Characterization of the role of MrpC in *Myxococcus xanthus* developmental cell fate determination

Dissertation

zur Erlangung des Doktorgrades
der Naturwissenschaften
(Dr. rer. nat.)

dem Fachbereich Biologie
der Philipps-Universität Marburg

vorgelegt von

Vidhi Bhardwaj

aus Delhi, Indien

Marburg (Lahn), April 2013

Die Untersuchungen zur vorliegenden Arbeit wurden von Oktober 2009 bis Dezember 2012 am Max-Planck-Institut für Terrestrische Mikrobiologie unter der Leitung von Dr. Penelope I. Higgs durchgeführt.

Vom Fachbereich Biologie der Philipps-Universität Marburg als Dissertation angenommen am: _____

Erstgutachter: Dr. Penelope Higgs
Zweitgutachter: Prof. Dr. Anke Becker

Weitere Mitglieder der Prüfungskommission:
Prof. Dr. Renate Renkawitz-Pohl
Prof. Dr. Michael Bölker

Tag der mündlichen Prüfung: 15.07.2013

Die während der Promotion erzielten Ergebnisse wurden und werden in folgenden Originalpublikationen veröffentlicht:

Lee B., Mann P., Grover V., *et al*. The *Myxococcus xanthus* Spore Cuticula Protein C Is a Fragment of FibA, an Extracellular Metalloprotease Produced Exclusively in Aggregated Cells. PLoS One. 2011; 6(12): e28968

Grover Bhardwaj V., Mann P. and Higgs P.I. (In preparation).

ERKLÄRUNG

Ich erkläre, dass ich meine Dissertation

„Characterization of the role of MrpC in *Myxococcus xanthus* developmental cell fate determination“

selbstständig, ohne unerlaubte Hilfe angefertigt und mich dabei keiner anderen als der von mir ausdrücklich bezeichneten Quellen und Hilfen bedient habe. Die Dissertation wurde in der jetzigen oder einer ähnlichen Form noch keiner anderen Hochschule eingereicht und hat noch keinen sonstigen Prüfungszwecken gedient.

Marburg, 14.05.2013

Vidhi Bhardwaj

Dedicated to my parents

KURZFASSUNG

Myxococcus xanthus ist ein exzellentes Modelsystem für multizelluläres prokaryotisches Verhalten und Gram-negative Differenzierung. Unter nahrungslimitierenden Bedingungen beginnt die Population ein komplexes multizelluläres Entwicklungsprogramm in welchem sich die Zellen in mindestens drei verschiedene Zelltypen differenzieren können: Sporulation in multizellulären Fruchtkörpern; Differenzierung in eine Art Dauerform names „Periphere Stäbchen“ und Zelllyse. Ein vierter, weniger verstandener Zelltyp namens „Zellcluster“ wird ebenfalls vermutet. Das hungerinduzierte Entwicklungsprogramm ist durch temporale und spatiale Expression von spezifischen Genen streng reguliert. Einer dieser Regulatoren heißt *mrpC*, welcher einen wichtigen Transkriptionregulator in der Entwicklung kodiert. Wir nehmen an, dass MrpC, welches für die Induktion von Aggregation und Sporulation wichtig ist und in die Zelllyse involviert sein soll, als Masterregulator für die Zelltypbestimmung verantwortlich sein könnte. Es wurde gezeigt, dass MrpC in entwicklungsbedingten Subpopulation unterschiedlich akkumuliert und dass die Fehlakkumulation dieses Proteins in gestörter Zelltypsegregation resultiert. MrpC ist sehr genau reguliert. Es wurde bereits vorgeschlagen, dass MrpC seine eigene Expression positiv reguliert. Die Transkriptionsaktivität von MrpC ist vermutlich reguliert – MrpC wird durch Phosphorylierung deaktiviert und durch proteolytische Prozessierung zu der kürzeren Isoform MrpC2 aktiviert.

In der vorgestellten Arbeit habe ich die Regulation des Transkriptionsfaktors MrpC mit Hilfe von genetischen und fluoreszenten Techniken untersucht und meine Daten deuten an, dass MrpC seine eigene Transkription negativ reguliert. Meine Analysen zeigten ebenfalls, dass die unterschiedlichen Akkumulationsmuster des MrpC Proteins in den entwicklungsbedingten Subpopulationen nicht auf Unterschiede in der Transkription oder Translation zurückzuführen sind, sondern wahrscheinlich durch Proteinabbau in der aggregierten Zellpopulation entstehen. Mit Hilfe von genetischen und biochemischen Methoden habe ich die zwei bekannten aktiven Formen von

MrpC untersucht. Meine detaillierten *in vivo* Analysen zeigten, dass die bereits veröffentlichten Ergebnisse aus *in vitro* Studien neu bewertet werden müssen um einer Isoform von MrpC eine biologische Rolle zuordnen zu können. Mit Hilfe von fluoreszenten Reporterkonstrukten der Promotoraktivität, habe ich die Expression verschiedener Gene in einzelnen Zellen der entwicklungsbedingten Subpopulationen bestimmt. Es konnte gezeigt werden, dass Ziele von MrpC nicht dem Akkumulationsmuster von MrpC folgten. Des Weiteren konnten Subpopulationen nicht auf Grund von Zelltyp-spezifischen Transkriptionsmarkern oder Chromosomenstatus unterschieden werden.

Die Studie unterstreicht die Bedeutung der Regulation des Schlüsselregulators MrpC, welche von den bereits veröffentlichten abweicht. Sie stellt ein Gerüst für die Aufarbeitung des vorgeschlagenen Models der komplexen MrpC Regulation und wie diese zu verschieden Zellschicksalen führen kann, dar.

ABSTRACT

Myxococcus xanthus is an excellent model system for multicellular prokaryotic behaviour and Gram-negative differentiation. Under nutrient-limited conditions, the population enters a complex multicellular developmental program wherein cells undergo at least three distinct known cell fates: sporulation within multicellular fruiting bodies; differentiation into persister-like state termed peripheral rods and cell lysis. A fourth distinct, relatively less understood cell type, called the cell clusters is also thought to exist. This starvation-induced developmental program is tightly regulated by the temporal and spatial expression of specific genes. One of them is *mrpC*, which codes for an important developmental transcriptional regulator. We hypothesized that MrpC, which is necessary for inducing aggregation and sporulation and was implicated in mediating developmental cell lysis, may act as a master cell fate regulator in *M*. *xanthus*. MrpC has been shown to accumulate heterogeneously in developmental subpopulations and its misaccumulation results in perturbed cell fate segregation. MrpC is known to be highly regulated. It has previously been proposed that MrpC positively regulates its own expression. The transcriptional activity of MrpC is thought to be regulated- MrpC is inactivated by phosphorylation and activated by proteolytic processing to the shorter isoform MrpC2.

In the presented thesis, using a combination of genetic and fluorescent techniques, I characterized the regulation of the transcription factor MrpC and my data suggests that MrpC negatively regulates its own expression. My analysis further revealed that the MrpC protein heterogeneity in developmental cell subpopulations is not due to transcriptional or translational differences but likely regulated by a protein turnover in the aggregated cell population. Using genetic and biochemical techniques, I addressed the two known activity states of MrpC. My detailed *in vivo* analysis revealed that the previously published *in vitro* data needs to be re-evaluated in order to assign a biological role to an isoform of MrpC. Using fluorescent reporters of promoter activity, I analyzed single-cell expression of various genes in developmental subpopulations. It was revealed that targets of MrpC do not follow the differential accumulation of MrpC. Moreover, cell subpopulations cannot be distinguished by means of cell-fate specific transcriptional markers or chromosome status.

This study emphasizes on the implications of regulation of the key developmental regulator MrpC being different than previously proposed and provides the framework to re-investigate the proposed models of MrpC regulation in order to aid an appropriate understanding of how this complicated system functions to enable cells to adopt distinct cell fates. .

TABLE OF CONTENTS

ABBREVIATIONS

h	hours
daH_2O	demineralized autoclaved water
min	minute
rpm	rotations per minute
kDa	kilo Dalton
DNA, RNA	deoxyribonucleic acid, ribonucleic acid
bp	base pairs
gDNA	genomic DNA
cDNA	single stranded complementary DNA
Pr	promoter
qRT-PCR	quantitative real time PCR
RT	room temperature
rbs	ribosome binding site
(p)ppGpp	guanosine tetra or pentaphosphate
GFP	Green Fluorescent Protein
X-Gal	5-bromo-4-chloro-3-indolyl- β -D-galactopyranoside
IPTG	isopropyl β-D-1-thiogalactopyranoside
DTT	dithiothreitol
DMSO	dimethylsulfoxide
DMF	dimethylformamide
EDTA	ethylenediamine tetraacetic acid
CYE	casitone yeast extract medium
CTT	casitone tris phosphate medium
LB	Luria-Bertani medium
MOPS	morpholinepropanesulfonic acid
MMC	MOPS-magnesium-calcium
Tris	tris-(hydroxymethyl)-aminomethane
TE	Tris-EDTA
TAE	Tris-acetate-EDTA
SDS	sodium dodecylsulfate
PAGE	polyacrylamide gel electrophoresis
APS	ammonium persulfate
TEMED	*N,N,N',N'*-tetramethylethylendiamine
ATP	adenosinetriphosphate
HPLC	high pressure liquid chromatography
BLASTp	Basic Local Alignment Search Tool (protein query mode)
Mxan	*Myxococcus xanthus* gene locus
Ni-NTA	nickel-nitroloacetic acid
HABA	hydroxy-azophenyl-benzoic acid
DMF	dimethyl formamide

1. INTRODUCTION

1.1 Multicellular development and differentiation in prokaryotes

Development in multicellular organisms results in the generation of specialized cells. For instance, during human embryogenesis, a totipotent blastocyst differentiates to pleuripotent stem cells which further differentiate into distinct organ-specific cell types (Odorico *et al*., 2001). For a long time, multicellular differentiation was considered to be a characteristic of eukaryotes alone and prokaryotes were treated as a uniform group of genetically identical cells. However, in the past decade, many tools have become available to facilitate studies at a single cell level. Thus, it is now well recognized that genetically identical bacteria differentiate into specialized cell types (Lopez *et al*., 2009; Veening *et al*., 2008). One of the earliest examples of phenotypic heterogeneity was of the catabolic enzyme synthesis for lactose utilization in *E. coli* where upon treating a clonal population of cells with a sub-saturating concentration of TMG, a non-metabolizable lactose analogue, a stable differentiated population consisting of induced and non-induced cells is produced (Novick & Weiner, 1957). Some other well defined examples are the differentiation of some cyanobacteria like *Anabaena* sp. into non-nitrogen fixing and specialized nitrogen-fixing cells called heterocysts (Kumar *et al*., 2010); the differentiation of *Bacillus* into motile cells, spores, cannibals, competent cells or matrix-producers (Lopez & Kolter, 2010), the differentiation of *Caulobacter* into swarmer and stalked cells (Amon, 1998); and the occurrence of antibiotic resistant and non-resistant cells in various pathogenic bacterial populations (Balaban *et al*., 2004).

1.1.1 Benefits of population heterogeneity

It is crucial to understand what advantages population heterogeneity can have for a bacterial community. The presence of variable phenotypes allows a population to be prepared and better adapted for sudden changes in the environment (Lopez *et al*., 2009). It is often considered as a 'bet-hedging' strategy to provide an evolutionary edge in the survival of a species (Veening *et al*., 2008). For example, in case of persister cells, phenotypic variation helps cells to evade the immune response and ensure survival of the population into the next generation (Lewis, 2007). The division of labour in a heterogeneous population allows efficient utilization of the resources available to a community. Only certain cells specialize to exhibit a metabolic trait and the rest are also benefitted by it, for example, only a small proportion of *B .subtilis* cells produce matrix but all the cells encased in it are resistant to environmental stress (Lopez & Kolter, 2010). Phenotypic heterogeneity has been speculated as a strategy to utilize different niches within an ecosystem. For instance, in case of a

population consisting of motile and non-motile cells, the sessile cells exploit the existing niche whereas the motile cells are nomadic that can swim away in search of new nutrient sources (Dubnau & Losick, 2006). Alternatively, phenotypic variation might serve as an advantage to generate genetic diversity and repair damaged DNA through homologous recombination, thereby increasing the overall fitness of a species e.g. competent cells are naturally capable of taking up DNA available in the local environment and integrating it into their genome (Maamar *et al*., 2007; Smits *et al*., 2006).

1.1.2 Mechanisms that generate population heterogeneity

Population heterogeneity can result from either genetic or non-genetic factors. Genetic factors involve alterations in the genome, such as DNA methylation, slipped-strand mispairing, or genome re-arrangements. For example, synthesis of Pap pili to mediate attachment of uropathogenic *E. coli* in host cells, is dependent upon the Dam methylation of newly replicated DNA (Owen *et al*., 1996). Slipped-strand mispairing within homopolymeric regions of DNA can cause a frameshift mutation resulting in an altered gene regulation and phase variation in *Neisseria* (Meyer *et al*., 1990) and *Bordetella pertussis* (Stibitz *et al*., 1989). A chromosomal inversion causes phase variation in *Salmonella* giving rise to a mixed population of cells expressing one of two forms of flagella (Graumann, 2006). Non-genetic factors involve no alteration in the genetic makeup of an organism and phenotypic variation arises either due to a dedicated regulatory genetic network, or due to the relative spatial positioning of cells within a multicellular biofilm possessing different microenvironments (Lopez *et al.*, 2009; Vlamakis *et al*., 2008). I will focus only on epigenetic phenotypic heterogeneity in this thesis.

Heterogeneity in gene expression & the concept of bistability

Genes can sometimes be expressed in a non-uniform fashion in an isogenic heterogeneous population. When the gene expression is distributed such that the population bifurcates into distinct cell types, this phenomenon is termed as ‘bistability’ (Dubnau & Losick, 2006; Chai *et al*., 2008). True bistability occurs only when the differentiation into the distinct cell types is a random event and not pre-determined. The non-linear induction of gene expression leads to bistability. This can occur when transcriptional factors require forming multimers, binding DNA cooperatively or phosphorylation (Veening *et al*., 2008). Bistable gene expression is controlled by two mechanisms (Lopez *et al*., 2009) (Fig. 1.1).

(a) Positive autoregulation: The product of a gene induces itself in a non-linear fashion after the basal level of the product is reached (Fig. 1.1A).

(b) Negative autoregulation: The product of a gene represses the expression of its own repressor. The effect of such a double negative feedback loop is similar to positive autoregulation *i.e.* activation (Fig. 1.1B).

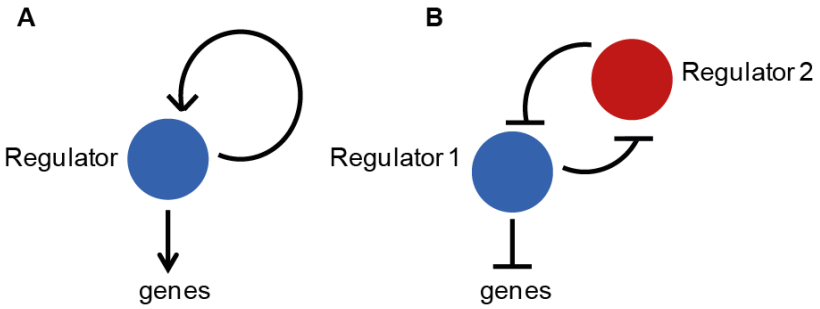

Fig.1.1 Mechanisms controlling bistable gene expression. A. Positive autoregulation. The gene product induces its own expression. B. Negative autoregulation. The gene product represses a repressor of its own expression (Figure modified from Lopez *et al*., 2009).

Threshold

The basal level of a gene product necessary for the non-linear induction of a gene and for the population to differentiate is called 'threshold'. Bistability occurs only when certain cells of a population are above the threshold and others are not. No bistability is observed if feedback loops are absent in a biological system (Smits *et al*., 2006) (Fig. 1.2).

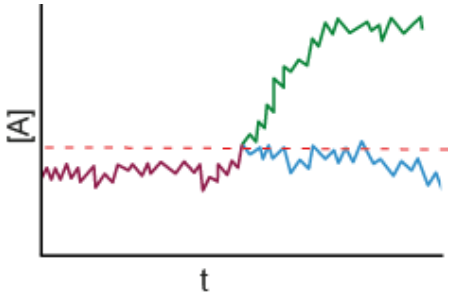

Fig.1.2 Threshold. The graph depicts the concentration of protein A [A] over time (t). Protein levels vary over time. When the levels exceed the threshold (red dotted line), high levels of the protein accumulate in the presence of a positive or double negative feedback loop (green line). No bistability is observed in the absence of a feedback loop (blue line) (Figure modified from Smits *et al*., 2006).

Noise

Another key determinant of phenotypic heterogeneity is the random variation in the expression of a gene, referred to as 'noise' (Maamar *et al*., 2007; Tyagi, 2010; Smits *et al*., 2006 & references therein). Noise can be of two kinds- intrinsic and extrinsic. Intrinsic noise arises due to the fluctuations in biochemical processes such as transcription and translation (depending on the rate of synthesis and degradation of a gene product). Extrinsic noise arises due to the variation in the metabolic capacities of different cells owing to the

difference in the number of polymerases, ribosomes *etc*. It has been demonstrated that noise is more abundant when small number of molecules are involved (Fig. 1.3). Transcription factors are generally present in limited numbers in a cell. Also, stress responses cause a decrease in the number of transcription factors leading to phenotypic variability.

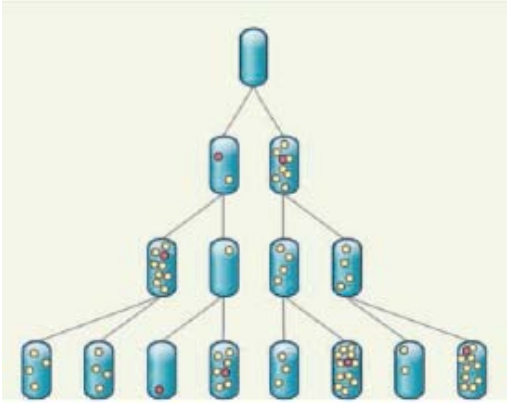

Fig.1.3 Noise associated with inheritance of cellular components. At any time, the number of mRNA molecules (red dots) and corresponding protein molecules (yellow dots) can vary among isogenic cells of a population. Noise arises due to differences in the life spans of mRNAs, which are relatively short lived and proteins, which can persist longer than the time required for cell division. The surviving protein molecules are randomly distributed into daughter cells, resulting in an unequal distribution if the number of protein molecules is small (Figure modified from Tyagi, 2010).

The expression of any gene is a matter of probability and it is always distributed across a population (Fig. 1.4). The generation of phenotypic heterogeneity owing to a variable gene expression depends on the genetic circuitry of a system. In other words, noise in gene expression does not give rise to phenotypic heterogeneity as long as it is suppressed by negative feedback but it becomes important when amplified by a positive feedback loop (Smits *et al*., 2006; Davidson & Surette, 2008 and references therein)

The differentiation of a population to generate distinct cell fates can either be stochastic / random, based on the feedback architecture of genetic networks and the noise characteristic of various cellular biochemical processes or deterministic *i.e.* linked to the cell cycle. A classic example of each of these two types of cell fate differentiation is described in section 1.1.3 (*Bacillus subtilis*) and section 1.1.4 (*Caulobacter crescentus*), respectively.

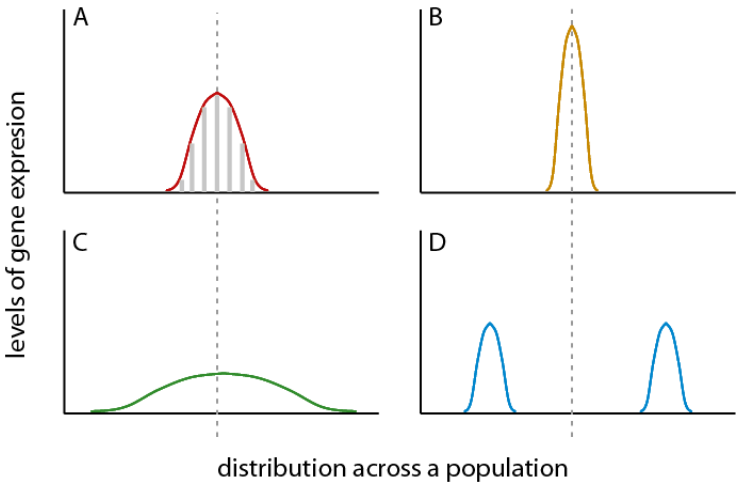

Fig.1.4 Distribution of gene expression in populations with the same average expression. The grey dotted line represents the average expression and the curve(s) depicts the distribution of expression levels of a gene in each case. (A) A characteristic distribution of gene expression across a population; grey bars represent the histogram of the expression levels of individual cells. In case of an alteration in the regulation of the system, the distribution of gene expression may narrow (B) or broaden (C) without changing the average expression level in the population. (D) Variation in gene expression can generate a bistable population in the presence of positive or double negative feedback loops (Figure modified from Davidson & Surettte, 2008).

1.1.3 Cell differentiation in *Bacillus subtilis*

Bacillus subtilis has been an excellent model system to study stochastic phenotypic heterogeneity as it differentiates into distinct specialized cell types by virtue of several defined developmental pathways (Dubnau & Losick, 2006; Lopez *et al*., 2009). Cells of a community communicate with each other via extracellular signals to coordinate this differentiation. The induction of a distinct developmental program is initiated by the phosphorylation of the three master regulators, Spo0A, DegU and ComA such that each cell fate is mutually exclusive of the other (Lopez & Kolter, 2010).

Figure 1.5 is a schematic showing all the distinct cell fates that cells adopt in a *Bacillus subtilis* community, classified according to the master regulator controlling the particular fate. Some of these cell fates are briefly described below with reference to the master regulator involved in the decision and the level of control it is subject to.

Competence

During the stationary phase, ~10-20% cells of the total *Bacillus* population become naturally capable of taking up DNA from the environment and incorporating it in their genome. The development of competence is regulated by the master transcription factor ComK, which is responsible to induce the

expression of genes involved in DNA binding and transport. A positive feedback loop associated with a non-linear response at the *comK* promoter plays a pivotal role in the regulation of competence (Maamar & Dubnau, 2005). In this biological system, the criteria for bistability are met and phenotypic heterogeneity is achieved.

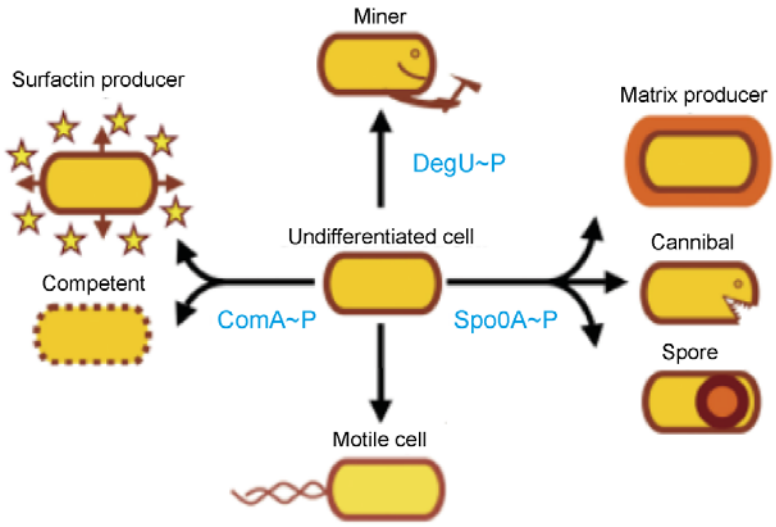

Fig.1.5 Differentiation of distinct cell types in *Bacillus subtilis*. Each cell type is caricaturized based on its most representative feature. Cell types are sub-grouped according to the master regulator that controls their differentiation. Arrows indicate the differentiation process. The master regulator involved is highlighted in blue. The differentiation into motile cells does not require any master regulator (Figure modified from Lopez & Kolter, 2010).

The synthesis and activity of ComK is regulated through proteolytic degradation, quorum-sensing and transcriptional control (reviewed in Lopez *et al*., 2009; Leisner *et al*., 2008; Dubnau & Losick, 2006; Lopez & Kolter, 2010) as described below (Fig. 1.6).

(a) Control through proteolytic degradation and quorum sensing: During the exponential growth phase, ComK binds an adapter protein MecA and is targeted for degradation by the ClpCP protease. As the stationary phase approaches, the expression of *comK* is activated by the phosphorylation of the master transcriptional regulator ComA by a quorum sensing mechanism. Briefly, the pheromone ComX is sensed by the histidine kinase ComP which then phosphorylates ComA. ComA~P induces expression of the *sfr* (surfactin) operon encoding the small protein ComS that binds to MecA and prevents ComK from degradation.

(b) Control at the level of transcription: ComK induces its own expression by binding to its promoter (P_{comK}). This positive feedback loop involves a non-linear expression of *comK*. Additional proteins control the expression of *comK* by

binding to the promoter as activators or repressors. For example, the pleiotropic regulator DegU increases ComK affinity for P_{comK} and acts as an activator while AbrB, CodY and Rok act as repressors during exponential growth.

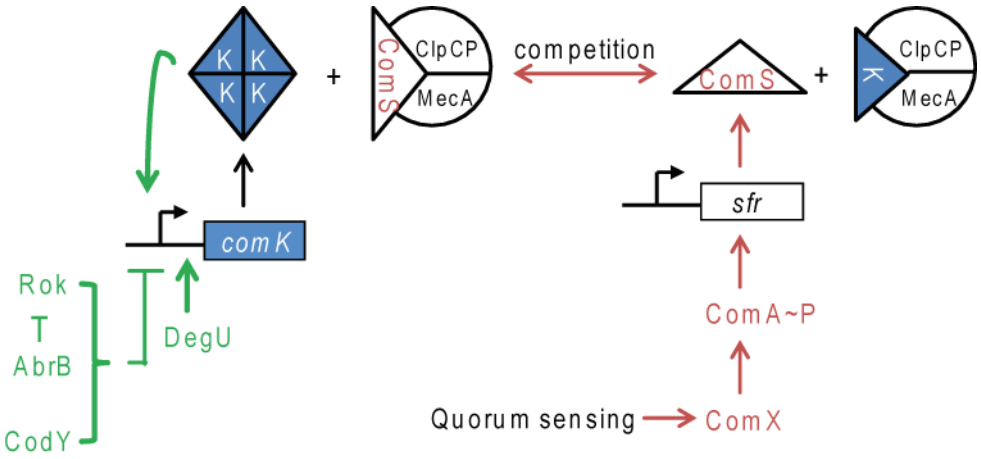

Fig.1.6 Regulatory network governing competence development. Transcriptional control of *comK* is depicted in green and proteolytic control of ComK is depicted in red. Arrows and T-bars indicate positive and negative regulation, respectively; kinked arrows indicate promoter regions; K, ComK; ~P, phosphorylated (Figure modified from Leisner *et al*., 2008).

Sporulation and Cannibalism

Another example of bistability in *Bacillus* is the differentiation into environmentally resistant spores under nutrient limited conditions to ensure survival of cells upon the return of favorable conditions (Lopez *et al*., 2009). The master regulator of sporulation, Spo0A, is a member of the response regulator family of transcription factors (Fujita & Losick, 2003). Spo0A is regulated at the level of activity by phosphorylation and at the level of transcription, directly and indirectly (Fig. 1.7).

Spo0A activity is regulated by phosphorylation via a phosphorelay pathway that involves a series of histidine kinases and two relay proteins, Spo0F and Spo0B. Further, several phosphatases interact with the phosphorelay proteins or phosphorylated Spo0A (Spo0A~P) itself to dephosphorylate Spo0A (Fujita & Losick, 2005; Dubnau & Losick, 2006 and references therein). Additionally, Spo0A synthesis is regulated by two feedback mechanisms (Veening *et al*., 2005). Spo0A~P induces the expression of *spo0A* directly via a positive feedback loop and indirectly via a double negative feedback loop. Spo0A~P represses the expression of *abrB*, a gene that encodes the repressor of *sigH*. The gene *sigH* codes for an RNA polymerase sigma factor (sigma-H) which induces the transcription of *spo0A* and of genes involved in Spo0A phosphorylation such as *spo0F*. It has been proposed that the phosphorelay is a noise generator in this system such that only cells that reach a threshold level

of Spo0A~P are able to sporulate (Chastanet *et al*., 2010). Thus, the master regulator Spo0A stimulates both its synthesis and activity to generate a bistable population.

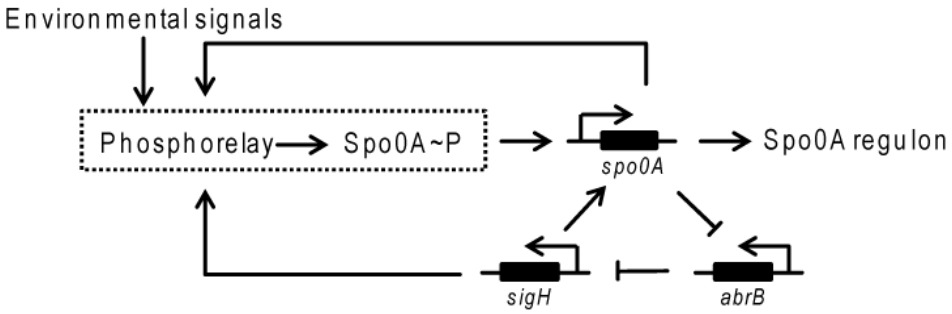

Fig.1.7 Regulatory network governing the initiation of sporulation. The master regulator Spo0A is regulated at the level of transcription by Spo0A~P and SigH and at the level of phosphorylation by a series of kinases and phosphatases. Arrows and T-bars indicate positive and negative feedback loops, respectively. ~P; phosphorylated (Figure modified from Veening *et al*. 2005).

Sporulation is an energy intensive process. Before being irreversibly committed to sporulation, *B. subtilis* differentiates into another subpopulation of cells that can cannibalize their siblings by the production of two toxin proteins; Skf (sporulation killing factor) and Sdp (sporulation delaying protein). These specialized cells, called cannibals secrete toxins but at the same time express immunity proteins in order to resist the action of the toxins. This phenomenon of killing sister cells to obtain food temporarily under nutrient limited conditions, thereby delaying the onset of sporulation, is termed as cannibalism (reviewed in Lopez & Kolter, 2010 and Lopez *et al*., 2009). Low levels of the master regulator Spo0A~P are sufficient to induce the expression of the *skf* operon directly and the expression of the *sdp* operon indirectly, by repressing the repressor AbrB (Fig. 1.8).

A nutrient limited population of *Bacillus* differentiates into Spo0A-ON (sporulating) and Spo0A-OFF (non-sporulating) cells (Dubnau & Losick, 2006). Spo0A-ON cells become cannibalistic before eventually sporulating and kill their siblings to use them as food. These cells express the immunity proteins to protect themselves. However, the Spo0A-OFF cells are non-immune as the repression on the immunity operon expression by AbrB is not relieved. Thus, cell fate is governed by the levels of Spo0A~P: low levels activate cannibalism while high levels activate sporulation (reviewed in Gonzalez-Pastor *et al*., 2011). Thus, from the above examples, it is clear how a master regulator coordinates differentiation in a multicellular organism; cells adopt distinct cell fates owing to bistable gene regulatory networks.

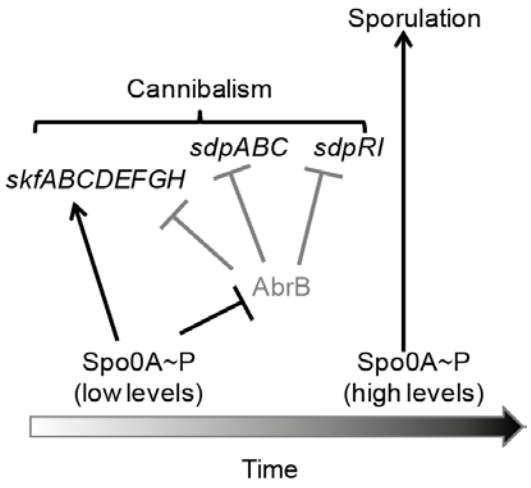

Fig.1.8 Regulatory network governing cannibalism. Different levels of phosphorylated Spo0A (Spo0A~P) control cannibalism and sporulation. The operons encoding the toxin/immunity proteins are activated by a low level of Spo0A~P while genes involved in sporulation are turned on at high levels of Spo0A~P. *skfA-H* & *sdpABC* are the toxin gene operons while *sdpRI* codes for immunity proteins. Arrows and T-bars indicate positive and negative feedback loops, respectively (Figure modified from Gonzalez-Pastor *et al*., 2011).

1.1.4 Cell differentiation in *Caulobacter crescentus*

Heterogeneity in the aquatic α-proteobacterium *Caulobacter* is thought to be deterministic and innately hardwired into the cell cycle. The organism divides by asymmetric cell division (Amon, 1998) such that after each round, a differentiated progeny consisting of a motile swarmer and a sessile stalked cell is produced (Fig. 1.9). Both these cell types are morphologically distinct and possess different regulatory programs. The stalked cell can immediately replicate its DNA and divide while the swarmer cell can only initiate a new round of DNA replication and cell division after it has differentiated into a stalked cell.

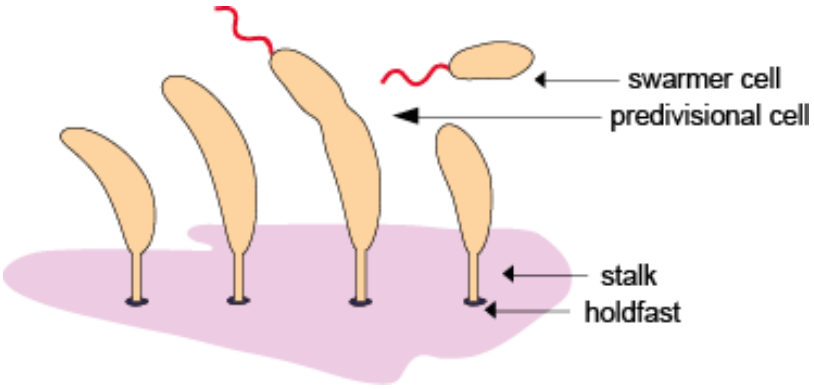

Fig.1.9 Life cycle of *Caulobacter crescentus*. A sessile stalked cell attached to a surface by an adhesive holdfast at the end of the stalk divides at the end of each cell cycle to give rise to a motile swarmer daughter cell (Figure modified from Laub *et al*., 2007).

A vast amount of knowledge is now available at the molecular level on the sophisticated cell cycle control system of this bacterium, but only the overall different mechanisms of control of the key players involved in the regulation of such a genetic circuit are briefly outlined.

The progression of the cell cycle in *C. crescentus* is controlled by four master regulatory proteins namely, CtrA, GcrA, DnaA and CcrM. CtrA and DnaA are transcription factors while GcrA and CcrM influence transcription indirectly. These proteins together control the expression of at least 200 genes. They are produced successively during the cell cycle with a spatial and temporal control over their concentrations at the level of transcription, proteolysis and activation by phosphorylation (Østerås & Jenal, 2000; Laub *et al*., 2007 and references therein) as described below (Fig. 1.10).

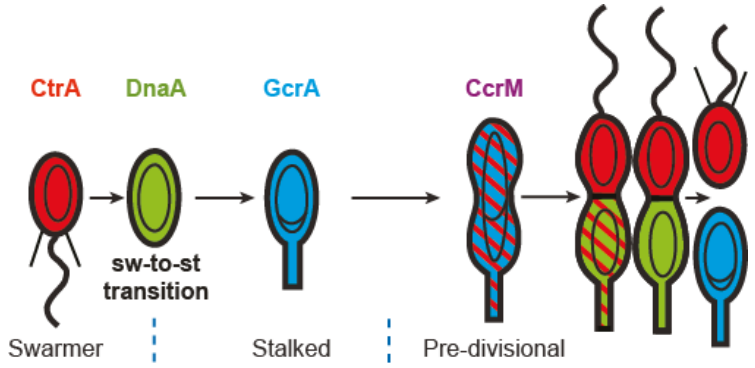

Fig.1.10 Regulation of cell differentiation in *C. crescentus*. The concentrations of the master regulatory proteins are changed both in space and time to synchronize the progression of the asymmetric cell cycle. CtrA (red), DnaA (green), GcrA (blue). The interior circles in the cell represent the chromosome. Curved line and straight line shown at the cell pole represent flagellum and pili respectively (Figure taken from Laub *et al*., 2007).

CtrA is an essential transcription factor that governs the transcription of genes involved in flagellar biosynthesis, cell division, DNA replication and methylation. CtrA is active only if it is phosphorylated (CtrA~P). In the swarmer cells, it prevents DNA replication by binding to the origin of replication and also represses the transcription of *gcrA*. CtrA~P is specifically degraded by proteolysis in the stalked cell compartment of a predivisional cell and during the swarmer-to-stalked cell transition to allow DNA replication to proceed. At this stage, the DNA replication inititator protein DnaA is synthesized to initiate DNA replication and induce *gcrA* transcription. DnaA is dynamically proteolysed in order to prevent the reinitiation of DNA replication. Further as the cell cycle progresses, GcrA induces the transcription of *ctrA*. CtrA~P accumulates gradually and its concentration increases rapidly owing to the positive feedback of CtrA~P on its own promoter. CtrA~P is responsible to induce the expression of *ccrM* that encodes CcrM, a DNA methyltransferase which controls the expression of genes by regulating the methylation state of their promoter. CcrM

is produced only very shortly near the end of the DNA replication cycle to remethylate the genome and is inactivated thereafter. The transcription of *ctrA* can be re-induced only if its promoter is in a hemimethylated state, after the replication has passed the *ctrA* gene. Thus, multiple signals are used by *Caulaobacter* to track the progress of chromosome replication and cell division to give rise to dimorphic phenotypes at the end of each cell cycle.

In summary, complex genetic circuits are regulated to give rise to population heterogeneity either stochastically due to the existence of bistable switches owing to noise or deterministically so that cell differentiation is obligatorily linked to the cell cycle.

1.2 Cell differentiation in *Myxococcus xanthus*

The Myxobacteria have long been considered excellent model systems for multicellular bacterial behaviour and Gram-negative differentiation. *Myxococcus xanthus* is the best studied among this group of bacteria.

1.2.1 Life cycle of *M. xanthus*

The rod-shaped delta-proteobacterium *M. xanthus* inhabits the soil or herbivore dung. The cells swarm in groups by gliding motility and obtain nutrients cooperatively by degrading organic matter or preying on other microorganisms by secreting antibiotics and hydrolytic enzymes (Reichenbach, 1999; Rosenberg, 1977). The bacterium exhibits a complex life cycle that includes both vegetative growth and multicellular development (Fig. 1.11).

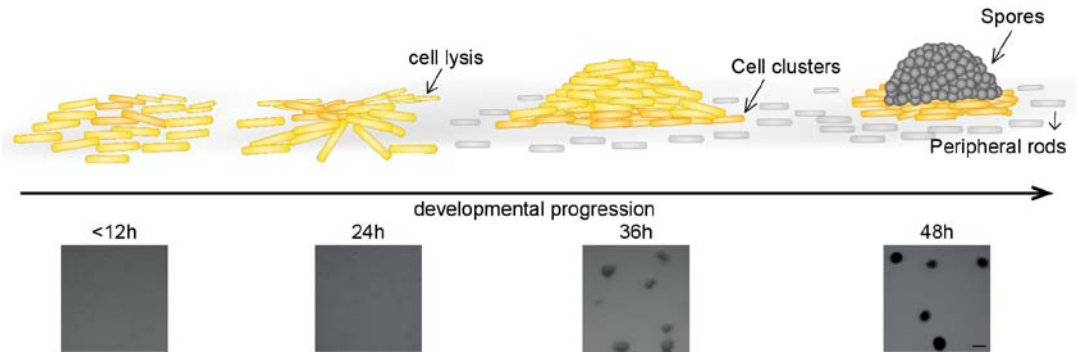

Fig.1.11 Life cycle of *Myxococcus xanthus*. Scheme of the vegetative and developmental cycle of *M. xanthus*. Upon starvation, cells begin to aggregate into fruiting bodies within which they differentiate into environmentally resistant spores. Some cells that do not enter these aggregates and remain outside are called the peripheral rods. Another cell type termed cell clusters, distinct from the cells induced to aggregate into mounds is also thought to exist (top). Development of Wild type DZ2 in laboratory conditions (bottom). The pictures denote the various stages of the developmental program shown in A. Scale, 100 µm.

Under nutrient-limited conditions, the population enters a complex multicellular developmental program wherein cells undergo at least three distinct known cell fates: sporulation within multicellular fruiting bodies (Shimkets, 1990; Dworkin & Kaiser, 1993); differentiation into persister-like state termed peripheral rods (O'Connor & Zusman, 1991a, b, c) and cell lysis (Wireman & Dworkin, 1977; Nariya & Innoye, 2008; Lee *et al*., 2012). A fourth distinct although relatively less understood cell type, called the cell clusters is also thought to exist (Lee *et al*., 2012). On the return of favourable nutrient-rich conditions, the spores germinate and cells undergo vegetative growth.

1.2.2 Regulation of the starvation induced developmental program

The starvation-induced developmental program in *M. xanthus* is tightly regulated by the temporal and spatial expression of specific genes under the influence of a series of sophisticated intra- and intercellular signaling events that must be coordinated and integrated to ensure proper fruiting body formation and sporulation (Kaiser, 2004) (Fig. 1.12). Starvation triggers the stringent response that causes an increase in (p)ppGpp levels (Laue & Gill, 1995; Harris *et al*., 1998) that trigger A-signalling (Singer & Kaiser, 1995) which is proposed to be a population (quorum-) sensing mechanism (Kaplan & Plamann, 1996). The A-signal is a mixture of amino acids and small peptides and induces the transcription of several early developmental genes (Kuspa *et al.*, 1992). One of the genes upregulated in response to the A-signal is *mrpC* which encodes for a transcriptional regulator protein belonging to the cyclic AMP receptor protein (CRP) family and is necessary for aggregation and sporulation (Sun & Shi, 2001a,b). MrpC is subject to post-translational modification which is proposed to control its affinity to target promoters. MrpC is thought to be phosphorylated (MrpC~P) under vegetative conditions and binds target sequences with a low affinity. However, under developmental conditions, MrpC can no longer be phosphorylated and is proposed to be proteolysed to MrpC2, a shorter isoform lacking the N-terminal 25 amino acid residues. MrpC2 binds target sequences with a higher affinity *in-vitro* (Nariya & Inouye, 2005, 2006) and is proposed to induce their transcription more efficiently. One of the targets of MrpC2 is the developmental transcriptional regulator gene *fruA* (Ueki & Inouye, 2003; Nariya & Inouye, 2006).

FruA is an orphan response regulator of the two-component signal transduction family with a DNA binding output domain and is essential for aggregation and sporulation (Ogawa *et al*., 1996). It is proposed to be activated by phosphorylation in response to the C-signal generated as a result of cell-to-cell contact (Ellehauge *et al*., 1998). The C-signal (p17) is a developmentally regulated proteolytic product of the cell-surface-associated CsgA (p25) protein (Lobedanz & Søgaard-Andersen *et al*., 2003). It is proposed that the C-signal is

sensed by an unidentified receptor on a neighboring cell and the activation of FruA is initiated in an unknown manner. Low levels of activated FruA are proposed to trigger aggregation by stimulating the methylation of the methyl-accepting chemosensory protein FrzCD (Blackhart & Zusman, 1985; McBride *et al*., 1992; McBride & Zusman, 1993; Shi *et al*., 1996; Søgaard-Andersen & Kaiser, 1996). Increased cell-cell contact between aggregated cells leads to higher levels of C-signalling and activated FruA (Søgaard-Andersen *et al*., 1996; Ellehauge *et al*., 1998). Higher levels of activated FruA are proposed to trigger sporulation by inducing several downstream target genes, for example, the *dev* locus (Vishwanathan *et al*., 2007), which is necessary for the induction of another sporulation specific gene Mxan_3227 (Licking *et al*., 2000). Furthermore, one of the products of the *dev* locus (DevT) is required for stimulation of *fruA* transcription, thus, providing a positive feedback loop on *fruA* expression (Boysen *et al*., 2002). FruA sometimes acts in combination with MrpC2 to control the transcription of genes expressed late during the developmental program (Mittal & Kroos, 2009a, b; Lee *et al*., 2011; Son *et al*., 2011). Thus, MrpC/MrpC2, FruA, C-signal and FrzCD form the core components in the regulation of this sophisticated multicellular developmental program.

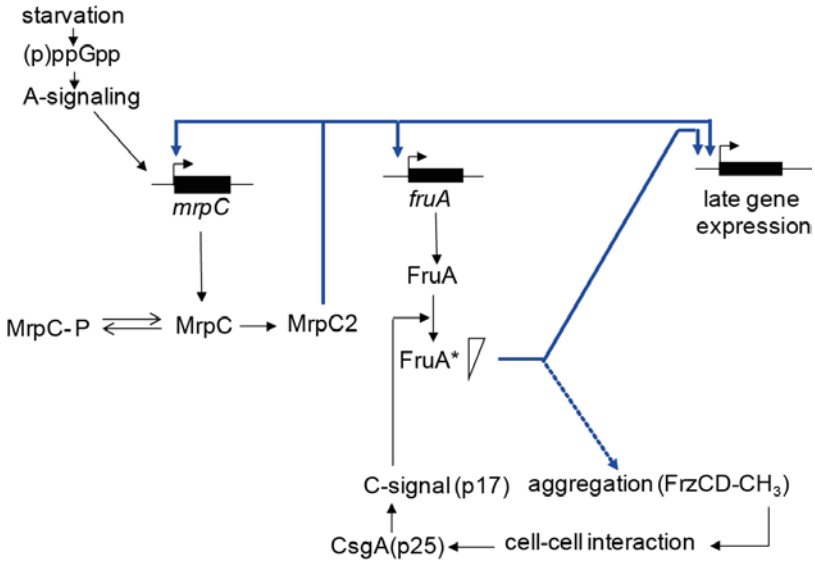

Fig.1.12 A simplified model for molecular events during the starvation induced developmental program of *M. xanthus*. The various genes are shown with kinked arrows representing the respective promoters; * depicts FruA activation, triangle indicates levels of FruA, arrows indicate activation, blue line depicts positive auto-amplification loops.

1.2.3 Cell population heterogeneity during development

As mentioned previously (section 1.2.1), *M. xanthus* cells adopt distinct fates during the starvation induced developmental program. Each of these is described in detail below.

Cell clusters

It has been shown previously that cells growing as a lawn can be separated by differential centrifugation into those found in aggregates (aggregated cells) and those which are not (non-aggregated cells) (Lee *et al*., 2011, 2012). 25% of the total population of aggregated cells (under the conditions tested) is termed as cell clusters in order to differentiate them from the cells which are induced to aggregate into mounds during the developmental program. Cell clusters can be isolated under vegetative conditions and early during development, at least until the onset of aggregation. This subpopulation of cells displays distinct characteristics in comparison to the cells not found in aggregates. These include: increased EPS production, increased methylation of the chemosensory protein FrzCD and the exclusive production of the EPS-associated protein- the metalloprotease FibA (Lee *et al*., 2012) (Fig. 1.13). While the accumulation of C-signal (p17) in the cell clusters is similar to the non-aggregated cells, the major developmental regulators, MrpC and FruA, do not accumulate as rapidly nor to the same levels as in the non-aggregated cells (Fig 1.13B). It is therefore suggested that the cell clusters likely follow a different developmental program (Lee *et al*., 2012).

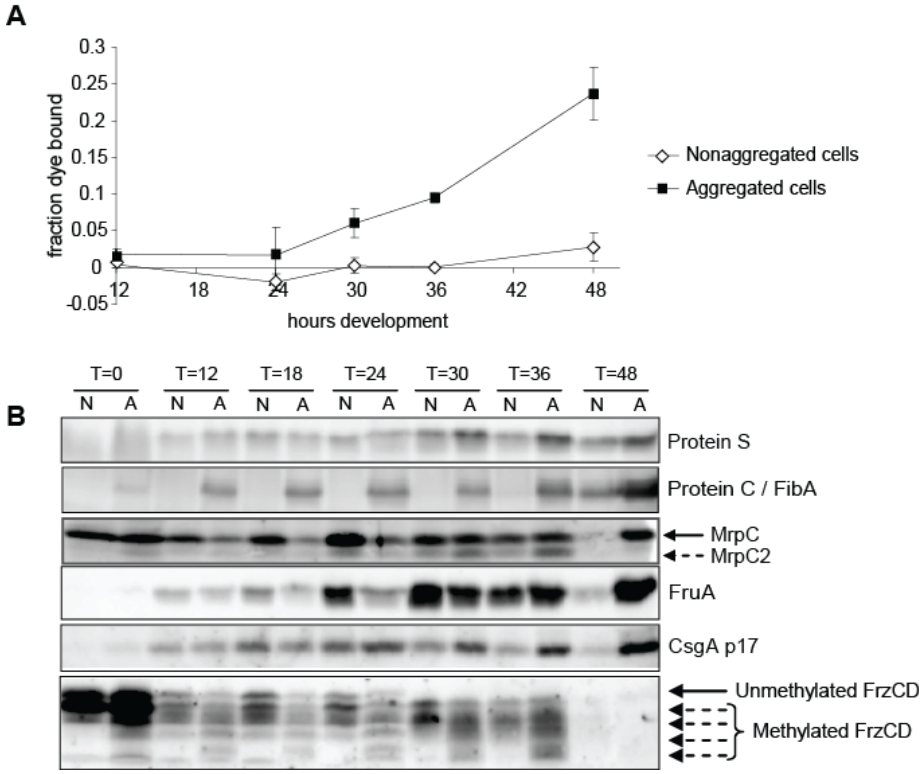

Fig.1.13 Developmental subpopulations of the non-aggregated and aggregated cells display distinct characteristics A. Relative EPS production in the non-aggregated (open diamonds) and aggregated cells (filled squares) is expressed as the fraction of dye bound to approx. $2.8x10^8$ of cells in each fraction at the indicated time points. B. Immunoblot analysis of cells from the non-aggregated and aggregated fractions using antibodies specific for protein S, FibA, MrpC, FruA, CsgA (p17) and FrzCD. Each lane contains total cell lysate prepared from $4x10^7$ cells (Figure modified from Lee *et al.,* 2012).

The exact role that these cell clusters play in the *M. xanthus* life cycle is not well understood. They might be a way to better adapt to changes in the environment in a way similar to the epiphytic aggregates of *Psuedomonas syringae* which are more resistant to dessication than single cells (Monier & Lindow, 2003, 2004). Some functions that can be envisioned for the cell clusters during developmental conditions are- they serve as a platform for the aggregating cells to build fruiting bodies (Curtis *et al*., 2007); they act as a spacing determinant for appropriate spacing between fruiting bodies (Xie *et al*., 2011) or that they mimic the more elaborate stalks observed in the related species, *M. stipitatus* (Reichenbach, 1993)

Fruiting bodies & spores

Fruiting bodies are the best characterized cell fate. When cells are separated by differential centrifugation very late during development, the aggregated cell fraction predominantly consists of fruiting bodies filled with mature spores (Lee *et al*., 2012). The formation of fruiting bodies is initiated under conditions of nutrient limitation when certain cells of the population are induced to aggregate into mounds of approximately 10^5-10^6 cells and then exclusively within these mounds, the cells differentiate to form environmentally resistant spores (Fig 1.11). The production of fruiting bodies requires a solid surface, a certain population density of motile cells and a series of inter- and intra- cellular signalling events coordinated both in space and time (refer to section 1.2.2). It is thought that the formation of fruiting bodies facilitates dispersal of groups of spores to nutrient replete environments and the germination of these groups of spores facilitates cooperative feeding (Rosenberg *et al*., 1977).

Peripheral rods

The peripheral rods, first documented and characterized by O'Connor & Zusman in 1991, are a distinct developmental subpopulation of cells. Originally, cells were harvested at the end of development as a suspension and the peripheral rods were separated as single rod-shaped cells from mature fruiting bodies based on a differential centrifugation technique (O'Connor & Zusman, 1991a). Multicellular fruiting bodies were enriched in the pellet while the non-aggregated peripheral rods were enriched in the supernatant. Peripheral rods are thought to be structurally no different than vegetative cells and have been shown to not accumulate intracellular lipid bodies which are characteristic of cells that aggregate and sporulate (Hoiczyk *et al*., 2009). They do not appear to be motile or divide *in situ* but both motility and cell division can be restored by adding nutrients suggesting that these cells are not irreversibly differentiated (O'Connor & Zusman, 1991b). It is not fully clear whether peripheral rods retain the capacity to aggregate because of contrasting observations from two independent studies (O'Connor & Zusman, 1991b; Hoiczyk *et al*., 2009). It has

been demonstrated that the proteome of peripheral rods is different from both vegetative and fruiting body cell fractions (O'Connor & Zusman, 1991a). This subpopulation of cells does not significantly accumulate extracellular polymeric substances (EPS), the extracellular metalloprotease FibA and also the important developmental regulators MrpC/C2 and FruA (Fig. 1.13) (Lee *et al*., 2012). Analysis of several developmentally regulated proteins such as Myxobacterial Hemagglutinin (MBHA) and spore coat protein S revealed that the expression patterns are different from vegetative or fruiting body cells (O'Connor & Zusman, 1991a, c). It has been demonstrated that the peripheral rods express two-fold less CsgA protein than the fruiting body cells and thus, it was proposed that peripheral rods which do less C-signalling do not also express the late genes necessary for fruiting body formation and spore differentiation (Julien *et al*., 2000).It has been suggested that peripheral rods contain a 1N genomic content, whereas spores are 2N (Tzeng & Singer, 2005).

In summary, these distinct features are reflective of distinct regulation of the core metabolic process and cell cycle in peripheral rods. It is proposed that the peripheral rods help *M. xanthus* to utilize low levels of nutrients available in the environment that are insufficient to either promote growth or to induce germination of spores within the fruiting bodies (O'Connor & Zusman, 1991b).

Programmed cell death / developmental autolysis

Developmental cell lysis in *M. xanthus* has been a matter of debate. It was first proposed that the majority of cells (~80% of the total population) undergo obligatory cell lysis during the developmental program (Wireman & Dworkin, 1977). On the other hand, O'Connor and Zusman strongly support the view that the proposed developmental cell lysis is in fact an artifact of the manipulation of fragile developmental cells (O'Connor & Zusman, 1988). Nearly 20 years later, it was proposed that developmental cell lysis was a programmed event mediated by a novel toxin-antitoxin (TA) system, consisting of MazF and MrpC. It was shown that a *ΔmazF* mutant does not lyse during development, whereas a *ΔmrpC* mutant constitutively producing MazF, produced higher levels of dead cells (Nariya & Inouye, 2008).

Interestingly, however, it was recently shown that the deletion of *mazF* in two different wild type *M. xanthus* laboratory strains did not significantly reduce developmental cell lysis, suggesting that MazF's role in programmed cell death (PCD) is an adaption to the mutant background strain DZF1 (Lee *et al*., 2012). More recently, it has been demonstrated that the discrepancy in MazF's role in PCD in DZF1 is due to the presence of the *pilQ1* allele that renders the strain partially deficient in social motility and cell adhesiveness (Boynton *et al*., 2013). Additionally, in contrast to the previously proposed role of MrpC to inhibit MazF

activity (Nariya & Inouye, 2008), it has been revealed that MrpC enhances the ribonuclease activity of MazF (Boynton *et al*., 2013). The exact role of MrpC in developmental cell lysis is not yet clear but the observation that a *csgA* mutant does not decrease in cell number during development suggests that lysis is related to the induction of a specific signaling mechanism involving CsgA (or C-signal) (Janssen & Dworkin, 1985; Lee *et al*., 2012).

1.3 MrpC and its possible role in cell fate determination

The transcription factor MrpC plays a central role in the regulation of the multicellular developmental program. It is known to be highly regulated and we think that it might be the master regulator of cell fate determination during the multicellular developmental program in *M*. *xanthus*.

The mrp genetic locus and the regulation of mrpC expression

The *mrpC* locus was identified via transposon mutagenesis as an essential locus for multicellular development (Sun & Shi, 2001a). The *mrp* locus consists of three genes, namely, *mrpA*, *mrpB*, and *mrpC* (Fig. 1.14A). These three genes comprise of two transcriptional units, *mrpAB* and *mrpC*. Based on the predicted amino acid sequences, MrpA is a cytoplasmic histidine kinase, MrpB is an NtrC-like response regulator with a σ^{54}-activation domain, and MrpC is a transcription factor of the cyclic AMP receptor protein (CRP) family of transcriptional regulators. It was shown that both *mrpB* and *mrpC* are required for cellular aggregation and sporulation and *mrpA* is required only for sporulation. It was also shown that the mutation of the putative phosphorylation site of MrpB, D58 to D58A causes defects in both aggregation and sporulation but a D58E mutation results only in a sporulation defect (Sun & Shi, 2001a).

The transcriptional factor MrpC is homologous to the CRP of *E.coli*, with 23% identity over 184 residues. It possesses a cyclic nucleotide (cNMP) binding domain; however, the residues that are known to bind cAMP in *E.coli* CRP are not conserved in MrpC. It has a DNA-binding domain homologous to the HTH-Xre family of transcription factors (Sun & Shi, 2001a) (Fig. 1.14B). As mentioned earlier, the expression of *mrpC* is induced early during development and depends on (p)ppGpp and the A-signal (Sun & Shi, 2001b). In the earliest study to understand the regulation of *mrpC* expression (Sun & Shi, 2001a), a *lacZ* reporter strain was constructed (Fig. 1.15A). A translational fusion of the first 97 amino acids of *mrpC* gene was made to the *lacZ* gene and this construct was integrated at the gene locus. The expression of *mrpC* was measured as ß-galactosidase specific activity over time during development (Fig. 1.15B). The expression of *mrpC* was found to be upregulated ~10-fold during development in the wild type DK1622 background and was no different in a Δ*mrpA* strain.

However, no *mrpC* expression was observed in a Δ*mrpB* as well as in a Δ*mrpC* strain. Thus, it was proposed that *mrpB* is essential for the expression of *mrpC* and that *mrpC* positively autoregulates its own expression.

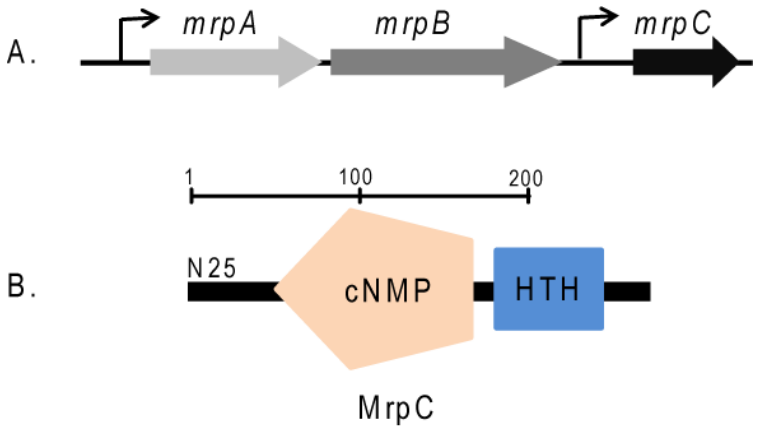

Fig. 1.14 A. Gene structure of the *mrp* locus. *mrpA and mrpB* are co-transcribed and *mrpC* is transcribed independently. B. Structure of MrpC. The first 25 amino-acid residues, N25, are missing in the isoform MrpC2, residues 45-138 correspond to the cyclic nucleotide binding domain (cNMP); residues 187-235 correspond to the Helix-Turn-Helix DNA binding domain (Figure information taken from the program SMART for protein domain architecture analysis).

MrpC is expressed during vegetative growth and is subject to post-translational modification. It has been shown that MrpC is phosphorylated by the Pkn8/Pkn14 Ser/Thr kinase cascade. Pkn8 is a Pkn14 kinase and Pkn14 is an MrpC kinase (Nariya & Inouye, 2005) *pkn8* and *pkn14* deletion strains (Δ*pkn8* and Δ*pkn14*) develop into fruiting bodies much faster than the wild type DZF1 strain. While *mrpC* is expressed at a low level in the DZF1 wild type during vegetative growth, it is expressed at high levels in Δ*pkn8* and Δ*pkn14* during vegetative growth and development as shown by *mrpC-lacZ* reporter analysis (Nariya & Inouye, 2005). The higher *mrpC* expression during vegetative growth induces untimely FruA expression at the early stationary phase and at the beginning of development in Δ*pkn8* and Δ*pkn14*, resulting in faster progression of development. *pkn14* expression increased at the mid- and late-log phases in the DZF1 wild type but decreased during development, suggesting that the Pkn8-Pkn14 kinase cascade appears to negatively regulate *mrpC* expression by phosphorylating MrpC during vegetative growth (Nariya & Inouye, 2005).

MrpC binds to at least eight sites in the upstream region of its promoter (Nariya & Inouye, 2006). The DNA binding activity of MrpC is greatly reduced upon its phosphorylation by Pkn14. It is thought that during development, MrpC is likely processed into a shorter isoform called MrpC2 by a proteolytic event involving the protease LonD. MrpC2 was isolated bound to the *fruA* promoter region and is thought to lack the N-terminal 25 residues of MrpC (Ueki and Inouye, 2003). It is only present in developing cells but not detectable in a *lonD* mutant in which

the expression of *fruA* is low (Nariya & Inouye 2005, 2006). It was shown by *in-vitro* DNA binding assays that MrpC2 has a higher affinity for *mrpC* and *fruA* promoter regions than MrpC itself. Thus, it was suggested that MrpC2 is a positive regulator of *mrpC* and *fruA* expression (Nariya & Inouye, 2006). Pkn14 does not phosphorylate MrpC2 and phosphorylates MrpC at Thr residue(s), thus Thr-21 and/or Thr-22 is (are) the likely sites of MrpC phosphorylation (Nariya & Inouye, 2006). Therefore, phosphorylation of MrpC (MrpC~P) inhibits not only the positive autoregulation but also its proteolytic processing to MrpC2 as it was present at high levels during vegetative growth in the *Δpkn8* and *Δpkn14* strains (Nariya & Inouye, 2006).

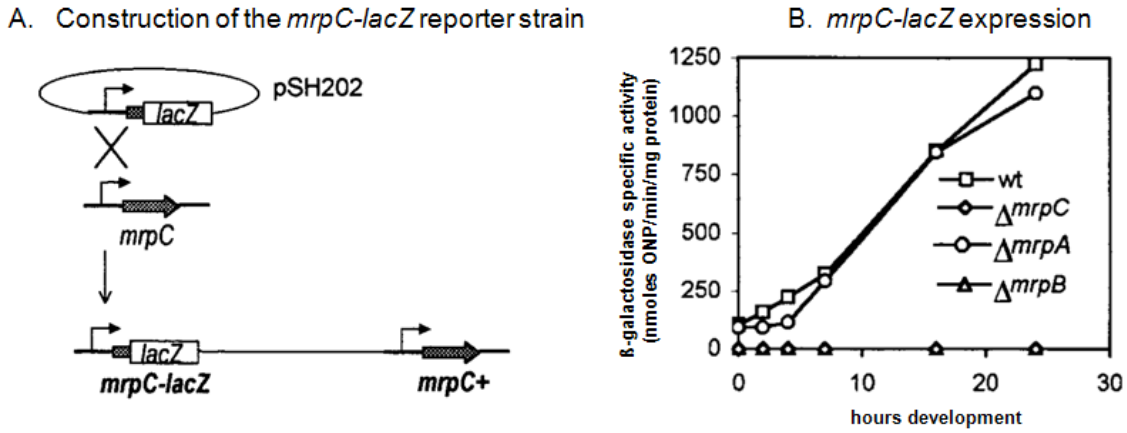

Fig. 1.15 A. Construction of the *mrpC-lacZ* reporter strain in wild type (DK1622) background. A translational fusion of the first 97 amino acids of *mrpC* gene was made to the *lacZ* gene. The reporter strain retained the wild-type copy of *mrpC* with its own promoter. B. β-galactosidase assay for the analysis of *mrpC-lacZ* expression in the *ΔmrpA*, *ΔmrpB, ΔmrpC* and wild type (DK1622) background (Figure taken from Sun & Shi 2001a).

MrpC and cell fate decisions

MrpC's accumulation affects cell fates. Developmental progression in *M. xanthus* is known to be negatively regulated by several genes, for example, *espA* (Cho & Zusman, 1999), *espC* (Lee *et al*., 2005), *redCDEF* (Higgs *et al*., 2005) and *todK* (Rasmussen & Søgaard-Andersen, 2003). All these genes are members of the two component signal transduction family of proteins and a null mutation in either of these causes an early developmental phenotype. Analysis of the accumulation pattern of the key regulatory protein MrpC during development in these mutants revealed an earlier accumulation in comparison to the wild type (Higgs *et al*., 2008; Lee, PhD Thesis 2009) (Fig. 1.16). Additionally, a quadruple mutant of the above-mentioned negative regulators of development forms more disorganised fruiting bodies than the single mutants and it has been shown that the proportions of cell populations *i.e.* the number of peripheral rods is perturbed in these mutants; the number of peripheral rods sporulating inappropriately outside of fruiting bodies increased with an increase

in the number of missing negative regulators of development (Fig. 1.17). It has been shown that the accumulation levels of MrpC/MrpC2 are perturbed also in the different developmental subpopulations of the negative regulator mutants e.g. *red* and *todK* in comparison to the wild type (Lee, PhD Thesis 2009).

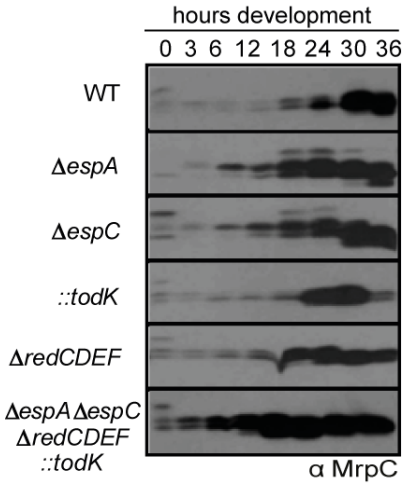

Fig 1.16 Analysis of MrpC accumulation pattern in the wild type (WT, DZ2) and mutants of negative regulators of development. Cell lysates from developmental samples containing equal proportions of cell culture for each strain were subjected to immunoblot analysis and probed with α-MrpC antibodies (Figure modified from Lee, PhD Thesis 2009).

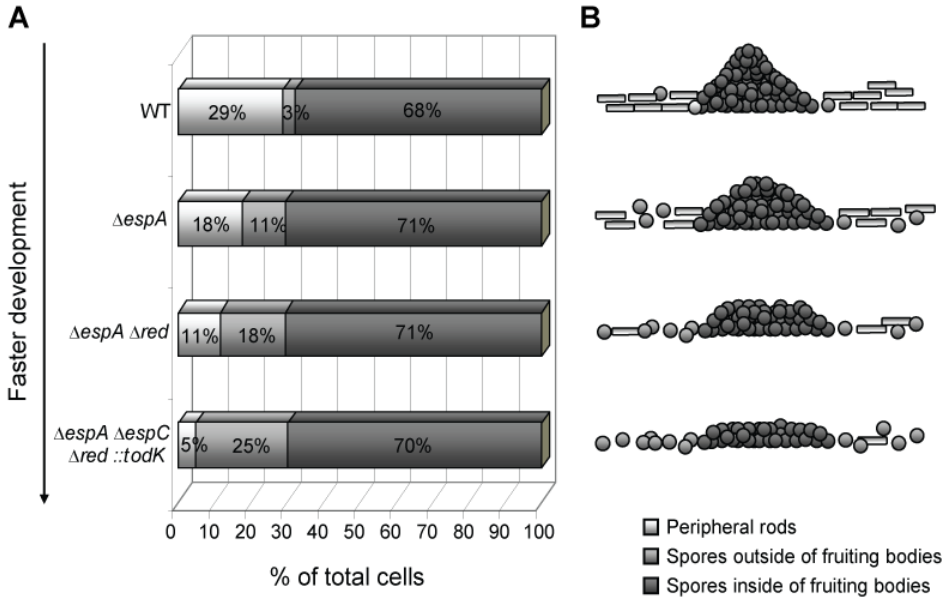

Fig 1.17 Analysis of developmental populations in negative regulator mutants A. Proportion of peripheral rods and spores in wild type (WT, DZ2), *ΔespA*, *ΔespA Δred*, and *ΔespA ΔespC Δred* todK mutants. Cells were grown in 24-well submerged culture plates and harvested after 5 days of development. The number of cells in each population was counted B. Schematic representation of the cell population in various mutants after 5 days (Figure modified from Lee, PhD Thesis 2009).

Moreover, as mentioned previously, the key transcription factor MrpC, a) accumulates heterogeneously in developmental subpopulations, the non-

aggregated and aggregated cell fractions (Fig 1.13); b) has been implicated in developmental lysis (Nariya & Inouye, 2008) and c) is necessary for aggregation and sporulation (Sun & Shi, 2001a).

In summary, all these facts were sufficient hints for MrpC to be a candidate to regulate alternate cell fates.

1.4 Aim of the study

Our hypothesis was that the highly regulated transcription factor MrpC may be the master of cell fate regulation in our model organism *M. xanthus* during its multicellular developmental program. Therefore, the aim of the present study was to characterize the role of MrpC in developmental cell fate determination. The specific questions addressed are as follows:

1) How is the differential accumulation of MrpC in developmental subpopulations regulated?

MrpC is known to accumulate differentially in the developmental subpopulations (Lee *et al*., 2012). To address if this differential accumulation was regulated at the level of transcription, I constructed a fluorescent transcriptional reporter and assayed *mrpC* promoter activity in the different subpopulations. My analysis revealed that the differential MrpC levels in the developmental subpopulations were regulated at the post-transcriptional level. Subsequently, I addressed if the differential accumulation of MrpC was regulated at the level of translation or a turnover.

2) How do levels of MrpC influence cell fates?

As mentioned previously, we think that the accumulation of MrpC has a link to cell fate. Therefore, I examined how MrpC distribution at the single cell level and over-expression/constitutive induction in developmental subpopulations could regulate the differentiation into distinct cell types.

3) How does the activity state of MrpC influence cell fates?

MrpC has been previously proposed to be regulated at the post-translational level and exist in various isoforms- MrpC2 and MrpC~P (Ueki & Inouye, 2003; Nariya & Inouye, 2005). To gain information on how MrpC activity influences cell fate segregation, I generated and analysed several mutants that produce only a particular activity state of MrpC (MrpC2 and MrpC/MrpC~P). Furthermore, the gene downstream of MrpC, which was found to be co-transcribed with MrpC in this study, was characterized to examine if its

interaction with MrpC could somehow affect MrpC activity and its role as a cell fate determinant.

4) Can a population-specific marker be assigned to developmental subpopulations?

As a second part of the project, I adopted a reverse approach in order to understand the role of MrpC in cell fate differentiation. I investigated if developmental subpopulations could be distinguished by means of a cell-specific marker. The ultimate goal was to later correlate the MrpC levels in a particular cell fraction. Thus, I analyzed the expression of two of the targets of MrpC and the aggregated cell fraction specific metalloprotease FibA in the developmental subpopulations. Additionally, I also investigated if the chromosome state of cells could be used as a marker to distinguish between cell populations.

2. RESULTS

2.1 Analysis of the differential accumulation of MrpC in developmental subpopulations

Mechanisms regulating control over the differentiation of *M. xanthus* cells into distinct cell types (clusters, lysed cells, spores and peripheral rods) during development are yet unknown. We hypothesized that the key transcription factor MrpC, necessary for the induction of aggregation and sporulation (Sun & Shi *et al*., 2001a) and previously implicated in mediating cell lysis (Nariya & Inouye, 2008) may act as a master cell fate regulator in *M*. *xanthus*. MrpC has been reported to accumulate heterogeneously in the non-aggregated and aggregated cell subpopulations (Lee *et al*., 2012) and its accumulation can be linked to cell fate segregation (Lee, PhD Thesis, 2009). As a first step, I set out to examine if the differential accumulation of this important developmental regulatory protein was due to differences in transcription.

2.1.1 MrpC is a negative autoregulator

Cell-fate specific promoter fusions to fluorescent proteins have been generated in the past to track individual cell fates in heterogeneous cell populations (Vlamakis *et al*., 2008) at the transcriptional level. To look at the *mrpC* promoter activity in the separated cell populations, I employed a P_{mrpC}-*mCherry* construct containing the promoter region of *mrpC* (334 bp upstream of and including the *mrpC* start codon; P_{mrpC}) fused to the second codon of the gene mCherry (P_{mrpC}-*mCherry*).

To first test whether the reporter was working appropriately, the construct was inserted at the exogenous Mx8 phage attachment (*attB)* site in the wild type and *ΔmrpC* strains. Cells grown under submerged developmental conditions were harvested, dispersed and the average fluorescence (normalised to the total protein) was measured through a developmental time course using a plate reader (Fig. 2.1). *mrpC* expression was upregulated; ~10 fold in the wild type and even higher in the *ΔmrpC* strain.

In comparison to an earlier study (Sun & Shi *et al*., 2001a), the expression of *mrpC* was consistent in the wild type but contrasting in the *ΔmrpC* strain. Previously, no *mrpC* expression was observed in *ΔmrpC* strain and it was proposed that MrpC positively autoregulates its expression (Sun and Shi 2001a, Fig. 1.15B). My results, however, were in accordance with initial preliminary research (Mensch, Bachelor thesis, 2009) done in our lab and suggested that MrpC is a negative autoregulator.

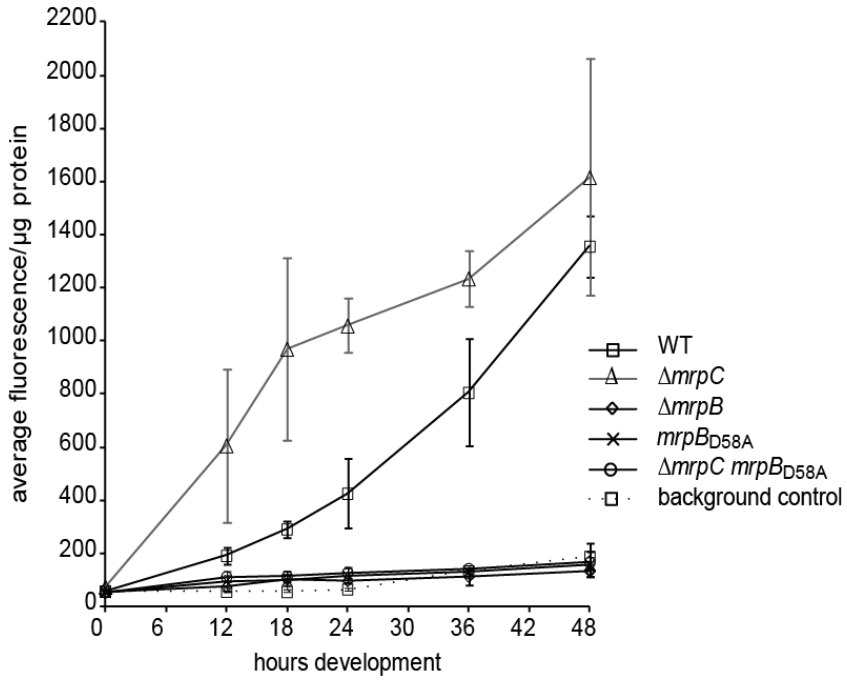

Fig. 2.1 Analysis of *mrpC* promoter activity. WT (DZ2), *ΔmrpC*, *ΔmrpB*, $mrpB_{D58A}$ and *ΔmrpC* $mrpB_{D58A}$ strains bearing the P_{mrpC}-*mCherry* construct were developed under submerged conditions in 24-well dishes, harvested and analyzed for mCherry fluorescence with a plate reader at the indicated time points. The line graph represents the average fluorescence normalised to the total protein. Error bars represent the standard deviation of three biological replicates. WT, wild type; Background control, wild type strain without the reporter construct.

From previous literature, it is known that MrpB, a response regulator, encoded by the *mrpAB* genetic locus, is essential for the expression of *mrpC* (Sun & Shi *et al*., 2001a). No *mrpC* expression was observed in a *ΔmrpB* strain which fails to develop like the *ΔmrpC* strain (Sun & Shi *et al*., 2001a). Additionally, an $mrpB_{D58A}$ strain carrying a mutation in the putative phosphor-accepting residue also fails to aggregate and sporulate (Sun and Shi 2001a). To confirm the previously published *mrpB* dependent regulation of *mrpC* and also that the above result was not an artefact of my reporter system, I generated *ΔmrpB,* $mrpB_{D58A}$ and *ΔmrpC* $mrpB_{D58A}$ mutant strains and examined their developmental phenotype under submerged conditions (Fig. 2.2). Subsequently, the P_{mrpC}-*mCherry* construct was transformed into all these mutant strains and *mrpC* expression was analyzed (Fig. 2.1) as described earlier.

The *ΔmrpC, ΔmrpB, mrpBD58A* strains failed to aggregate and sporulate as published previously (Sun and Shi 2001a) and the *ΔmrpC mrpBD58A* strain phenocopied them. The reporter construct in these backgrounds caused no alteration in the phenotype (data not shown). The WT *attB*::P_{mrpC}-*mCherry* strain developed ~3 h earlier in comparison to the parent strain lacking the reporter

that developed visible aggregates between 24 to 36 h during development. No significant fluorescence/*mrpC* expression was observed in the *ΔmrpB* reporter strain, as published previously (Sun and Shi 2001a), as well as in the $mrpB_{D58A}$ *and ΔmrpC* $mrpB_{D58A}$ reporter strains. Also, the fluorescence of all the parent strains lacking the reporter was negligible (data shown only for the wild type).

As a final proof of the functionality of the fluorescent reporter construct and the negative autoregulation of *mrpC,* the *mrpC* mRNA levels of 24-hour developed cell samples were directly assessed by a quantitative real-time qPCR (RT-qPCR) in the different strain backgrounds. The total *mrpC* mRNA levels were quantitated relative to the wild type using primers specific to the 5' UTR of the *mrpC* gene which is still present in the *ΔmrpC* strain (Fig. 2.3).

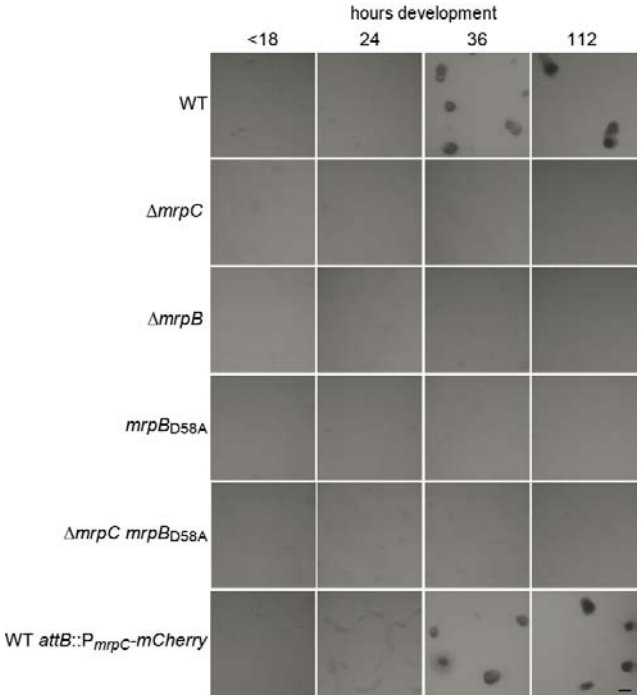

Fig. 2.2 Analysis of developmental phenotype under submerged culture. WT (DZ2), *ΔmrpC*, *ΔmrpB*, *mrpBD58A*, *ΔmrpC* $mrpB_{D58A}$, and WT *attB*::P_{mrpC}-*mCherry* strains were developed under submerged conditions in 24-well dishes. Pictures were recorded with a stereo microscope at the indicated time points during development. WT *attB*::P_{mrpC}-*mCherry*, wild type strain bearing the reporter construct; WT, wild type; scale bar, 100µm.

The levels of *mrpC* mRNA in the *ΔmrpC* strain were found to be at least 2.38 fold higher compared to the wild type, while no significant expression was observed in the *ΔmrpB, mrpBD58A and ΔmrpC mrpBD58A* strains. This result corresponds to the result of the plate reader experiment. One possible interpretation from these analyses could be that MrpC is a negative regulator of its own expression.

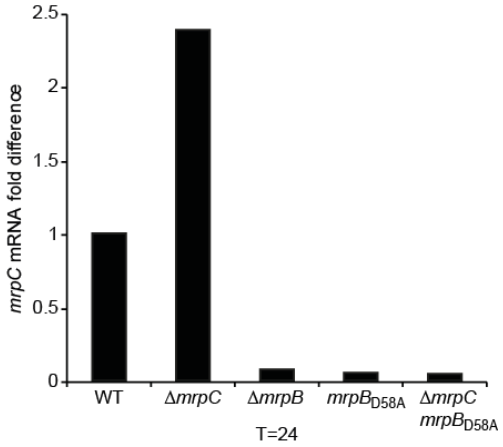

Fig. 2.3 Analysis of *mrpC* expression levels with quantitative real-time PCR. WT (DZ2), *ΔmrpC*, *ΔmrpB*, *mrpBD58A*, *ΔmrpC mrpB*$_{D58A}$ strains were developed in 16 ml submerged culture format and cells were harvested at 24 hours. RNA was isolated and reverse transcribed into cDNA. Primers specific to the 5' UTR of the *mrpC* gene were used for real-time qPCR analysis. The levels of *mrpC* transcript normalised to the 16S rRNA and expressed relative to the wild type (WT) are shown.

2.1.2 MrpC's differential accumulation is regulated at the post-transcriptional level, at least early during development

Having addressed that our reporter responds appropriately, I wanted to address the initial question of whether the differential accumulation of MrpC in developmental subpopulations is due to differences in transcription. Cells of the WT *attB*::P$_{mrpC}$-*mCherry* strain were developed under submerged culture, harvested and subjected to a low-speed centrifugation-based cell separation assay (Lee *et al.,* 2012) to separate the developmental subpopulations into aggregated and non-aggregated cell fractions at various time points (as described in section 4.3.5). Lysates prepared from equal numbers of cells in each fraction were subjected to both anti-MrpC and anti-mCherry immunoblot analysis (Fig. 2.4A). To examine the single cell mCherry accumulation in the two populations, dispersed cells from the two fractions were examined under a fluorescence microscope and the fluorescence intensity of single background-subtracted cells (n ≥ 250) was quantified (Fig. 2.4B).

In the immunoblot analysis, at 18 h, the non-aggregated fraction was enriched for MrpC while little was detected in the aggregated cell fraction, confirming previous results (Lee *et al*., 2011). At 36 h, late during development, MrpC was specifically upregulated in the aggregated cell fraction. The shorter, more active isoform of MrpC, MrpC2 could be detected as a band (~25kDa) that migrated just below the full length MrpC (~28kDa). mCherry was detected at nearly equal intensity in both the cell fractions at 18 h, however, at 36 h, a higher mCherry

signal was detected in the aggregated cell fraction consistent with a higher MrpC protein signal.

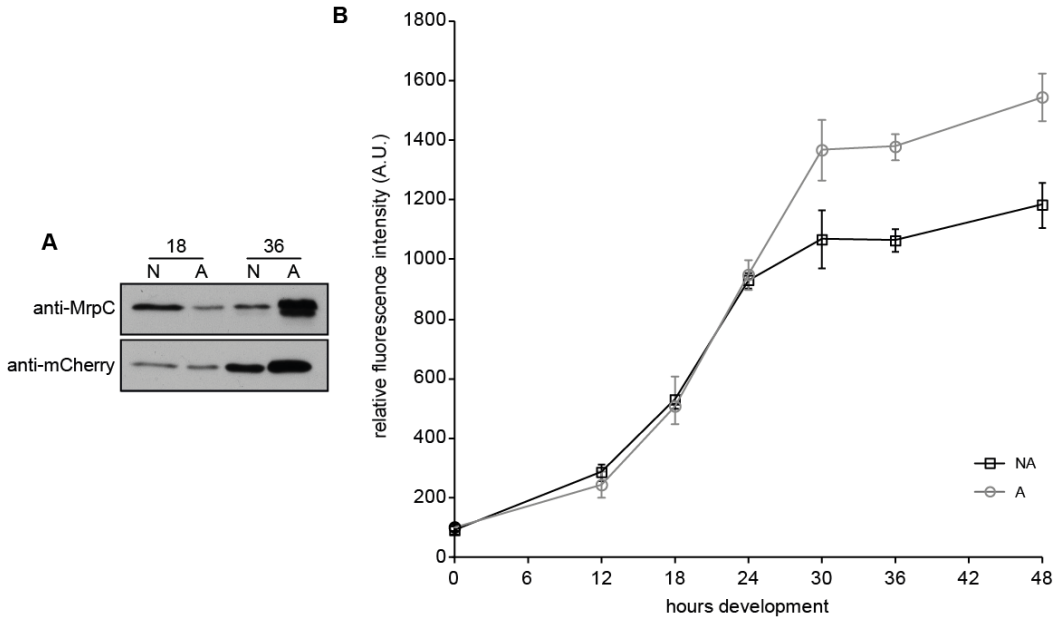

Fig. 2.4 Analysis of *mrpC* promoter activity in developmental subpopulations. A. Anti-MrpC (top) and anti-mCherry (bottom) immunoblot analysis of the WT *attB*::P_{mrpC}-*mCherry* strain. Cells were developed in 16 ml submerged culture format, harvested, and cell fractions were separated by differential centrifugation at the indicated time points. Lysates were prepared from equal numbers of cells in non-aggregated (NA) and aggregated (A) cells. Results from one assay are shown, but similar results were produced in biological replicates. B. Fluorescence quantification of non-aggregated and aggregated cell fractions. Cell in each fraction were dispersed, single cells (n≥ 100) were examined under a fluorescent microscope and the fluorescence intensity of single-background subtracted cells was quantified. The line graph represents the average mCherry fluorescence of the two populations at the indicated time points during development. Error bars represent the standard deviation of three biological replicates.

In the fluorescence analysis, the mCherry fluorescence intensity was found to be equal in both the cell fractions until 24 h of development after which it increased specifically in the aggregated cell fraction. This upregulation of *mrpC* transcription in the aggregated cell fraction could be correlated with the proposed role of MrpC2 as a positive autoregulator (Nariya & Inouye, 2006) late during development when the cells are present in mounds and eventually induced to sporulate. The results from the fluorescence analysis corresponded with the results from the immunoblot analyses. The single cell mCherry fluorescence variation between the two populations was only slightly different at 18 h. A very few cells fluoresced with higher intensity in the non-aggregated population. On the other hand, at 36 h, more cells fluorescing with higher intensities were recorded in the aggregated cell fraction which accounted for the overall higher mcherry signal (Fig. 2.5).

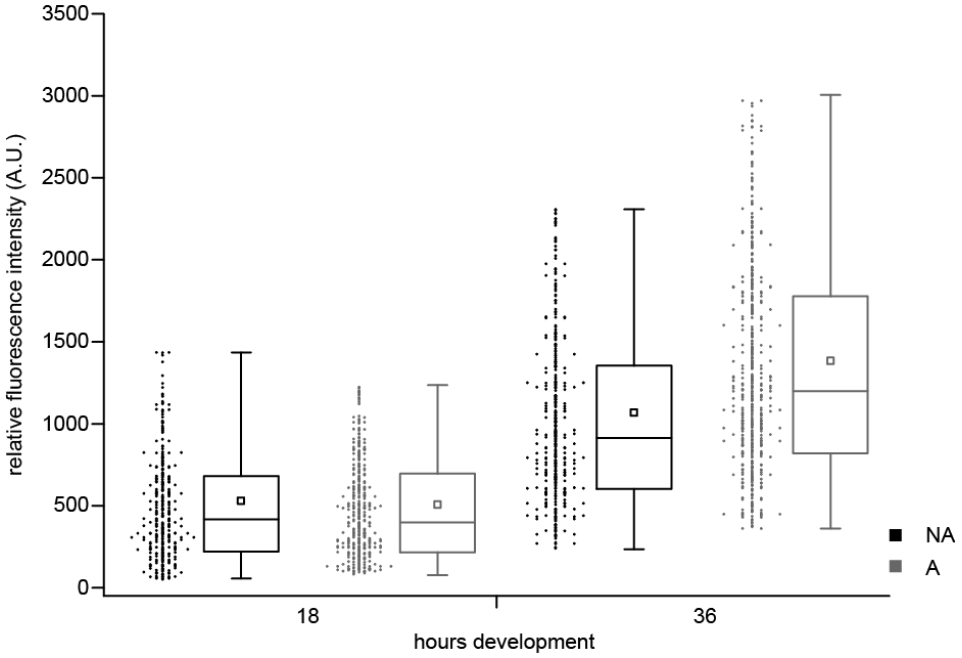

Fig. 2.5 Single cell analysis of *mrpC* promoter activity in developmental subpopulations. The box plot depicts the distribution of the mCherry fluorescence intensities of the non-aggregated (NA) and aggregated (A) population samples of Fig. 2.4B. The box and the whiskers represent 50% and 5-95% of the data, respectively. The middle line and the small square within the box represent the median and the average of the total population, respectively. The dots denote the intensity measurements of single cells (bin size 3). Data from the three biological replicates was pooled for the two cell fractions.

To further confirm *mrpC* expression in the separated cell populations, the *mrpC* mRNA levels were directly assessed by a quantitative real-time PCR (qRT-PCR) in the native wild type strain in order to rule out any artefacts due to the presence of an extra copy of the promoter in the fluorescent reporter strain. Cell populations were separated from the wild type strain developed in submerged culture for 18 and 36 h and the mRNA levels were quantitated by qRT-PCR using primers specific to the *mrpC* gene (Fig. 2.6).

At 18 h, the non-aggregated/aggregated cell fraction ratio of *mrpC* transcript was found to be ~1 (1.04). This meant that the average *mrpC* mRNA levels in the two cell fractions were equal. However, at 36 h, the non-aggregated/aggregated cell fraction ratio of *mrpC* transcript was found to be 0.44. This meant that the *mrpC* mRNA levels in the aggregated fraction were higher than the non-aggregated cell fraction. As a reference, the non-aggregated/aggregated MrpC protein ratio (as quantified from immunoblots) for the WT *attB*::P_{mrpC}-*mcherry* strain was also plotted along with the quantitated *mrpC* mRNA ratios. It should be mentioned that the WT *attB*::P_{mrpC}-*mcherry* strain accumulates MrpC in the developmental populations with the same timing and levels as the wild type (data not shown). At 18 h, the non-

aggregated/aggregated cell fraction ratio of MrpC was found to be ~3.34. This meant that the amount of protein in the non-aggregated fraction was higher than the aggregated fraction. At 36 h, the non-aggregated/aggregated cell fraction ratio of MrpC was found to be ~0.33. This meant that the MrpC levels in the aggregated fraction were higher than the non-aggregated cell fraction. To conclude, at 18 h, the differential MrpC accumulation in the two cell fractions did not result from differential *mrpC* transcription while at 36 h, differences in MrpC accumulation correlated with differences in transcription. The qRT-PCR results on the separated populations matched those obtained earlier with the immunoblot and fluorescence analysis of the *mrpC* reporter strain, thus strengthening the fact that the fluorescent reporter measures *mrpC* expression in the separated cell populations as in the wild type scenario.

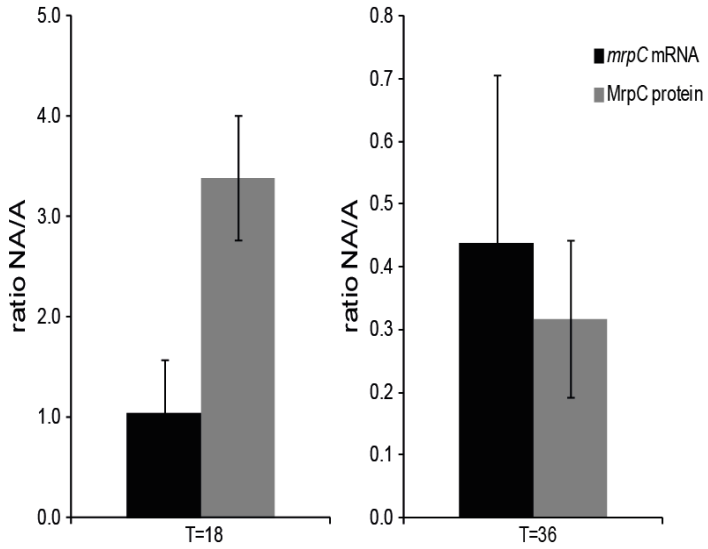

Fig. 2.6 Analysis of *mrpC* expression in developmental subpopulations of the wild type by quantitative real-time PCR. Wild type cells were developed in 16 ml submerged culture format and harvested at the indicated time points. RNA was isolated and reverse transcribed into cDNA. *mrpC* gene specific primers were used for real-time PCR analysis. To control for efficiency of RNA extraction and cDNA generation, the levels of *mrpC* mRNA were normalised to *E.coli* 16S rRNA isolated from *E. coli* cells spiked in proportion to the number of *M. xanthus* cells in each fraction (see methods). The graph depicts the *mrpC* mRNA NA/A ratio (NA, non-aggregated cells; A, aggregated cells) for the wild type as quantitated by qRT-PCR and the MrpC protein NA/A ratio for the WT *attB*::P_{mrpC}-*mcherry* strain as quantitated from immunoblots for comparison. Error bars represent the standard deviation of three biological replicates.

In summary, these data indicated that the *mrpC* transcription is similar in both populations, early during development (18 hours) but there is an upregulation of transcription late during development (36 hours) specifically in the aggregated cell fraction. Although MrpC accumulates heterogeneously in cell subpopulations, this difference in accumulation early during development (18 hours) is not due to transcriptional differences.

2.2 Analysis of the post-transcriptional regulation of MrpC

From the results presented above (section 2.1.2), it was clear that the differential accumulation of MrpC in developmental subpopulations is due to post-transcriptional regulation. This meant that the heterogeneous accumulation of MrpC in the non-aggregated and the aggregated subpopulations must arise either due to differences in translation or a protein turnover. Therefore, I set out to address the post-transcriptional regulation of MrpC's differential accumulation as described in the following two sections.

2.2.1 MrpC's differential accumulation is likely not due to translational regulation

To address whether MrpC's differential accumulation in the developmental subpopulations was regulated at the level of translation, I generated a reporter construct to measure the relative level of *mrpC* translation *vs* transcription in the two developmental subpopulations *in vivo*. This reporter system combined a translational reporter (mCherry fused to the first 180 amino acids of MrpC; P_{mrpC}-$mrpC_{180}$-*mCherry*) followed by a transcriptional reporter (Gfp fused to the ribosome binding site of the characterized *pilA* transcript (Wu & Kaiser, 1997); rbs_{pilA}-*gfp*). The principle behind such a reporter was to be able to measure the ratio of mCherry to Gfp signal per cell in the two developmental subpopulations. The mCherry signal is a measure of both transcription and translation while the Gfp signal is a measure of transcription alone as Gfp would be translated under the $rbs_{pilA,}$ independent of mCherry. In the case of no translational regulation, the mCherry/Gfp ratio would be equal between the two cell populations. However, in the case of a translational upregulation in the non-aggregated cell fraction (or a translational repression in the aggregated cell fraction), the mCherry to Gfp signal ratio would be higher in the non-aggregated cell fraction relative to the aggregated cell fraction.

To confirm that the two reporters were functioning correctly, I generated two additional constructs as a control. In one, the start codon of *mrpC* was mutated (ATG to CAT) to confirm that Gfp production is not dependent on mCherry production. In the second, the rbs_{pilA} preceding the *gfp* was mutated (AGGACC to CCTCCC) to confirm that translation of mCherry is independent of Gfp. Each of these constructs was inserted into the wild type strain at the *attB* site.

In order to first confirm if the system works as expected, the two control strains were developed under submerged conditions. Cells were harvested and the non-aggregated and aggregated subpopulations were separated at 18 hours of development. Lysates prepared from equal numbers of cells in each fraction were subjected to both anti-mCherry and anti-Gfp immunoblot (Fig. 2.7A). To

examine the single cell mCherry and Gfp accumulation in the two populations, dispersed cells from the two fractions were examined under a fluorescence microscope and the fluorescence intensity of single background-subtracted cells (n ≥ 100) was quantified (Fig. 2.7B).

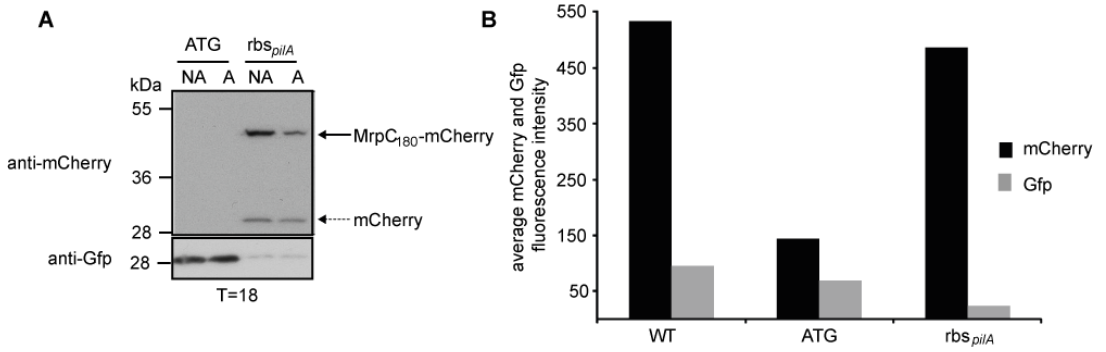

Fig. 2.7 Analysis of the controls for the translational reporter strain. A. Anti-mCherry (top) and anti-Gfp (bottom) immunoblot analysis of the control translational reporter strains. Cells were developed in 16 ml submerged culture format, harvested and cell fractions were separated at 18 hours. Lysates were prepared from equal numbers of cells in non-aggregated (NA) and aggregated (A) cells. ATG, control strain with the *mrpC* start codon mutated; *rbs$_{pilA}$*, control strain with the *pilA* ribosome binding site mutated. B. Fluorescence analysis. The non-aggregated (NA) and aggregated (A) cell fractions of the two control strains harvested as described in A were dispersed, single cells were examined under a fluorescent microscope. The mCherry and Gfp fluorescence intensity of single-background subtracted cells (n≥ 100) was quantified. The column graph represents the average per cell mCherry and Gfp fluorescence intensity of the total cell population calculated by averaging the individual values of the two cell fractions. For reference, the respective values for the WT *attB*::P$_{mrpC}$-*mrpC*$_{180}$-*mCherry-gfp* strain (Fig. 2.9) are also depicted on this graph.

In the immunoblot analysis, no mCherry signal could be detected in the control strain with the mutated *mrpC* start codon while abundant Gfp levels could be detected (Fig. 2.7A). These results suggested that production of Gfp was independent of mCherry production. Furthermore, only minor levels of Gfp could be detected in the control strain with the mutated *rbs$_{pilA}$* suggesting that Gfp was not significantly translationally coupled to MrpC$_{180}$-mCherry and the mCherry levels were not perturbed. This result was consistent with the result of the fluorescence analysis as in the control strain with the mutated *mrpC* start codon (ATG), the average Gfp fluorescence was similar to the wild type (WT *attB*::P$_{mrpC}$-*mrpC*$_{180}$-*mCherry-gfp*) strain while the mCherry fluorescence dropped significantly. Additionally, in the mutated *rbs$_{pilA}$* control strain (*rbs$_{pilA}$*), the average mCherry fluorescence was comparable to that of the wild type but the Gfp fluorescence was barely detectable. Hence, these results confirmed that mCherry and Gfp were translated independent of each other in the translational reporter construct and it could be used to address the translational regulation of MrpC.

As a first step, the developmental phenotype of the WT *attB*::P$_{mrpC}$-*mrpC*$_{180}$-*mCherry-gfp* strain was assessed under submerged conditions (Fig 2.8). The reporter strain and the wild type both developed visible aggregates at ~27h.

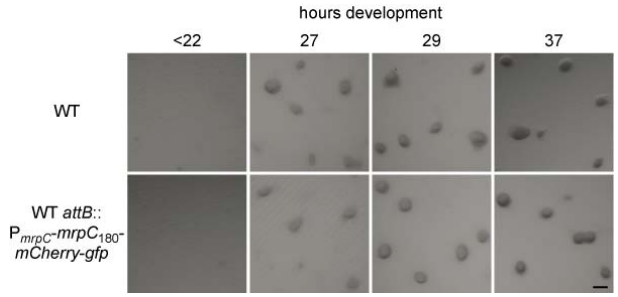

Fig. 2.8 Developmental phenotype analysis of the translational reporter strain. WT (DZ2) and WT *attB*::P$_{mrpC}$-*mrpC*$_{180}$-*mCherry-gfp* strains were developed under submerged conditions in 24-well dishes. Pictures were recorded with a stereo microscope at the indicated time points during development. WT, wild type; scale bar, 100µm.

Having confirmed that the translational reporter construct causes no alteration in the developmental phenotype, I proceeded to address the initial question of whether MrpC production is translationally regulated. The WT *attB*::P$_{mrpC}$-*mrpC*$_{180}$-*mCherry-gfp* strain was developed in submerged culture and subpopulations were separated at 18 and 36 hours. Immunoblot analysis using anti-MrpC, anti-mCherry and anti-Gfp antibodies (Fig 2.9A) as well as fluorescence analysis (Fig 2.9B) was performed as previously explained for the control strains.

In the immunoblot analysis, the MrpC antibody detected two distinct bands, the ~48 kDa MrpC$_{180}$-mCherry fusion protein and the ~28 kDa native MrpC. MrpC accumulation was detected to be nearly equal in the non-aggregated and aggregated cell fractions at 18 h, however, at 36 h, MrpC was found to be specifically enriched in the aggregated cell fraction as expected. The mCherry antibody also detected two bands like the MrpC antibody. The ~48 kDa corresponded to the MrpC$_{180}$-mCherry fusion protein. The lower ~28 kDa band was mCherry that was likely cleaved from the fusion protein as it migrated exactly at the same size as native mCherry. Since, this cleavage product was detected in the subpopulations in proportional amounts as the fusion product; it was assumed that this did not interfere in the analysis. At 18 h, ~1.2 fold higher mCherry signal was detected in the non-aggregated cell fraction compared to the aggregated cell fraction and at 36 h, the mCherry signal was ~5 fold higher in the aggregated cell fraction in comparison to the non-aggregated cell fraction. The anti-Gfp antibody detected a ~28 kDa band as expected from the estimated molecular mass of Gfp. The Gfp signal at 18 h was almost equal in the two cell fractions while at least 2 fold higher in the aggregated cell fraction at 36 h.

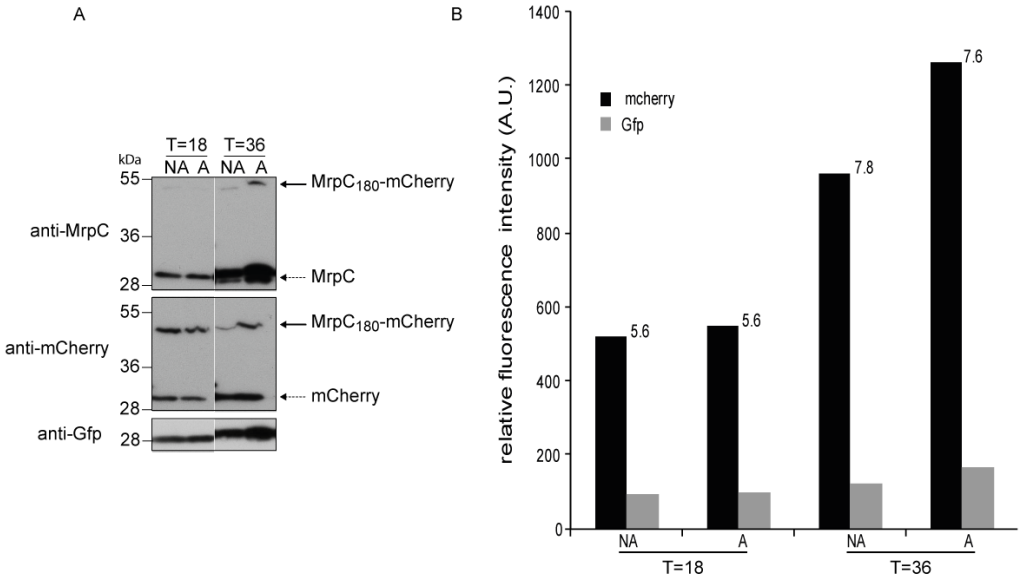

Fig. 2.9 Analysis of the translational reporter strain. A. Anti-MrpC (top), anti-mCherry (middle), anti-Gfp (bottom) immunoblot analysis of the WT *attB*::P$_{mrpC}$-*mrpC*$_{180}$-*mCherry-gfp* strain. Cells were developed in 16 ml submerged culture format, harvested and cell fractions were separated at 18 and 36 h. Lysates were prepared from equal numbers of cells in non-aggregated (NA) and aggregated (A) cells. B. Fluorescence analysis. The non-aggregated (NA) and aggregated (A) cell fraction harvested as described in A were dispersed, single cells (≥ 100) were examined under a fluorescent microscope and the mCherry and Gfp fluorescence intensity of single-background subtracted cells was quantified. The bar graph represents the average mCherry and Gfp fluorescence and the data labels on top of the bars represent the per cell mCherry/Gfp fluorescence ratio.

From the fluorescence analysis, it was observed that the average fluorescence intensity for both mCherry and Gfp in the non-aggregated and aggregated cell populations was almost similar at 18 h but was higher in the aggregated cell fraction at 36 h of development. These results were consistent with the immunoblot results with mCherry and Gfp antibodies. The average mCherry to Gfp ratio per single cell was nearly equal for both populations at 18 and 36 h. Additionally, in the single cell population analysis, the mCherry to Gfp ratio single cell profiles was also not very different for cells of the non-aggregated and aggregated cell fractions both at 18 and 36 hours (Fig. 2.10).

Taken together, these results suggested that translational differences might not account for the differential accumulation of MrpC in the two developmental subpopulations.

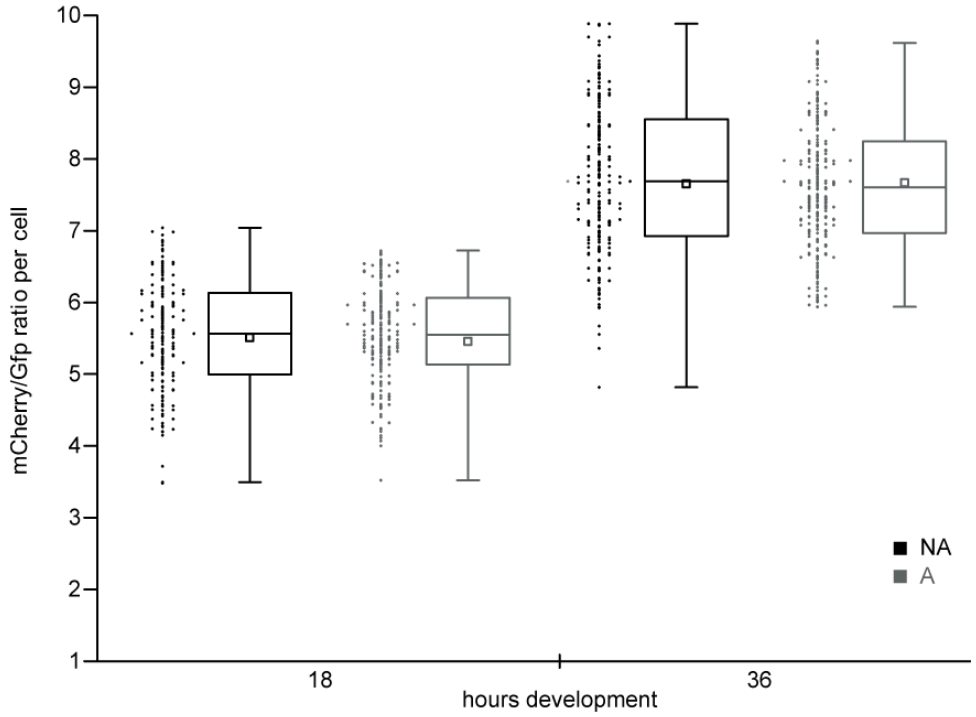

Fig. 2.10 Single cell analysis of developmental subpopulations of the WT *attB*-P$_{mrpC}$-*mrpC*$_{180}$-*mCherry-gfp* translational reporter strain. Cell samples are as described in Fig. 2.9. Single cells of the non-aggregated (NA) and aggregated (A) subpopulations were examined under a fluorescence microscope. The mCherry and Gfp fluorescence intensity of single background-subtracted cells ($n \geq 100$) was quantified and the per cell mCherry/Gfp ratio distribution is depicted by box plot. The box and the whiskers represent 50% and 5-95% of the data, respectively. The middle line and the small square within the box represent the median and the average of the total population, respectively. The dots denote the intensity measurements of single cells (bin size 1).

2.2.2 MrpC's differential accumulation appears to be due to a protein turnover event

Often, the level of protein present in a cell is regulated by the mechanism of controlled proteolysis so as to ensure efficient control over regulatory processes. It has been demonstrated that the accumulation MrpC early during development is controlled by proteolysis in the total cell population (Schramm *et al*., 2012). Thus, my second question was whether MrpC's differential accumulation early during development a result of MrpC turnover in the aggregating cell population. To address this, I adapted a protein turnover assay that had been already established in the lab. Wild type cells were developed in submerged culture for 18 hours and the non-aggregated and aggregated cell fractions were separated. The two cell fractions were blocked for *de novo* protein synthesis by the addition of chloramphenicol, and the MrpC protein levels in the two cell fractions were examined over a period of 40 minutes (Fig. 2.11A). As controls, the two cell fractions were simultaneously also treated with

a protease inhibitor cocktail to block protein degradation or with ethanol as a control for the chloramphenicol treatment.

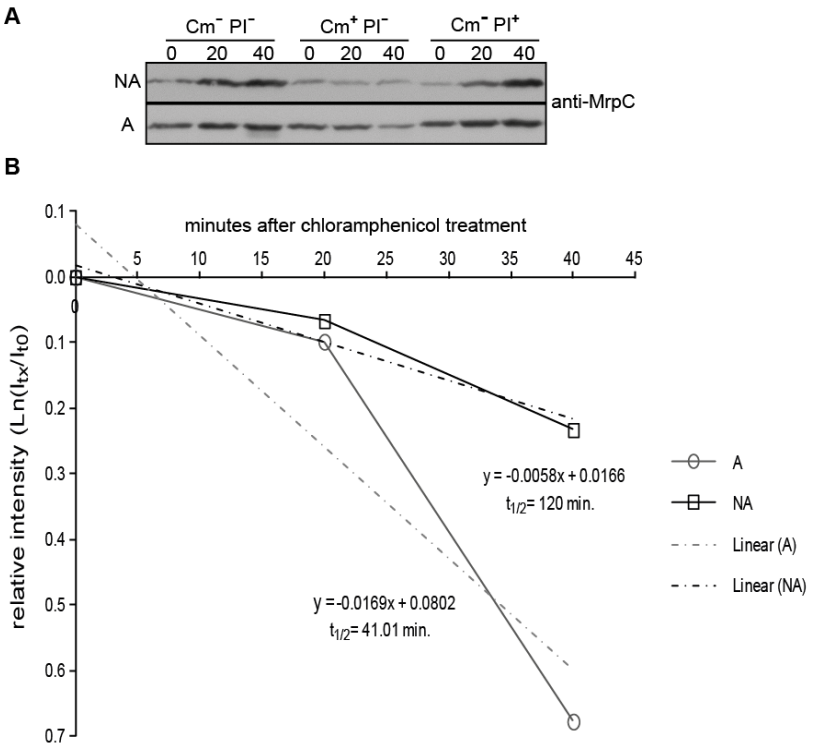

Fig. 2.11 Analysis of MrpC turnover in the developmental subpopulations. A. Chloramphenicol chase of MrpC. Wild type (DZ2) cells were developed in 16-ml submerged culture format for 18 hours. Cells were harvested from three plates and the two cell fractions separated from each plate were pooled together and resuspended in MMC buffer to have an equivalent number of cells in both the fractions. Each fraction was treated either with ethanol, chloramphenicol, or a protease inhibitor cocktail for the indicated minutes. Lysates with equal number of cells in both fractions were subjected to anti-MrpC immunoblot. NA, non-aggregated fraction; A, aggregated fraction. Cm, chloramphenicol; PI, protease inhibitor ; -/+, with/without B. Calculation of half-life ($t_{1/2}$) of MrpC. Chloramphenicol chase experiment as indicated in A (Cm^+PI^-) was performed and the MrpC band intensity for each time point was normalized to T=0 in the respective sample. The natural log of the average intensities was plotted *vs.* the minutes of chloramphenicol treatment. The slope of a linear fit of the data was used to calculate the MrpC half-life in wild type cells as described in materials and methods.

In the non-aggregated cell fraction, in the cell samples without treatment, the MrpC levels increased. In contrast, in the cell samples treated with chloramphenicol, a slight decrease in MrpC protein was observed over a period of 40 minutes. In the aggregated cell fraction, in the cell samples without treatment, the MrpC levels increased as expected. In the chloramphenicol treated aggregated cells, a gradual decrease in MrpC protein could be observed over time. The half-life of MrpC was calculated to be 120 minutes in the non-aggregated cell fraction and 41 minutes in the aggregated cell fractions (Fig. 2.11B). These results suggested that MrpC was only very slightly turned over in

the non-aggregated cell fraction but the MrpC protein in the aggregated cell fraction was subject to a strong turnover.

To conclude, the heterogeneous accumulation of MrpC in the developmental subpopulations is not due to transcriptional or translational differences between the two cell populations but instead due to a protein turnover event that occurs specifically in the aggregated cell fraction.

2.3 Analysis of single cell distribution of MrpC in developmental populations

We envisioned that the non-aggregated cell fraction, which is enriched in MrpC early during development (18 hours), is a broadly heterogeneous population consisting of cells that are destined to aggregate, undergo lysis or become peripheral rods through the course of development. As cells of this population progress through development, the MrpC levels drop at later stages of development i.e. by the end of 36 hours. Therefore, it was worth to examine how single cell accumulation of MrpC in this heterogeneous population could influence cell fate segregation.

2.3.1 Tagging MrpC with mCherry alters its activity and/or turnover

To examine the single cell accumulation of MrpC in the developmental subpopulations, I generated an MrpC protein fusion construct containing the *mrpC* promoter and the full length *mrpC* gene fused via a Gly-Gly-Gly-Gly-Ser-Gly-Gly-Thr linker to the second codon of the fluorescent protein mCherry. This construct was integrated at the *attB* site in the wild type and *ΔmrpC* strain. As a first step, the phenotype of these strains was characterized under submerged developmental conditions (Fig. 2.12). In the WT *attB*::P_{mrpC}-*mrpC-mCherry* strain, visible aggregates were first observed at 24 h, approximately 3 h earlier than the wild type. The *ΔmrpC* strain did not develop, while the *ΔmrpC attB*::P_{mrpC}-*mrpC-mCherry* strain formed visible aggregates at ~20 h and developed even earlier than the WT *attB*::P_{mrpC}-*mrpC-mCherry* strain suggesting that tagging of mCherry to MrpC likely interfered with its function and/or degradation.

Next, to examine whether these strains bearing the protein fusion construct produced stable protein, lysates were prepared from developmental samples and subjected to both anti-MrpC and anti-mCherry immunoblot (Fig 2.13). In the wild type, no MrpC could be detected at T=0. The ~28 kDa MrpC band could be first detected at ~6 h and the signal continued to increase through development. No protein was detected with mCherry antibody. In the WT *attB*::P_{mrpC}-*mrpC*-

mCherry strain, bands of three different sizes could be detected on the MrpC immunoblot. The ~60 kDa band, corresponded to the full length MrpC protein (248 amino acid residues) fused to mCherry; the ~40 kDa band likely corresponded to a degraded/clipped form of the fusion protein and the third, ~28 kDa band was that of the native MrpC. Summing up the three band intensities, more MrpC was present at 6 h in comparison to the wild type. After a drop between 6 to 12 h, the level increased between 12 and 27 h after which, it was almost double than in the wild type. A linear increase in signal from 0 till 27 h was observed with the mCherry antibody that detected only the full length fusion protein at ~60 kDa. The *ΔmrpC attB*::P_{mrpC}-*mrpC-mCherry* strain when compared to the wild type also had more MrpC starting at 6 h. The protein only increased through development with the highest levels detected at 27 h. A linear but even earlier mCherry accumulation could be detected in comparison to the wild type bearing the protein fusion.

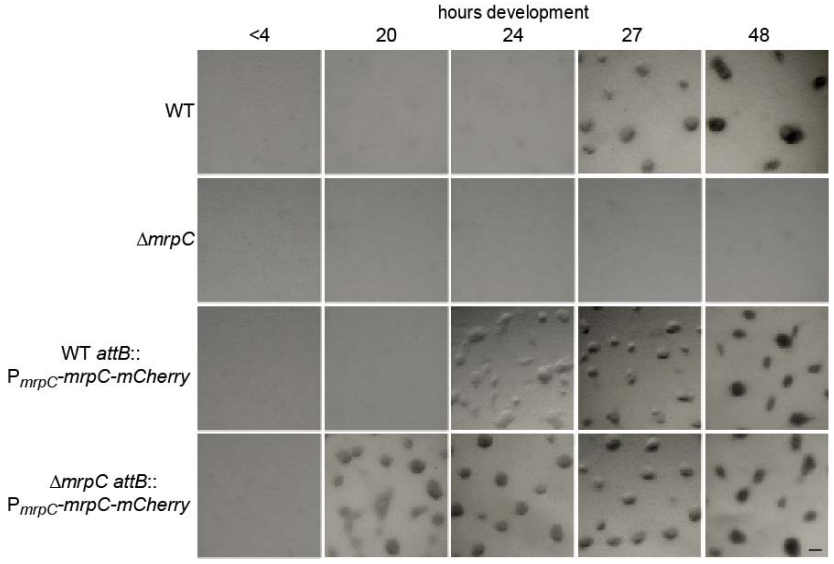

Fig. 2.12 Developmental phenotype analyses of strains bearing the MrpC-mCherry protein fusion construct. WT (DZ2), *ΔmrpC*, WT *attB*::P_{mrpC}-*mrpC-mCherry* and *ΔmrpC attB*::P_{mrpC}-*mrpC-mCherry* strains were developed under submerged conditions in 24-well dishes. Pictures were recorded with a stereo microscope at the indicated time points during development. WT, wild type; scale bar, 100µm.

Although the strains bearing the MrpC fusion construct had an early developmental and protein accumulation phenotype, I examined if they could still prove useful to analyze the single cell distribution of MrpC in the separated cell fractions during development. Both the strains bearing the MrpC-mCherry fusion and the wild type were developed under submerged conditions and the non-aggregated and aggregated cell fractions were separated at 6, 12 and 18 h of development. Lysates prepared from equal numbers of cells in each fraction were subjected to both anti-MrpC and anti-mCherry immunoblot (Fig 2.14). Simultaneously, to examine the single cell mCherry accumulation in the two

populations, dispersed cells from the two fractions were examined under a fluorescence microscope and the fluorescence intensity of single background-subtracted cells (n ≥ 100) was quantified (Fig 2.15).

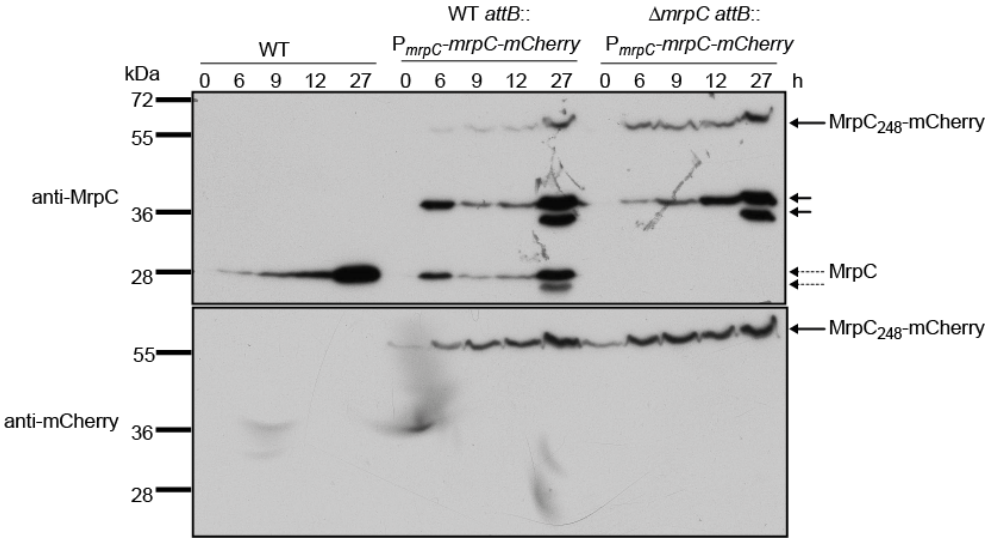

Fig. 2.13 Analysis of protein accumulation in the strains bearing the MrpC-mCherry protein fusion construct. Anti-MrpC (top), anti-mCherry (bottom) immunoblot analysis. Cells of the WT (DZ2), *ΔmrpC*, WT *attB*::P$_{mrpC}$-*mrpC-mCherry* and *ΔmrpC attB*::P$_{mrpC}$-*mrpC-mCherry* strains were developed in 16 ml submerged culture format and harvested by TCA precipitation at the indicated hours of development. Lysates were prepared and 20 µg total protein was analyzed.

In the immunoblot analysis, in the wild type strain, both at 6 and 12 h in development, the non-aggregated fraction was specifically enriched for MrpC while little was detected in the aggregated cell fraction. At 18 h, the accumulation was heterogeneous as for 6 and 12 h, but the difference in MrpC accumulation between the non-aggregated and aggregated cell fraction was reduced. This could be due to the day-to-day variability in the development of the wild type. In the strains bearing the protein fusion, MrpC antibody detected 3 distinct bands (as explained earlier) with the difference that the middle, ~40 kDa band was only very faint in this analysis. This could be attributed to the fact that the time needed to harvest separated cell populations was greater than that needed to harvest total cells. In the former case, the ~40 kDa degradation product was likely specifically proteolysed completely. In the WT *attB*::P$_{mrpC}$-*mrpC-mCherry* strain, the accumulation pattern of MrpC in the two cell populations was similar to the wild type at all time points. The *ΔmrpC attB*::P$_{mrpC}$-*mrpC-mCherry* strain showed higher levels of the fusion protein at 6 and 12 h, the proportions between the two populations being less heterogeneous in comparison to the other two strains. The mCherry signal in the developmental subpopulations of the protein fusion bearing strains could be correlated with the respective MrpC signal, while no signal was detected for the wild type, as expected. In the mCherry immunoblot, apart from the ~60 kDa band of the fusion protein, a second faint band could be detected at ~30 kDa.

This might correspond to the mCherry protein which could be produced as a result of clipping of mCherry from the C-terminus of the MrpC fusion protein and was detected in proportions similar to the fusion protein in the non-aggregated and aggregated cell fractions. For measuring the single cell mCherry fluorescence of the separated cell fractions, the WT *attB*::P_{mrpC}-*mrpC-mCherry* strain was analyzed (Fig 2.14). At all time points, the average mcherry fluorescence signal was nearly equal in the non-aggregated and aggregated subpopulations (Fig 2.15). This data did not correlate with the differential MrpC-mCherry accumulation recorded in the immunoblot analysis suggesting that the fluorescence of the fusion protein was likely quenched.

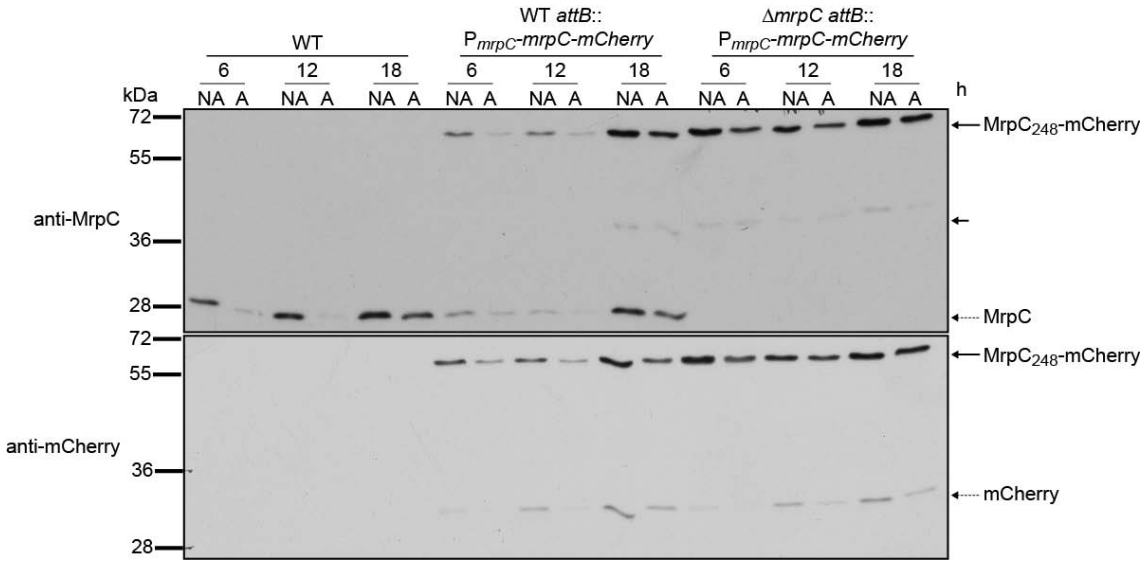

Fig. 2.14 Analysis of protein accumulation in the developmental subpopulations of the MrpC-mCherry protein fusion strains. Anti-MrpC (top), anti-mCherry (bottom) immunoblot analysis. WT (DZ2), *ΔmrpC*, WT *attB*::P_{mrpC}-*mrpC-mCherry* and *ΔmrpC attB*::P_{mrpC}-*mrpC-mCherry* strains were developed in 16 ml submerged culture format, cells were harvested and cell fractions were separated at the indicated time points. Lysates were prepared from equal numbers of cells ($4x10^7$) in non-aggregated (NA) and aggregated (A) fraction (short arrow on the anti-MrpC immunoblot represents the faint ~40 kDa degradation product).

Apart from the *attB* site MrpC fusion strains, strains carrying either a C- or an N-terminal mCherry fusion to MrpC at the endogenous locus were generated and analyzed. These also displayed a similar early developmental phenotype (data not shown).

Taken together, these data suggested that tagging MrpC either at the C- or N-terminus interferes with its activity and/or turnover, thereby having an effect on the phenotype and MrpC accumulation. Hence, I concluded that the MrpC-mcherry protein fusion was not useful to address the single cell accumulation of MrpC because the mCherry fluorescence did not correlate with the MrpC accumulation pattern in the non-aggregated and aggregated cell fractions.

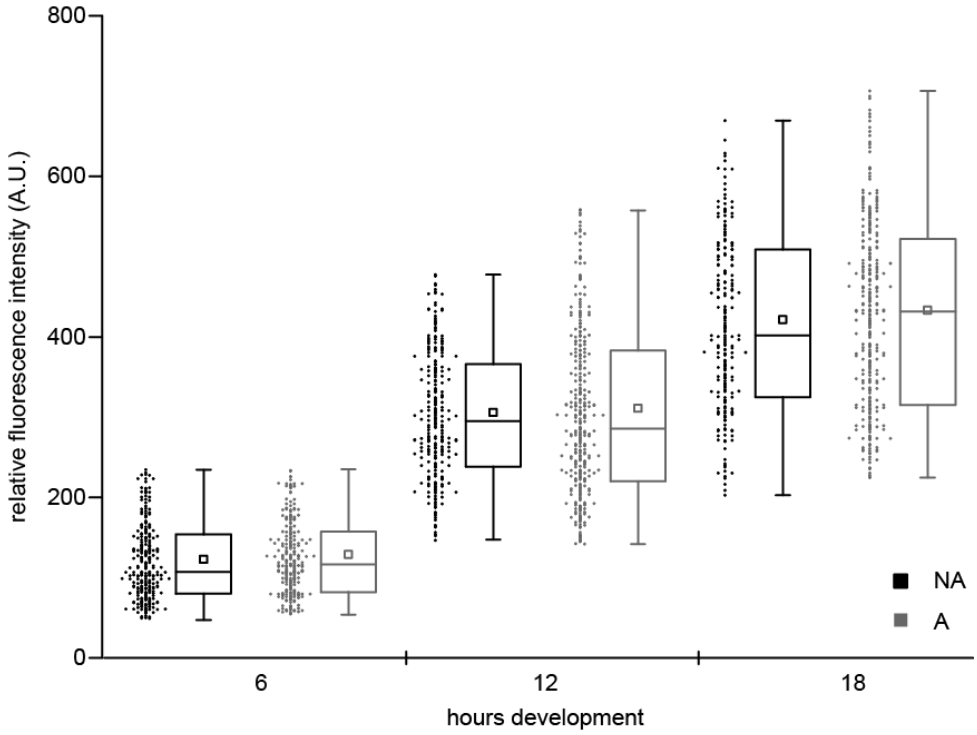

Fig. 2.15 Single cell mCherry analysis of developmental subpopulations of the WT *attB*::P$_{mrpC}$-*mrpC-mCherry* strain. Cell samples are as described in Fig. 2.14. Single cells of the non-aggregated (NA) and aggregated (A) subpopulations were examined under a fluorescence microscope. The fluorescence intensity of single background-subtracted cells ($n \geq 100$) was quantified and the distribution of mCherry intensities of cells is depicted in the box plots. The box and the whiskers represent 50% and 5-95% of the data, respectively. The middle line and the small square within the box represent the median and the average of the total population, respectively. The dots denote the intensity measurements of single cells (bin size 1).

2.4 Over-expression of MrpC to understand its effect in cell fate determination

The fact that the levels of MrpC were important for development and that accumulation of MrpC was linked to cell fates was evident from the inappropriate sporulation of peripheral rods in the negative regulator mutants (Lee, PhD Thesis, 2009). Therefore, I wanted to uncouple the production of MrpC from its own regulation and over-express it in order to understand how it affects cell population distribution during development. I expected to observe an early developmental phenotype associated with an imbalance in the distribution of the cell populations. The induction of MrpC was attempted using two tools (as described below) that have been successfully used in the past to achieve inducible expression of genes in *Myxococcus*.

2.4.1 MrpC could not be induced under the *pilA* promoter

The first approach to achieve the constitutive induction of *mrpC* was based on the *pilA* promoter. This well-characterized promoter, responsible for the induction of pilin subunits of the type IV pili in *M. xanthus*, was chosen as it is constitutively expressed at high levels both during growth and development (Wu & Kaiser, 1997). The *mrpC* gene was cloned in front of the *pilA* promoter (189 bp upstream of and including the *pilA* start codon; P_{pilA}-*mrpC*), and the plasmid containing this construct was inserted at the chromosomal *attB* site in the wild type and *ΔmrpC* strains. Simultaneously, as a control for the P_{pilA}-*mrpC* construct, I also cloned *mrpC* under its own promoter (P_{mrpC}-*mrpC*) and the plasmid containing this construct was inserted at the *attB* site in the wild type and *ΔmrpC* strain.

The WT *attB*::P_{pilA}-*mrpC*, *ΔmrpC attB*::P_{pilA}-*mrpC*, WT *attB*::P_{mrpC}-*mrpC*, *ΔmrpC attB*::P_{mrpC}-*mrpC*, WT and *ΔmrpC* strains were developed in submerged culture to assay the developmental phenotype (Fig. 2.16).

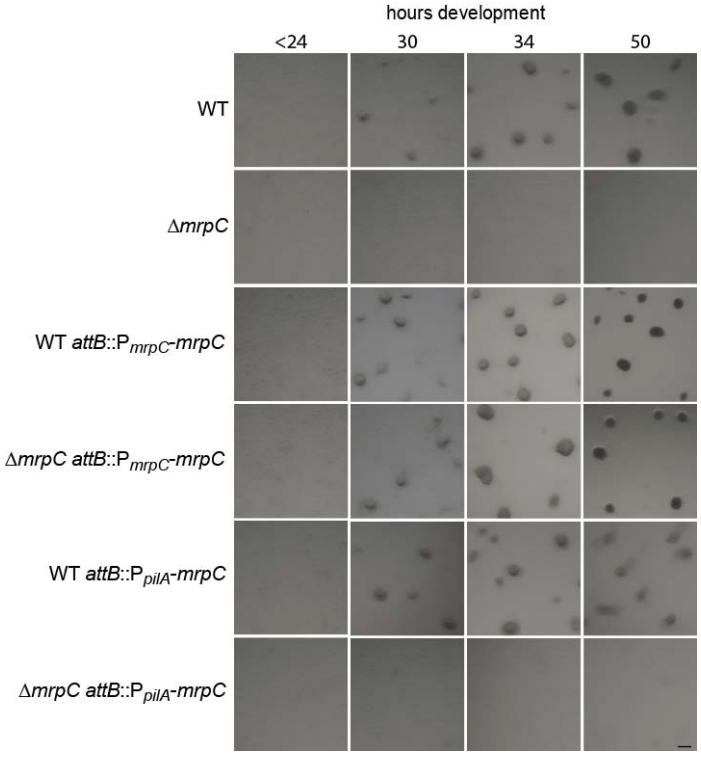

Fig. 2.16 Developmental phenotype analysis of the P_{pilA}-*mrpC* strains. WT (DZ2), *ΔmrpC*, WT *attB*::P_{mrpC}-*mrpC*, *ΔmrpC attB*::P_{mrpC}-*mrpC*, WT *attB*::P_{pilA}-*mrpC*, and *ΔmrpC attB*::P_{pilA}-*mrpC* strains were developed under submerged conditions in 24-well dishes. Pictures were recorded with a stereo microscope at the indicated time points during development. WT, wild type; scale bar, 100µm.

While all other strains developed visible aggregates between 24-30 h like the wild type, the *ΔmrpC* and the *ΔmrpC attB*::P_{pilA}-*mrpC* strains failed to develop at all. Importantly, the *ΔmrpC attB*::P_{mrpC}-*mrpC* strain could be complemented by expressing *mrpC* from its own promoter. Next, in order to examine the MrpC production in the above strains, cell lysates were prepared from 24 h old

developmental samples and subjected to immunoblot analysis with anti-MrpC antibody. MrpC was found to be present in equivalent amounts in the wild type, WT *attB*::P$_{pilA}$-*mrpC* and WT *attB*::P$_{mrpC}$-*mrpC* strains, while ~1.5 fold more MrpC was detected in the *ΔmrpC attB*::P$_{mrpC}$-*mrpC* strain. This was likely due to the negative autoregulation of *mrpC* due to an imbalance in the MrpC binding the two *mrpC* promoters present in this strain in comparison to the WT *attB*::P$_{mrpC}$-*mrpC* strain. However, no MrpC was detected in the *ΔmrpC* and the *ΔmrpC attB*::P$_{pilA}$-*mrpC* strains (Fig. 2.17).

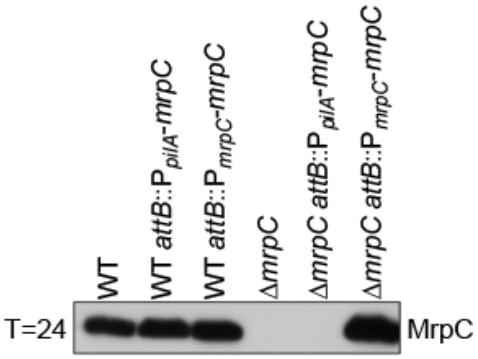

Fig. 2.17 Analysis of MrpC protein production in the P$_{pilA}$-*mrpC* strains. Anti-MrpC immunoblot. WT (DZ2), *ΔmrpC*, WT *attB*::P$_{mrpC}$-*mrpC*, *ΔmrpC attB*::P$_{mrpC}$-*mrpC*, WT *attB*::P$_{pilA}$-*mrpC*, and *ΔmrpC attB*::P$_{pilA}$-*mrpC* strains were developed in 16 ml submerged culture format. Cells were harvested at 24 hours of development, lysates were prepared and 20 µg total protein was analyzed. WT, wild type.

As a final step, to examine if *mrpC* was even induced under the *pilA* promoter, qRT-PCR was employed to quantitate the *mrpC* mRNA levels in the *ΔmrpC attB*::P$_{pilA}$-*mrpC* strain. Cells of the WT, *ΔmrpC* and *ΔmrpC attB*::P$_{pilA}$-*mrpC* strain were vegetatively grown overnight in liquid culture. Total RNA was extracted and the *mrpC* mRNA levels were quantitated relative the wild type using primers specific to the *mrpC* gene (Fig. 2.18). As expected, no *mrpC* transcript was detected in the *ΔmrpC* strain as the primers used for the qRT-PCR bind inside the *mrpC* gene. Interestingly, in the *ΔmrpC attB*::P$_{pilA}$-*mrpC* strain, *mrpC* mRNA levels were about half in comparison to the wild type. This result implied that there was at least some induction of the *mrpC* gene under the *pilA* promoter. However, under these conditions, no MrpC protein could be detected either in the wild type or in the *ΔmrpC attB*::P$_{pilA}$-*mrpC* strain. It was possible that the levels of the induced transcript were not sufficient to be able to detect induced MrpC protein and/or the induced protein was rapidly turned over under these conditions. To conclude, these results suggested that a strong constitutive induction could not be achieved by expressing *mrpC* under the *pilA* promoter.

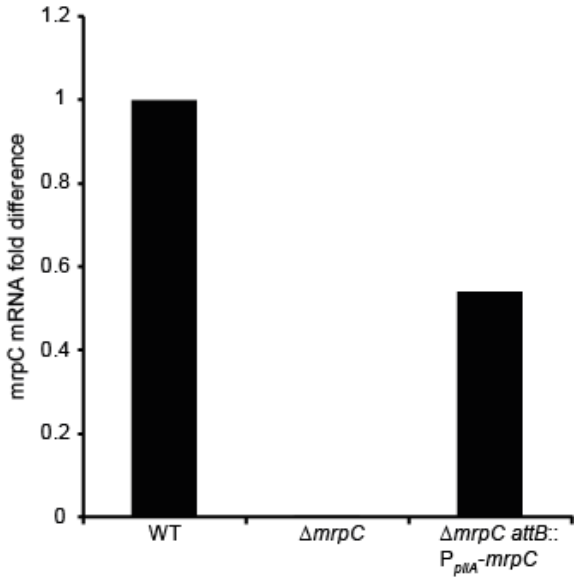

Fig. 2.18 Analysis of *mrpC* expression by quantitative real-time PCR in the *ΔmrpC attB*::P_{pilA}-*mrpC* strain. WT (DZ2), *ΔmrpC* and *ΔmrpC attB*::P_{pilA}-*mrpC* strains were grown overnight under vegetative broth conditions and cells were harvested. RNA was isolated and reverse transcribed into cDNA. *mrpC* gene specific primers were used for real-time PCR analysis. The levels of *mrpC* transcript normalised to the 16S rRNA and expressed relative to the wild type (WT) are shown.

2.4.2 MrpC could not be induced under the copper (*cuoA*) promoter

Since a strong MrpC over-expression could not be achieved under the *pilA* promoter, I used the multicopper oxidase *cuoA* promoter to force MrpC induction in a concentration dependent manner under the effect of copper. This approach was based on a set of plasmids which allow highly controlled copper-inducible gene expression in *M. xanthus* and whose functionality has been tested to induce the *pilB* gene, encoding for the ATPase essential for social motility (Gómez-Santos *et al*., 2012). The analysis of the effect of copper on the wild type strain DK1622 revealed that concentrations of upto 500 µM during growth and 60 µM during development did not affect physiological processes such as cell viability, motility or aggregation into fruiting bodies. A copper concentration of 120 µM was successfully used under vegetative conditions for the copper induced expression of the *pilB* gene to achieve the functional complementation of a *ΔpilB* mutant (Gómez-Santos *et al*., 2012).

I generated an expression vector that contained the multicopper oxidase *cuoA* promoter (P_{cuoA}, 824 bp upstream of and including the *cuoA* start codon) fused to the *mrpC* gene. This construct was integrated in the *attB* site of the wild type and *ΔmrpC* strain. Both of these strains bearing the construct along with the parent wild type and *ΔmrpC* strains were developed in submerged culture in the absence and presence of copper (40 µM and 200 µM) (Fig. 2.19). Strains that

were grown without copper developed normally; the wild type and WT *attB*::P_{cuoA}-*mrpC* strains developed visible aggregates at ~24 hours while the *ΔmrpC* and *ΔmrpC attB*::P_{cuoA}-*mrpC* strains did not develop. In contrast, when strains were grown in the presence of copper, the wild type and WT *attB*::P_{cuoA}-*mrpC* strains failed to develop. This data suggested that addition of copper interfered with the aggregation of cells into fruiting bodies. To additionally test for MrpC induction under these conditions, lysates were prepared from these developmental samples and subjected to anti-MrpC immunoblot analysis. No copper-induced MrpC could be detected (data not shown).

At this point, in order to ensure that the copper construct contained all the regulatory elements necessary for MrpC production, I generated another construct containing the P_{cuoA} (824 bp upstream of and including the *cuoA* start codon) fused to the transcriptional start of *mrpC* (58 bp upstream of the predicted start, Nariya & Inouye, 2005) including the full length gene. This vector was similarly integrated in the *attB* site in the wild type and *ΔmrpC* strain as the previous construct. Also, as an alternate strategy to avoid or at least lower the toxicity of copper, the time of exposure of cells to copper was reduced. Cells were first developed without any copper in the medium or starvation buffer for 24 hours and then incubated for 2 hours in the absence and presence of 40 µM copper. Cell samples were harvested and lysates were subjected to anti-MrpC immunoblot analysis. No copper-induced MrpC could be detected in the *ΔmrpC* strains bearing either of the two different copper-inducible constructs (data not shown).

Apart from testing copper-inducible MrpC expression under submerged developmental conditions, the induction was also tested under vegetative conditions. The aforementioned strains were grown overnight in shaking liquid cultures and induced overnight with varying concentrations of copper (100, 300 and 600 µM). Cell samples were harvested and cell lysates prepared were subjected to anti-MrpC immunoblot. Like earlier, no copper-inducible MrpC induction could be detected (data not shown). Another protein, KapC, could previously be successfully induced in *M. xanthus* under vegetative conditions (Mann & Higgs, unpublished data).

To conclude from my data, it seems that a copper concentration as low as 40 µM during development is toxic to the wild type strain DZ2 and no success could be achieved either during development or vegetative growth for the induction of MrpC using the multicopper oxidase *cuoA* promoter.

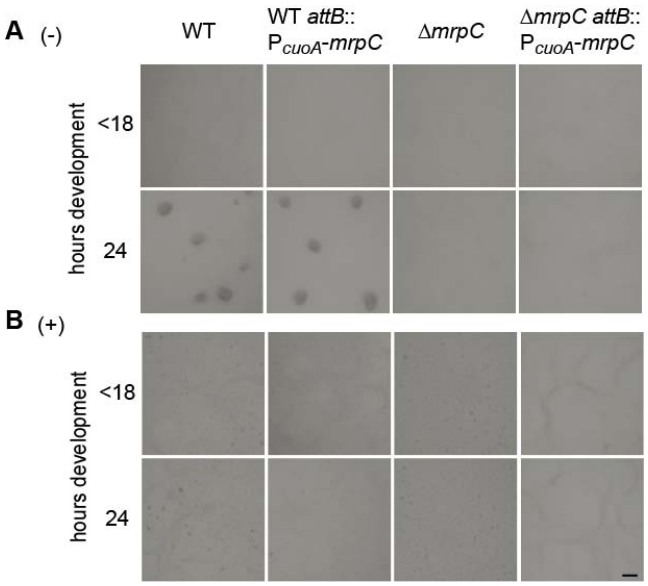

Fig. 2.19 Induction of MrpC under the copper *(cuoA*) promoter. WT (DZ2), *ΔmrpC*, WT *attB*::P_{cuoA}-mrpC and *ΔmrpC attB*::P_{cuoA}-*mrpC* strains were developed in 16 ml submerged culture format. Cells were first grown as a lawn in CTT medium for 24 hours in the absence A. (-) and B. (+) presence of 40 µM copper. At T=0, CTT was replaced with MMC starvation buffer containing no (-) or 40 µM copper (+) to induce starvation. Pictures were recorded with a stereo microscope at the indicated time points during development. WT, wild type; scale bar, 100µm. Protein samples were collected at 0, 18 and 24 hours of development. Lysates were prepared and 20ug total protein was analyzed on immunoblot with anti-MrpC antibody. The results were the same with a copper concentration of 200 µM.

2.5 Analysis of the activity state of MrpC and its role in developmental cell fate determination

MrpC is known to exist in various isoforms. It can be proteolysed to a transcriptionally more active form MrpC2 (Ueki & Inouye, 2003; Nariya & Inouye, 2006) and phosphorylated (MrpC~P) to be a less active transcription factor (Nariya & Inouye, 2005; 2006). The activity state of MrpC could be more important than its mere presence in a cell. Therefore, in order to gain an insight into how the activity state of MrpC could affect cell fate segregation, the rationale was to generate strains which would only express MrpC in a particular activity state and analyze their developmental phenotype.

2.5.1 MrpC2 does not induce development

2.5.1.1 The *mrpC$_{Δ1-25}$* strain does not develop

It was proposed that during development, the transcription factor MrpC is clipped into a transcriptionally more active version called MrpC2 which lacks the

N-terminal 25 residues of MrpC and also positively autoregulates its own expression (Nariya & Inouye, 2006). With this background knowledge, I started to investigate the biological role of MrpC2. At first, I adopted a genetic approach. I generated an *mrpC$_{Δ1-25}$* strain in which the first 25 amino acid residues of the full length *mrpC* were deleted so that only the more active form of the transcription factor *i.e.* MrpC2 would be produced in a cell. In the process of generation of this strain, the *mrpC$_{Δ1-25}$* strain was obtained at a frequency of 1/100 recombinants; most of them were wild type. The first step was to analyze the developmental phenotype of the *mrpC$_{Δ1-25}$* strain. The wild type, *ΔmrpC and mrpC$_{Δ1-25}$* strains were developed in submerged culture and pictures were recorded at various time points (Fig. 2.20). As expected, the wild type developed visible aggregates at ~28h and the *ΔmrpC* strain did not develop. Surprisingly, however, the *mrpC$_{Δ1-25}$* strain also did not develop. This result was contrary to the proposed role of MrpC2 as an autoinducer (Nariya & Inouye, 2006).

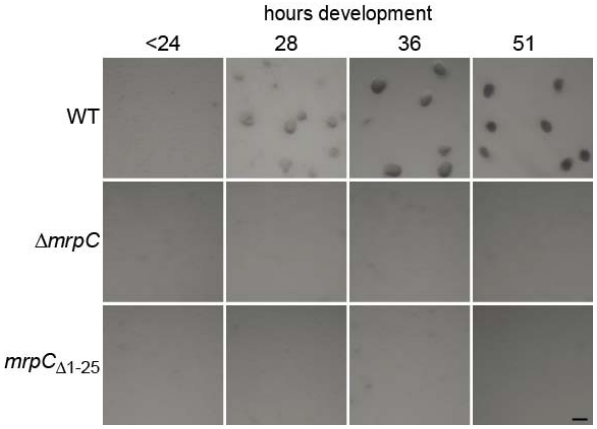

Fig. 2.20 Developmental phenotype analysis of the *mrpC$_{Δ1-25}$* strain. WT (DZ2), *ΔmrpC* and *mrpC$_{Δ1-25}$* strains were developed under submerged conditions in 24-well dishes. Pictures were recorded with a stereo microscope at the indicated time points during development. Scale bar, 100µm.

2.5.1.2 The *mrpC$_{Δ1-25}$* strain mimics the *ΔmrpC* strain in *mrpC* expression

To address the non-developing phenotype of the *mrpC$_{Δ1-25}$* strain, it was examined whether this strain produces MrpC2 and FruA; FruA is one of the targets of MrpC2 (Ueki & Inouye, 2003). The wild type, *ΔmrpC and mrpC$_{Δ1-25}$* strains were developed under submerged conditions and harvested at various points through development. Cell lysates were prepared and subjected to anti-MrpC and anti-FruA immunoblot analysis. MrpC2 (~25 kDa) could be detected in the *mrpC$_{Δ1-25}$* strain at levels comparable to the wild type MrpC/MrpC2. However, only basal levels of FruA were detected in the *mrpC$_{Δ1-25}$* strain in comparison to the wild type (P. Mann, data not shown).

Next, I wanted to examine the expression of *mrpC* in the *mrpC*$_{\Delta 1\text{-}25}$ strain background to understand how this activity state of MrpC influences the regulation of *mrpC*. For this reason, I employed the P$_{mrpC}$-*mCherry* construct (Section 2.1.1). Since it was not possible to transform the *mrpC*$_{\Delta 1\text{-}25}$ strain with the aforementioned construct, I adopted an alternate strategy which was to generate the *mrpC*$_{\Delta 1\text{-}25}$ mutation in the WT *attB*::P$_{mrpC}$-*mCherry* strain. Subsequently, cells of the wild type, *ΔmrpC and mrpC*$_{\Delta 1\text{-}25}$ strains bearing the P$_{mrpC}$-*mCherry* fluorescent reporter construct were developed under submerged conditions, harvested, and dispersed. The average fluorescence of cells was recorded with a plate reader and the number of cells in each strain was enumerated using a cell counter at various time points (Fig. 2.21).

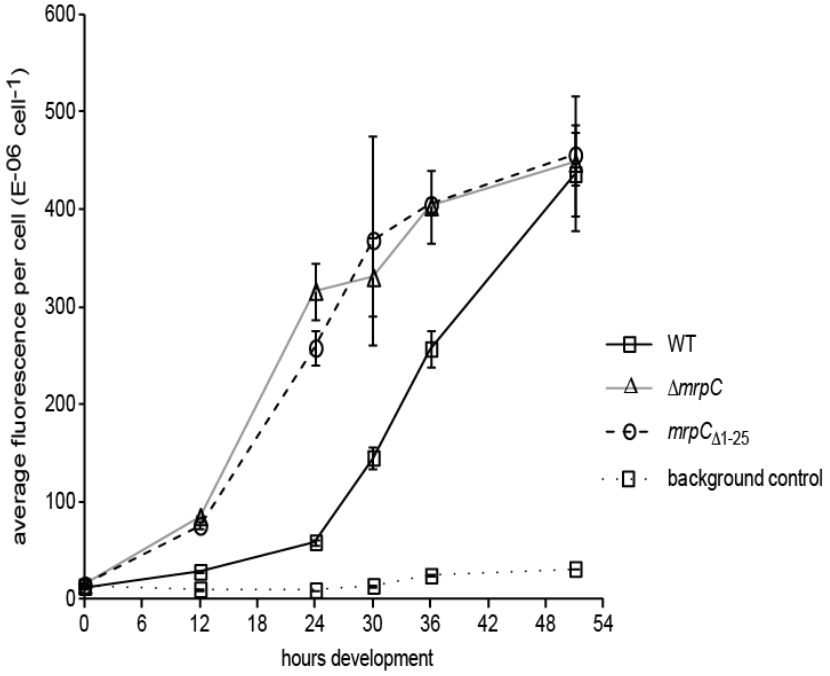

Fig. 2.21 Analysis of *mrpC* promoter activity in the *mrpC*$_{\Delta 1\text{-}25}$ strain. WT (DZ2), *ΔmrpC* and *mrpC*$_{\Delta 1\text{-}25}$ strains bearing the P$_{mrpC}$-*mCherry* construct were developed under submerged conditions in 24-well dishes, harvested and analyzed for mCherry fluorescence with a plate reader at the indicated time points during development. The total number of cells in each strain was counted with a cell counter. The line graph represents the average fluorescence normalised to the number of cells. Error bars represent the standard deviation of three technical replicates. Background control, wild type strain lacking the reporter construct; WT, wild type.

The expression of *mrpC* was upregulated soon after entry into development. In the wild type, the average fluorescence per cell increased gradually until 24 h but linearly thereafter. In the *ΔmrpC* strain*,* the expression at T=0 was equal to that in the wild type but increased very rapidly as early as 12 h. As reported earlier (section 2.1.1), *mrpC* expression in the *ΔmrpC* strain was higher than in the wild type, at least till 36 h. In the *mrpC*$_{\Delta 1\text{-}25}$ strain, the expression of *mrpC* was similar to that in the *ΔmrpC* strain.

In conclusion, the increased *mrpC* expression and the lack of FruA production in the *mrpC$_{Δ1-25}$* strain background together suggested that the MrpC2 produced in this strain is likely inactive or MrpC is naturally designed to be clipped to MrpC2 to render the protein inactive.

2.5.1.3 The *mrpC$_{Δ1-25}$* strain does not form glycerol induced spores

It has been reported that *mrpC* is essential for sporulation (Mueller *et al*., 2010). Therefore, I examined the *mrpC$_{Δ1-25}$* strain for its ability to form glycerol induced spores. Liquid cultures of the wild type, *ΔmrpC and mrpC$_{Δ1-25}$* strains were induced with 0.5 M glycerol for 18 hours and assayed for the formation of chemically induced glycerol spores (Fig.2.22). Vegetatively growing, uninduced, rod-shaped cells of the wild type transformed into round spores after only ~2h of induction with glycerol which became phase-bright by the end of 18 hours. However, like the *ΔmrpC* strain, the *mrpC$_{Δ1-25}$* did not form glycerol-induced spores. This observation further supported the idea that the MrpC2 produced in the *mrpC$_{Δ1-25}$* strain is likely not active.

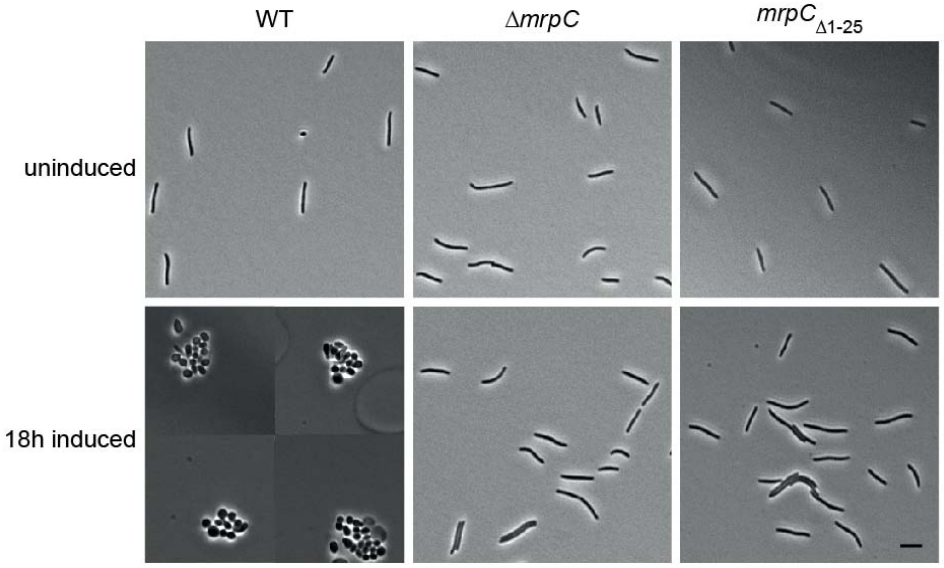

Fig. 2.22 Analysis of glycerol-induced sporulation in the *mrpC$_{Δ1-25}$* strain. WT (DZ2), *ΔmrpC* and *mrpC$_{Δ1-25}$* strains were grown under vegetative broth conditions and chemically induced for sporulation for 18 hours by the addition of 0.5 M glycerol. Phase contrast pictures of uninduced and induced samples were recorded with a microscope. WT, wild type; scale bar, 5µm.

2.5.1.4 The *mrpC$_{Δ1-25}$* strain has a growth defect

As I analyzed developmental cells under the microscope, many round cells could be observed in the *mrpC$_{Δ1-25}$* strain after ~24 h till the end of development while cells of the wild type and *ΔmrpC* strains were still rod-shaped (Fig.2.23).

Additionally, the freezer stocks of the *mrpC*$_{\Delta 1\text{-}25}$ strain were highly unstable. Thus, it appears that the *mrpC*$_{\Delta 1\text{-}25}$ strain has a growth defect due to the deletion of the first 25 amino acids of MrpC.

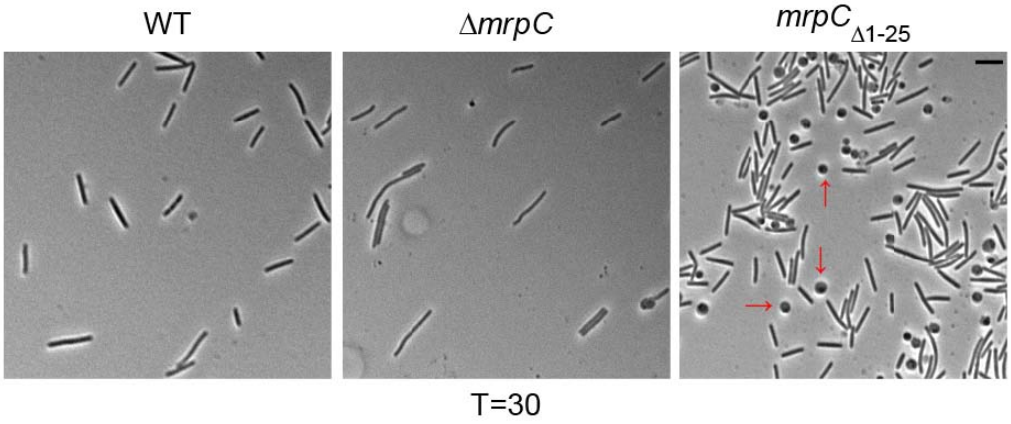

Fig. 2.23 Microscopic analysis of the *mrpC*$_{\Delta 1\text{-}25}$ strain late during development. WT (DZ2), *ΔmrpC* and *mrpC*$_{\Delta 1\text{-}25}$ strains were developed in 16-ml submerged culture format. Cells were harvested, dispersed and analyzed under a microscope at 30 h of development. DIC pictures were recorded. WT, wild type; arrows denote the round cells in the *mrpC*$_{\Delta 1\text{-}25}$ strain; scale bar, 5µm.

2.5.2 The activity of Pkn14 and MrpC phosphorylation appear important in starvation induced sporulation

Apart from MrpC2, the other activity state of MrpC is its phosphorylated state. It has been shown previously that MrpC can be phosphorylated via the Pkn8/Pkn14 Ser/Thr kinase cascade (Nariya & Inouye, 2005). Pkn8 phosphorylates Pkn14 which then phosphorylates MrpC. It was proposed that the kinase cascade negatively regulates *mrpC* expression by phosphorylating MrpC during vegetative conditions as the deletion of *pkn14* and *pkn8* resulted in an early developmental phenotype with elevated MrpC and FruA expression levels (Nariya & Inouye, 2005; 2006). It was shown that MrpC2 cannot be phosphorylated by Pkn14 *in vitro*. It was proposed that MrpC is phosphorylated at the Thr-21 and/or Thr-22 residue(s) and that the phosphorylation of MrpC prevents its proteolytic processing to MrpC2 (Nariya & Inouye, 2006).

Data from our lab showed that the deletion of *pkn14* in the DZ2 background resulted in a delayed developmental phenotype (P. Mann) contrary to previously published results (Nariya & Inouye, 2005). Moreover, MrpC phosphorylation point mutants (*mrpC*$_{T21A}$, *mrpC*$_{T22A}$ and *mrpC*$_{T21\text{-}22A}$) were previously generated in our lab. The likely phosphorylation site(s) (Threonine-21/22) in *mrpC* had been mutated in these strains to an alanine residue; however, all of these strains displayed only slight developmental defects (Mann & Bhardwaj, data not

shown). Thus, these observations altogether led to a detailed analysis of the phosphorylation state of MrpC and the role of Pkn14 in the same.

2.5.2.1 *Δpkn14* has a delayed developmental phenotype while *pkn14*$_{K48N}$ has a wild type phenotype

For an extended analysis of the phosphorylation state of MrpC, I employed the already available deletion mutant of the Pkn14 kinase, *Δpkn14* along with the newly generated Pkn14 autophosphorylation deficient mutant, *pkn14*$_{K48N}$ and the quadruple phosphorylation mutant of MrpC, *mrpC*$_{T21\text{-}22A,S23\text{-}24A}$. In the *mrpC*$_{T21\text{-}22A,S23\text{-}24A}$ strain, the proposed phosphorylation site(s) (Thr-21/22) and additionally, as a likely possibility, the Ser-23/24 residues have been mutated to an alanine. These strains were grown in submerged culture and their developmental phenotype was analyzed (Fig. 2.24A). The production of heat- and sonication-resistant spores was also assessed at the end of development (Fig. 2.24A). Simultaneously, cells were harvested at various time points and cell lysates of samples with equal protein were prepared and subjected to anti-MrpC immunoblot to analyze the MrpC accumulation pattern over development (Fig. 2.24B).

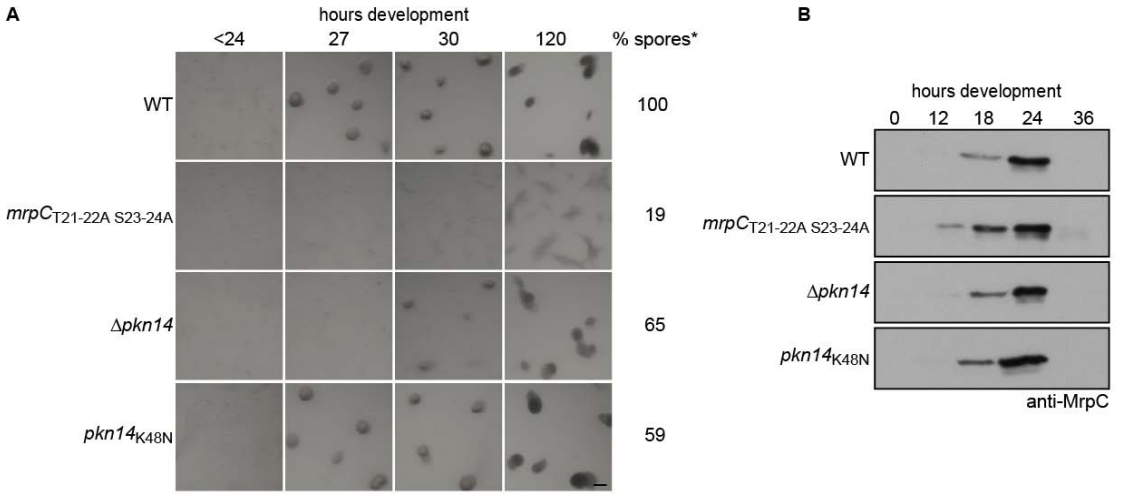

Fig. 2.24 Analysis of the MrpC phosphorylation mutants. A. Developmental phenotype and sporulation efficiency analysis. The WT, *Δpkn14, pkn14*$_{K48N}$ and *mrpC*$_{T21\text{-}22A,S23\text{-}24A}$ strains (DZ2 background) were developed in 16 ml submerged culture format. Pictures were recorded with a stereo microscope at the indicated time points. Spores were isolated at 120 h of development, heated, sonicated, dispersed and counted manually with a counting chamber. *, % heat- and sonication-resistant spores relative to the wild type (WT); scale bar, 100µm. B. Anti-MrpC immunoblot analysis. The WT, *Δpkn14, pkn14*$_{K48N}$ *and mrpC*$_{T21\text{-}22A,S23\text{-}24A}$ strains were developed as in A and cells were harvested at the indicated times. Lysates were prepared and 20 µg total protein was analyzed by immunoblot probed with anti-MrpC antibody. A. and B. Results from one experiment are shown but identical results were obtained in three biological replicates.

The wild type strain developed visible aggregates at ~27 h of development. It accumulated MrpC first at 18 h which peaked by 24 h and was no longer detected at 36 h. The quadruple phosphorylation mutant, *mrpC*$_{T21\text{-}22A,S23\text{-}24A}$ did not develop to form dark fruiting bodies like the wild type but formed aggregation flares as seen late during development between 30 to 120 h. MrpC was detected in this strain first at 12 hours of development; it increased sharply by 18 h, peaked at 24 h and later not detected at 36 h. The *Δpkn14* mutant exhibited a delayed developmental phenotype consistent with previous results (P. Mann) and a wild type MrpC accumulation pattern. This observation was in contrast to previously published data. The *Δpkn14* strain in the wild type DZF1 background displayed an early developmental phenotype (Nariya & Inouye, 2005) and an earlier and elevated production of MrpC/MrpC2 (Nariya & Inouye, 2006). Intriguingly, the *pkn14*$_{K48N}$ strain displayed a wild type phenotype and a wild type MrpC accumulation pattern. The effect of *pkn14*$_{K48N}$ on development was previously analyzed by its constitutive expression in the wild type DZF1 background and was shown to result in an early developmental phenotype (Nariya & Inouye, 2005). Thus, the *pkn14*$_{K48N}$ phenotype in the DZ2 background was also different than predicted based on previously published data. From the above results, it was obvious that the non-developing phenotype of the *mrpC*$_{T21\text{-}22A,S23\text{-}24A}$ mutant was not merely due to the absence or instability of the mutant MrpC protein. It was also clear that the delayed developmental phenotype of the *Δpkn14* mutant was not the result of a delayed MrpC accumulation.

Further, all the above mentioned phosphorylation mutant strains were reduced in the production of heat and sonication resistant spores in comparison to the wild type. An intriguing observation was that the *Δpkn14*, *pkn14*$_{K48N}$ and *mrpC*$_{T21\text{-}22A,S23\text{-}24A}$ strains produced 65%, 59% and 19% spores, respectively, relative to the wild type. To follow this up, I additionally analysed the sporulation efficiency of the already available *mrpC* phosphorylation point mutants that were previously tested and did not display any significant developmental phenotype (data not shown). Importantly, an *mrpC*$_{S23\text{-}24A}$ mutant was comparable (107%) to the wild type but an *mrpC*$_{T21\text{-}22A}$ mutant was reduced in sporulation (58%) like the *Δpkn14* and *pkn14*$_{K48N}$ strains (data not shown).

These results suggested that the activity of Pkn14 and the phosphorylation of MrpC at the Thr-21/22 residue(s) appear to be important for starvation induced sporulation.

2.5.2.2 The *Δpkn14* strain can be complemented

I wanted to complement the *Δpkn14* strain to confirm that the observed phenotype was a true effect of the gene deletion. I generated two constructs: the first contained the *pkn14* gene expressed under the *pilA* promoter (P$_{pilA}$-

Pkn14) and the second contained 385 bp upstream of the start of *pkn14* (putative *pkn14* promoter) followed by *pkn14* gene (P_{pkn14}-*Pkn14*). Both of these constructs were inserted into the DZ2 *Δpkn14* strain at the *attB* site, and the developmental phenotype was analyzed in submerged culture (Fig. 2.25). The *Δpkn14* strain expressing Pkn14 under the control of the *pilA* promoter developed aggregates at 24 h, 3 h earlier than the wild type. This could be attributed to the fact that the *pilA* promoter is constitutively active and thus, Pkn14 may have been expressed at levels higher than normal during development. The *Δpkn14* strain bearing the P_{pkn14}-*Pkn14* construct displayed a wild type phenotype. These results indicated that the delayed phenotype of the *Δpkn14* mutant in the DZ2 background was indeed due to the deletion of the *pkn14* gene.

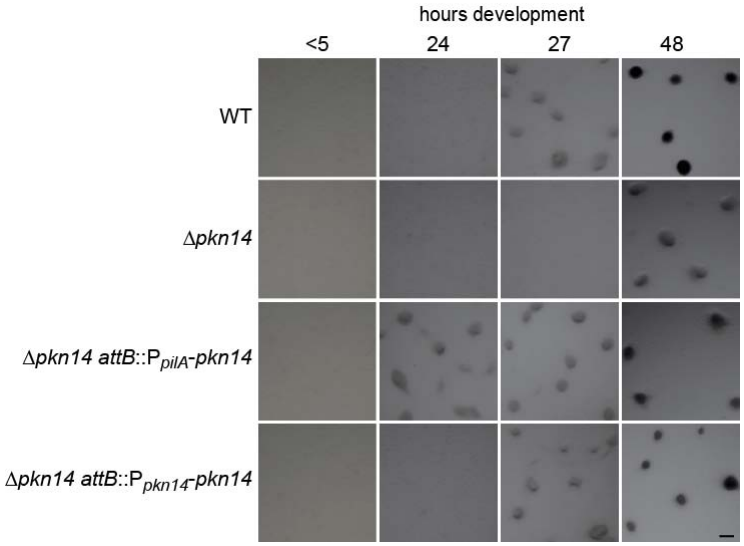

Fig. 2.25 Developmental phenotype analysis of the *Δpkn14* complementation strains (DZ2 background). WT, *Δpkn14, Δpkn14 attB*::P_{pilA}-*Pkn14* and *Δpkn14 attB*::P_{pkn14}-*Pkn14* strains were developed under submerged conditions in 24-well dishes. Pictures were recorded with a stereo microscope at the indicated time points during development. WT, wild type; scale bar, 100µm.

2.5.2.3 Pkn14 phosphorylates MrpC at the Thr-21 residue

Next, I tried to reproduce the results of the previously published *in vitro* analysis (Nariya & Inouye, 2005) in order to confirm the phosphorylation of MrpC by Pkn14. Recombinant Pkn14, $Pkn14_{K48N}$ (the published autophosphorylation deficient mutant of Pkn14) and MrpC proteins were over-expressed and purified. Pkn14 and $Pkn14_{K48N}$ were first tested for autophosphorylation in the presence of radioactive [γ^{32}P]-ATP (Fig. 2.26). While a radioactive band corresponding to Pkn14 could be readily detected, the corresponding band for $Pkn14_{K48N}$ was not detected indicating that Pkn14 was capable of autophosphorylation (Fig. 2.26, lanes 1 and 2). To test the subsequent

phosphotransfer to MrpC, either Pkn14 or $Pkn14_{K48N}$ were incubated with MrpC in the presence of radioactive [γ^{32}P]-ATP. As expected, when Pkn14 was incubated with MrpC, both proteins were labeled; however, when $Pkn14_{K48N}$ was incubated with MrpC, none of the proteins were labeled (Fig. 2.26, lanes 3 and 4). This indicated that Pkn14 phosphorylated MrpC. The above results were consistent with previously published data (Nariya & Inouye, 2005). Having confirmed that Pkn14 phosphorylated MrpC *in vitro*, I over-expressed and purified recombinant MrpC mutant proteins, in which the proposed phosphorylation site(s) had been mutated ($MrpC_{T21\text{-}22A,}$ $MrpC_{T22A}$, $MrpC_{T21\text{-}22A,S23\text{-}24A)}$, and MrpC2 (the N-terminal truncated version of MrpC). Each of these proteins was separately incubated with Pkn14 and radioactive [γ^{32}P]-ATP in order to confirm the exact phosphorylation site in MrpC (Fig. 2.26).

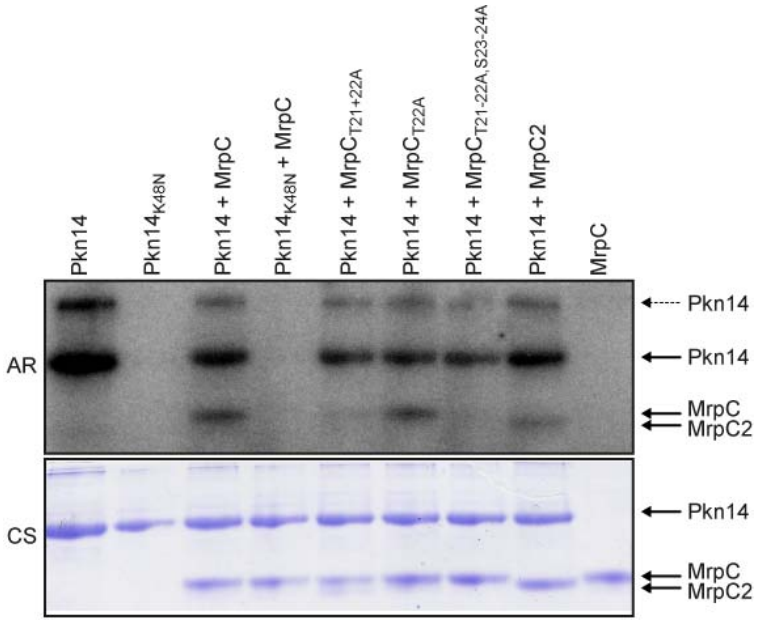

Fig. 2.26 *In vitro* phosphorylation of MrpC, MrpC2 and MrpC mutants by Pkn14. A. 10 µM of each recombinant protein was incubated in 30 µL of buffer P containing 175 µM ATP with 1.5 µCi of [γ^{32} P]-ATP for 30 minutes at 30ºC, quenched and analyzed on a 15% SDS-PAGE. The radiolabel was detected by exposure to a Storage Phosphor Screen (AR). The dashed arrow represents a phosphorylated Pkn14 oligomer B. The SDS-PAGE gel in A was subsequently stained with Coomassie brilliant blue to detect the total protein (CS).

Pkn14 could radiolabel $MrpC_{T22A}$, however, only a diminished label could be detected on $MrpC_{T21\text{-}22A}$ (Fig. 2.26, lanes 6 and 5). This observation suggested that MrpC was preferentially phosphorylated by Pkn14 at the Thr-21 residue. The quadruple phosphorylation mutant of MrpC, $MrpC_{T21\text{-}22A,S23\text{-}24A}$ could not be phosphorylated by Pkn14 (Fig. 2.26, lane 7). Interestingly, however, a weak radiolabel was detected on MrpC2, suggesting that Pkn14 could phosphorylate MrpC2 (Fig. 2.26, lane 8). This observation was contrary to previously published analysis as it was shown that MrpC2 could not be phosphorylated by Pkn14 (Nariya & Inouye, 2006). It further suggested that MrpC can be phosphorylated

at another site(s) than the Thr-21 and/or Thr-22 as previously proposed (Nariya & Inouye, 2005; 2006). As a control, MrpC was incubated alone under the same conditions and no radiolabel was detected on it (Fig. 2.26, lane 9) supporting the fact that MrpC did not autophosphorylate itself.

Taken together, these results suggest that the activity of Pkn14 and MrpC phosphorylation at Thr-21/22 might be important during development for sporulation. Pkn14 preferentially phosphorylates MrpC at the Thr-21 residue but MrpC can be additionally phosphorylated at a site(s) downstream of the N-terminal 25 residues.

2.6 Mxan_5126 does not appear to modulate MrpC's activity during development

Although MrpC was described to be a single gene (Sun & Shi, 2001a), analysis of its genetic context revealed the presence of a gene immediately downstream of MrpC. Mxan_5126 lies 49 bp downstream of MrpC and is a hypothetical protein of 217 amino acids. An interesting coincidence was that this protein contains an SMI1 domain which is common to immunity proteins in bacterial toxin systems that code for a variety of nucleases and nucleic acid deaminases (Zhang *et al*., 2011). I hypothesized that the interaction of MrpC with such a protein might influence its activity and thus, began to characterize the downstream gene Mxan_5126.

2.6.1 MrpC and Mxan_5126 co-occur only in *M. xanthus*

Since Mxan_5126 was annotated to be a hypothetical protein, I wanted to check if there were orthologs present in other bacteria. Orthologs were identified within the publically available Myxococcales genomes using a Reciprocal BLASTp analysis (Altschul *et al*., 1997) and within the unpublished genomes (Huntley S. & Søgaard-Andersen) using the Artemis Comparison Tool (Wellcome Trust Sanger Institute). An ortholog of Mxan_5126 could only be identified in the close relative *Anaermyxobacter dehalogenans*. Simultaneously, I also looked for orthologs of MrpC. Orthologs of MrpC were found in all Myxococcales genomes except in *Anaermyxobacter dehalogenans* and *Sorangium cellulosum*. From these analysis, interestingly, MrpC and Mxan_5126 were found to co-occur only in *M. xanthus* (Fig. 2.27).

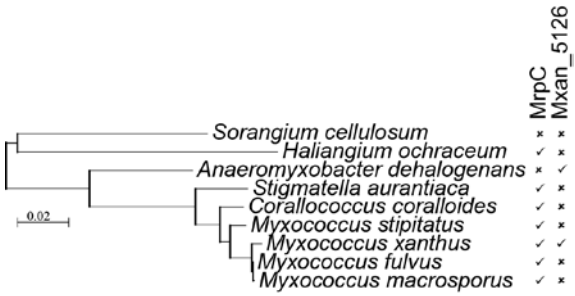

Fig. 2.27 Co-occurrence of MrpC and Mxan_5126 homologs in different Myxococcales genomes. The dendrogram represents the relationship of members of the order Myxococcales based on their 16sRNA (S. Huntley & L. Søgaard-Andersen). The coloured bars indicate the suborder, family of genus of the respective genomes (see key). Tick mark (√); present in the analyzed genome, cross mark (x); absent in the analyzed genome.

2.6.2 *mrpC* is co-transcribed with the downstream gene Mxan_5126

As seen from the bioinformatic analysis, since *mrpC* and Mxan_5126 were present together only in *M. xanthus,* oriented in the same direction separated by only 49 bp, I wanted to investigate whether they formed one transcriptional unit. PCR was performed on cDNA generated from 24 h-old developmental wild type cells by using gene specific primer combinations (Fig. 2.28). PCR products of the expected size were produced by both Mxan_5126 and *mrpC* specific primers from the cDNA generated using a primer that bound immediately downstream of the gene Mxan_5126. PCR products of comparable size were also produced when genomic DNA was used as a positive control for the gene specific PCR reactions. In each case, samples without added reverse transcriptase or RNA template for the cDNA synthesis produced no PCR product, thus, verifying the absence of contaminating genomic DNA in the cDNA. The results suggested that *mrpC* is co-transcribed with the downstream gene Mxan_5126.

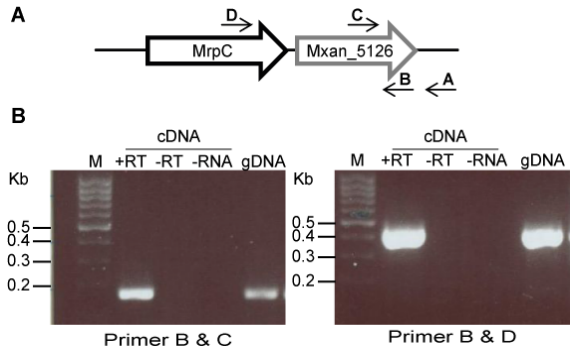

Fig. 2.28 Analysis of *mrpC* and Mxan_5126 as a transcriptional unit. A. Genetic organisation of *mrpC* and Mxan_5126. Arrows indicate the primers used for cDNA synthesis (A) and PCR (B, C and D) B. PCR results. cDNA from 24 hour old developmental wild type cells was analyzed by PCR using oligonucleotide primer pairs B&C for Mxan_5126 and B & D for MrpC. Wild type genomic DNA (gDNA) as positive control; +RT, reaction with reverse transcriptase; -RT, reaction without reverse transcriptase; -RNA, reaction without RNA; M, DNA ladder.

2.6.3 Mxan_5126 does not have a significant role during development

Since Mxan_5126 was found to be co-transcribed with *mrpC*, next I wanted to investigate the role of Mxan_5126 and its association with MrpC. I adopted a genetic approach and generated the deletion mutantΔMxan_5126 and the Δ*mrpC* ΔMxan_5126 double mutant. Strains were developed under submerged conditions and the developmental phenotype along with the production and germination ability of heat- and sonication-resistant spores at the end of development was assayed (Fig 2.29A). The strain ΔMxan_5126 phenocopied the wild type forming aggregates at ~27h while the Δ*mrpC* and Δ*mrpC* ΔMxan_5126 strains did not develop at all. The number of heat and sonication resistant spores produced at 120 h of development and the spore germination efficiency was similar but smaller colonies of germinated spores were observed for ΔMxan_5126 in comparison to the wild type (Fig 2.29B). This minor difference could be attributed to the fact that ΔMxan_5126 shares homology to proteins involved in the regulation of 1,3-β-glucan synthase activity and cell wall formation (Zhang *et al*., 2011).

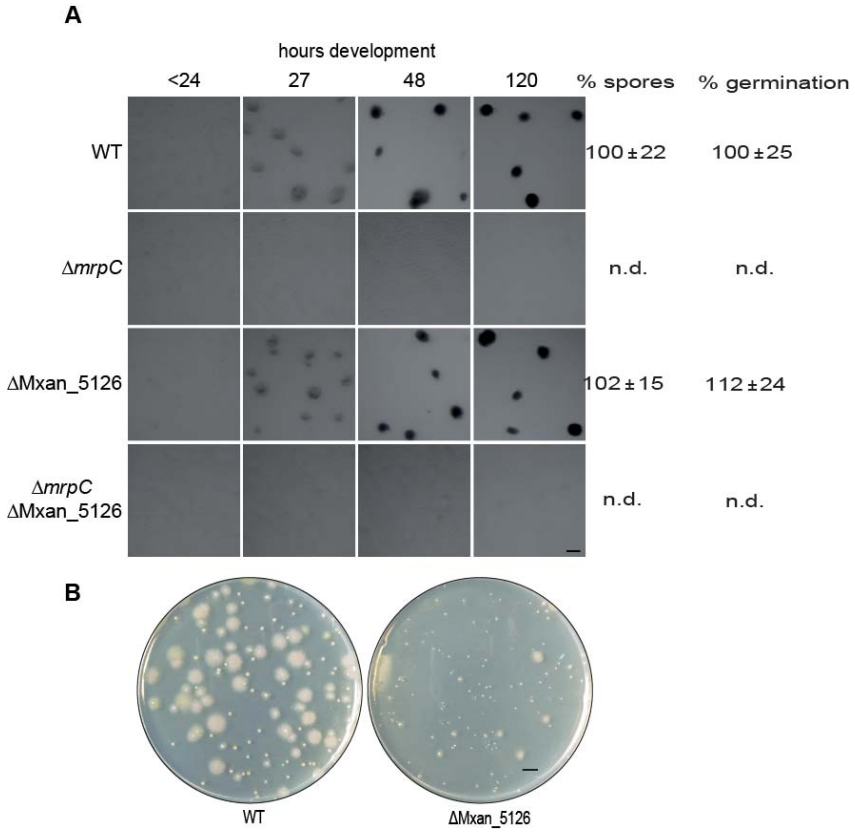

Fig. 2.29 Developmental phenotype and spore germination analysis of ΔMxan_5126 strains. A. Phenotype analysis. WT (DZ2), Δ*mrpC*, ΔMxan_5126 and Δ*mrpC* ΔMxan_5126 strains were developed under submerged conditions in 24-well dishes. Pictures were recorded with a stereo microscope at the indicated time points during development. WT, wild type; n.d., none detected. Scale bar, 100µm. B. Spore germination analysis. Various Spore dilutions were plated in top agar on CYE plates and incubated for 6 days at 32°C. The total number of colonies produced for each strain was counted and pictures of the spore germinated plates were recorded with a camera. Scale bar, 0.5 cm.

These results suggested that Mxan_5126 does not have a significant role during development in the wild type.

2.6.4 Mxan_5126 is a protein that is translated very weakly

The phenotype of the ΔMxan_5126 strain was indistinguishable from the wild type but given that Mxan_5126 is co-transcribed with MrpC, it could have a role in the MrpC pathway. Therefore, I wanted to characterize if the protein was produced and how it accumulated/localized in the cells during development. For this purpose, I constructed an insertion strain bearing a C-terminal mCherry fusion to the gene Mxan_5126 at the endogenous locus. The developmental phenotype of this strain was examined (Fig 2.30A). Cells were harvested at various time points during development and cell lysates were prepared and subjected to anti-mCherry immunoblot analysis. Additionally, the cells harvested were dispersed and single cells were analyzed under a microscope and the mCherry fluorescence was recorded (Fig 2.30B).

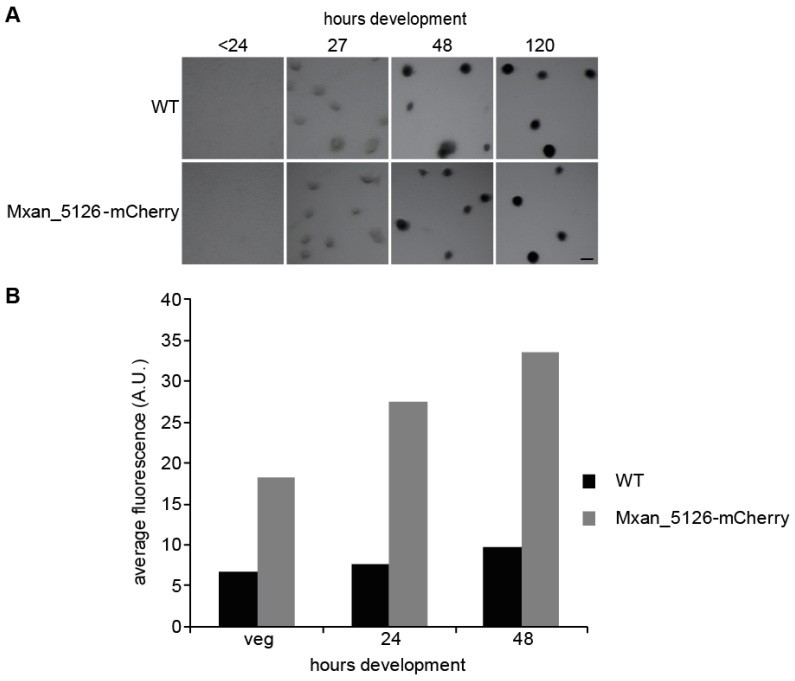

Fig. 2.30 Developmental phenotype and fluorescence analysis of Mxan_5126-mCherry fusion bearing strain. A. Phenotype analysis. WT (DZ2) and Mxan_5126-mCherry strains were developed in 16 ml submerged culture format. Pictures were recorded with a stereo microscope at the indicated time points during development. WT, wild type. Scale bar, 100µm. B. Fluorescence analysis. Vegetative cells grown overnight in CYE medium, 24 and 48 h old developmental cells (as developed in A) were harvested, dispersed and single cells were analyzed under a fluorescent microscope. The fluorescence intensity of single-background subtracted cells was quantified. The graph represents the per cell average mCherry signal at the indicated time points. WT, wild type.

The strain carrying the Mxan_5126-mCherry fusion at the endogenous locus developed exactly like the wild type, aggregates were observed at ~27h. No

protein could be detected in immunoblot with mCherry antibody (data not shown). However, in the fluorescence analysis, a weak mCherry signal which increased during development compared to vegetative conditions could be detected in the Mxan_5126-mCherry strain. This increase in the average signal was higher in comparison to the wild type which was used a control for auto fluorescence and consistent with the upregulation of *mrpC* transcription during development. These results suggested that Mxan_5126 is a weakly translated protein as the mCherry fluorescence signal for the Mxan_5126-mCherry fusion was insignificant relative to the strong signal observed in case of the MrpC-mCherry protein fusion (Fig. 2.15). Alternatively, the fusion protein is non-functional and degraded right away or Mxan_5126 is not a real protein.

Taken together, these results indicated that Mxan_5126 does not play a significant role during development or modulate the activity of MrpC to influence decisions pertaining to cell fate.

2.7 Analysis of markers to distinguish between subpopulations during development

A second part of my project was to identify markers to be able to distinguish between subpopulations. This approach was designed so as to first differentiate developmental cell populations with the help of transcriptional markers and ultimately, correlate the MrpC levels in a particular cell fraction in order to understand its role in cell fate determination.

2.7.1 Targets of MrpC do not follow the differential accumulation of MrpC

MrpC, the key developmental transcription factor, is known to bind to the promoters of several developmentally regulated genes and is also necessary for their induction (Sun & Shi *et al.,* 2001a, b; Ueki & Inouye, 2003; Nariya & Innoye, 2008). As a first step, the expression of two of the targets of MrpC was analyzed in the developmental populations.

The first target of MrpC/C2 to be examined was the gene *fruA* (Ueki & Inouye, 2003). Like MrpC, FruA is also a transcriptional regulator necessary for the induction of aggregation (Ogawa *et al*., 1996) and has been previously shown to accumulate heterogeneously in the non-aggregated and aggregated cell subpopulations during development (Lee *et al*., 2012). We hypothesized that *fruA* could be a subpopulation marker for the aggregated cell fraction as it known to induce the expression of some late developmental genes (those involved in sporulation), sometimes by acting in combination with MrpC/MrpC2 (Mittal & Kroos, 2009a, b).

In order to assess the promoter activity of *fruA,* a fluorescent reporter construct containing the putative promoter region of *fruA* (491 bp upstream of and including the start codon; P_{fruA}) fused to the second codon of mCherry (P_{fruA}-*mCherry*) was generated. This construct was inserted at the *attB* site in the wild type which was then developed under submerged conditions to assay the effect on the developmental phenotype. The reporter caused no alteration in the wild type phenotype (data not shown). Additionally, as a control, the expression of this construct was tested in the *ΔmrpC* strain and no mCherry expression could be detected (data not shown). This observation was consistent with the idea that MrpC is necessary for *fruA* induction (Ueki & Innoye, 2003) and further suggested that the reporter is responding appropriately.

Cells of the WT *attB*::P_{fruA}-mCherry strain were developed under submerged culture, harvested and separated into aggregated and non-aggregated fractions at various time points. Cells were dispersed for examination under a fluorescent microscope and the fluorescence intensity of single background-subtracted cells (n ≥ 100) was quantified (Fig. 2.31). In both the cell fractions, the expression of *fruA* was induced between 12 to 18 h of development. It peaked at 30 h of development but dropped steeply thereafter, till 48 h of development.

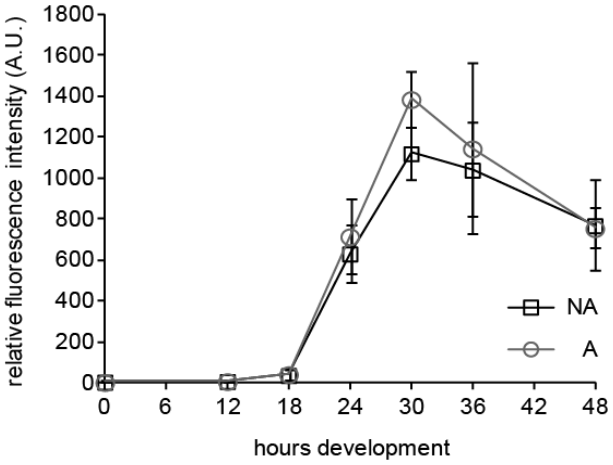

Fig. 2.31 Analysis of *fruA* promoter activity in developmental subpopulations. Cells of the WT *attB*::P_{fruA}-*mCherry* strain were developed in 16 ml submerged culture format, harvested and non-aggregated (NA) and aggregated (A) cell fractions were separated at the indicated time points. Cells of the two fractions were dispersed and single cells (n≥ 100) were examined under a fluorescent microscope. The fluorescence intensity of single-background subtracted cells was quantified. The line graph represents the average mCherry fluorescence of the two populations. Error bars represent the standard deviation of three biological replicates.

The expression of *fruA* has previously been tested in the total population of the wild type by qRT-PCR (Higgs *et al*., 2008). In this former study, the expression was induced ~2h in development and the maximum expression was seen at 24 h of development. The difference in *fruA* expression between the former and the current study can be attributed to the use of difference methods. However, the

fluorescent reporter system employed in this study was suitable for our purpose as it offered the advantage of single cell analysis. At the average population level, no significant differences in *fruA* promoter activity could be observed between the non-aggregated and the aggregated sub-populations through the course of development (Fig. 2.31). Although the average expression was similar, it was possible that there was heterogeneity in *fruA* expression in single cells of the two populations. Therefore, the single cell mCherry fluorescence of the two populations was also analyzed (Fig. 2.32). While MrpC was previously seen to accumulate heterogeneously also at 24 h (Lee *et al*., 2012), the single cell *fruA* expression between the two populations was not significantly different except the fact that a few cells fluorescing with higher intensities were detected in the aggregated cell fraction that also displayed a higher average mCherry signal in comparison to the non-aggregated cell fraction. A similar single cell profile was also seen for the two separated cell fractions at 36 h. To summarize, since *fruA* promoter activity was similar in both the cell fractions at the population as well as single cell level, these data suggested that the difference in accumulation levels did not translate into a differential *fruA* expression in the developmental populations.

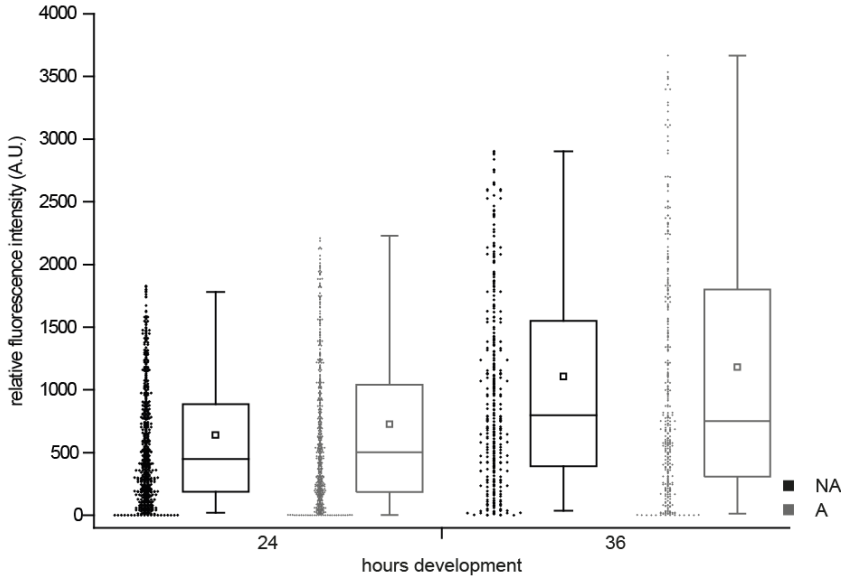

Fig. 2.32 Single cell analysis of *fruA* promoter activity in developmental subpopulations of the WT *attB*::P_{fruA}-*mCherry* strain. The box plots depict the distribution of the mCherry fluorescence intensities of the non-aggregated (NA) and aggregated (A) population samples of Fig. 2.31 at the indicated time points. The box and the whiskers represent 50% and 5-95% of the data, respectively. The middle line and the small square within the box represent the median and the average of the total population, respectively. The dots denote the intensity measurements of single cells (bin size 4). Data is from the three biological replicates.

The next target of MrpC to be tested was *mazF*, a gene encoding an endoribonuclease MazF, which at the time of these experiments, was implicated in mediating cell lysis to cause programmed cell death during development

(Nariya & Inouye, 2008). It is known that MrpC/MrpC2 binds the *mazF* promoter and activates its transcription (Nariya & Inouye, 2008). It was possible that *mazF* was specifically expressed in cells that were destined to lyse and could serve as a marker to differentiate this subpopulation of cells from the rest of the population. Therefore, to assess the promoter activity of *mazF*, a wild type bearing a P_{mazF}-*mCherry* construct (597 bp upstream of and including the *mazF* start codon fused to mCherry) was generated on similar lines as the WT *attB*::P_{fruA}-*mCherry* strain (described above). Cells of the WT *attB*::P_{mazF}-*mCherry* strain were developed under submerged conditions, harvested and separated into aggregated and non-aggregated fractions at various time points. Cells were dispersed for examination under a fluorescent microscope and the fluorescence intensity of single background-subtracted cells ($n \geq 100$) was quantified (Fig. 2.33). No significant differences in *mazF* promoter activity could be recorded in the non-aggregated and the aggregated sub-populations throughout the course of development. Also, from the single cell analysis for mCherry fluorescence, the variation between the non-aggregated and aggregated cell fractions was insignificant with a similarly broad range of expression seen within both the populations (Fig. 2.34). No fluorescence was detected in a wild type lacking the reporter and the construct did not alter the phenotype of the wild type strain (data not shown). Additionally, no fluorescence was detected in a *ΔmrpC attB*::P_{mazF}-*mCherry* strain, consistent with the idea that MrpC is required for the induction of *mazF* (Nariya & Inouye, 2008).

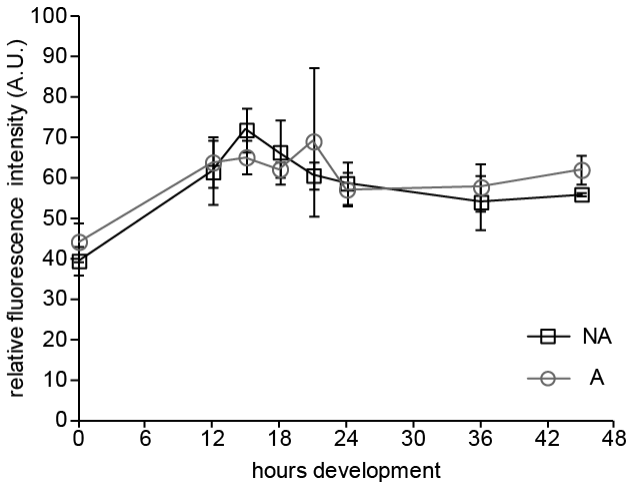

Fig. 2.33 Analysis of *mazF* promoter activity in developmental subpopulations. Cells of the WT *attB*::P_{mazF}-*mCherry* strain were developed in 16 ml submerged culture format, harvested and non-aggregated (NA) and aggregated (A) cell fractions were separated at the indicated time points. Cells of the two fractions were dispersed and single cells ($n \geq 100$) were examined under a fluorescent microscope. The fluorescence intensity of single-background subtracted cells was quantified. The line graph represents the average mCherry fluorescence of the two populations. Error bars represent the standard deviation of three biological replicates.

Together, these data suggested that targets of MrpC did not follow the differential accumulation pattern of the master regulator MrpC in the distinct developmental subpopulations.

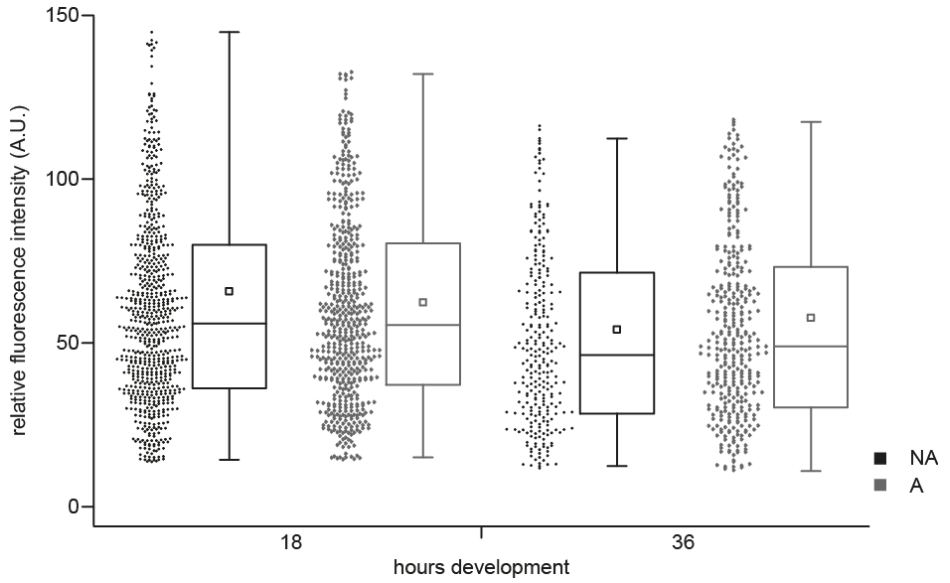

Fig. 2.34 Single cell analysis of *mazF* promoter activity in developmental subpopulations of the WT *attB*::P_{mazF}-*mCherry* strain. The box plots depict the distribution of the mCherry fluorescence intensities of the non-aggregated (NA) and aggregated (A) population samples of Fig. 2.33. The box and the whiskers represent 50% and 5-95% of the data, respectively. The middle line and the small square within the box represent the median and the average of the total population, respectively. The dots denote the intensity measurements of single cells (bin size 1). Data from the three biological replicates was pooled for the two cell fractions.

2.7.2 FibA, the aggregated fraction specific metalloprotease is likely regulated post-transcriptionally

As seen above, neither the key developmental regulator MrpC nor its targets are expressed differentially in the developmental subpopulations at the level of transcription. The comparison of several developmental and structural proteins in the separated subpopulations revealed remarkable heterogeneity in their accumulation profiles (Fig. 1.13 & Lee *et al.*, 2012). FibA, an extracellular metalloprotease, is one of the structural proteins reported to be exclusively present in the aggregated cells (Lee *et al.*, 2011, Lee *et al*., 2012). Next, I wanted to examine whether *fibA* could serve as a transcriptional marker to exclusively differentiate the cell clusters from the other developmental subpopulations. To address this, I employed a strain bearing a P_{fibA}-*mCherry* construct at the *attB* site. The construct contains the putative promoter region of *fibA* (575 bp upstream of and including the *fibA* start codon; P_{fibA}) fused to the second codon of the gene containing the fluorescent reporter protein mCherry (P_{fibA}-*mCherry*). The strain has a sporulation phenotype but still produces FibA

exclusively in the aggregated cells at levels comparable to the wild type (Lee *et al*., 2011).

Cells were developed in triplicate biological replicates under submerged culture for 24 h, separated into aggregated and non-aggregated fractions, and lysates prepared from equal numbers of cells in each fraction were subjected to both anti-mCherry and anti-FibA immunoblot (Fig. 2.35A). FibA was detected almost exclusively in the aggregated cell fraction while mCherry was detected nearly equally (relative intensity ratio aggregated/non-aggregated of 0.97±0.02) in both cell fractions. This suggests that in average, the putative *fibA* promoter activity is similar in both populations.

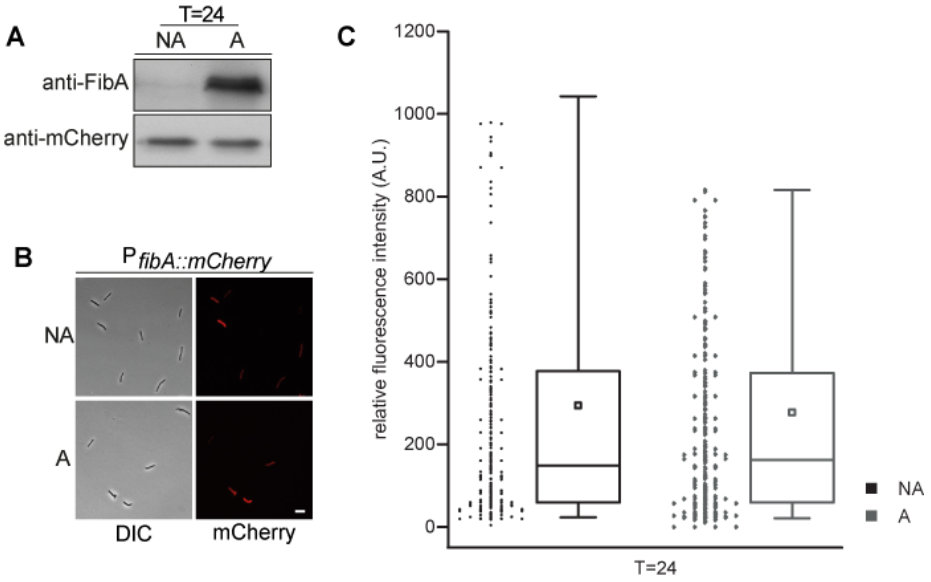

Fig. 2.35 Analysis of *fibA* promoter activity in developmental subpopulations. A. Anti-FibA (top), anti-mCherry (middle) immunoblot analyses of the WT *attB*::P_{fibA}-mCherry strain. Cells were developed in 16 ml submerged culture format for 24 hours, harvested and cell fractions were separated. Lysates were prepared from equal numbers of cells in each fraction. NA, non-aggregated cells; A, aggregated cells. B. Fluorescent microscope pictures. Single cells (n ≥ 250) of the two developmental populations were examined under a fluorescent microscope and the fluorescence intensity of single-background subtracted cells was quantified. Scale bar, 5µm. C. Single cell analysis of *fibA* promoter activity in the separated cell populations. The box plot depicts the distribution of mCherry fluorescence intensities of single cells of the two separated cell populations. The box and the whiskers represent 50% and 5-95% of the data, respectively. The middle line and the small square within the box represent the median and the average of the total population, respectively. The dots denote the intensity measurements of single cells (bin size 1). Results from one assay are shown, but triplicate biological repetitions produced identical results.

Further, to examine if the *fibA* expression was still somewhat different at the single cell level, dispersed cells from the two fractions were examined under a fluorescence microscope and the fluorescence intensity of single background-subtracted cells (n ≥ 250) was quantified (Fig. 2.35B). The population average

aggregated/non-aggregated mCherry fluorescence ratio was 0.87±0.09, which is similar to the results from the immunoblot analyses. The single cell mCherry fluorescence variation in these two populations was slightly different with more cells in the non-aggregated population fluorescing with higher intensity (Fig. 2.35C). No significant fluorescence could be detected in the wild type cells lacking the reporter (data not shown).

Together, these results indicated that although FibA accumulates heterogeneously in the aggregated cell fraction, *fibA* transcription is not a marker exclusively for the cell cluster subpopulation. These data also suggest that fibA/FibA is likely post-transcriptionally regulated (Lee *et al*., 2012).

2.7.3 Chromosome status is not a marker to distinguish between developmental subpopulations

From the results presented above, it was clear that a transcriptional marker cannot be assigned to the different developmental subpopulations. It has been demonstrated that DNA replication during the early aggregation phase is essential for the progression of development (Tzeng & Singer, 2006). Furthermore, it has been published that peripheral rods contain only one copy of the genome while all myxospores contain two copies of the genome (Tzeng & Singer, 2005). Therefore, I wanted to investigate whether a cell's chromosome status could be used as a marker to exclusively distinguish the peripheral rods in the non-aggregated cell fraction early during development. For this purpose, I generated a strain harbouring a P_{parB}-*parB-yfp* construct (Harms & Søgaard-Andersen, unpublished) in our wild type background. The construct encodes under the native promoter, the *Myxococcus* ParB protein C-terminally fused to Yfp (yellow fluorescent protein) and was integrated at the *M. xanthus* Mx8 phage attachment (*attB*) site. The WT *attB*::P_{parB}-*parB-yfp* strain was confirmed to have a wild type phenotype (data not shown).

The ParA and ParB proteins are a part of the bacterial chromosome partitioning system that work together with one or more cis-acting centromere-like *parS* sequences to ensure proper predivisional partitioning. The *parS* sequences nucleate the binding of ParB and titrate sufficient protein to create foci which can be visualized by fluorescence microscopy. These foci normally follow the chromosomal replication *oriC* complexes. ParA is a membrane-associated ATPase that is essential for the symmetric movement of the ParB foci (Bignell & Thomas, 2001). The WT *attB*::P_{parB}-*parB-yfp* strain was used as a tool to determine the chromosome copy number of a cell as the number of Yfp foci within a cell should correspond to the number of chromosomes.

Cells of the WT *attB*::P$_{parB}$-*parB-yfp* strain were grown under vegetative conditions. Exponentially growing cells were harvested, dispersed and examined under a fluorescent microscope (Fig. 2.36A). The number of ParB-YFP loci in single cells (n ≥ 100) was quantified (Fig. 2.36B). Approximately 90% of the cells had two ParB-Yfp foci and hence, contained two copies of the chromosome (2N; N= number of chromosome) while the remaining 10% of cells had one focus and were 1n. The average number of chromosomes per cell was 1.9. This result was in line with previous studies that demonstrated a population of vegetatively growing *M. xanthus* cells to contain an average of 1.7 chromosomes per cell (Zusman & Rosenberg, 1970).

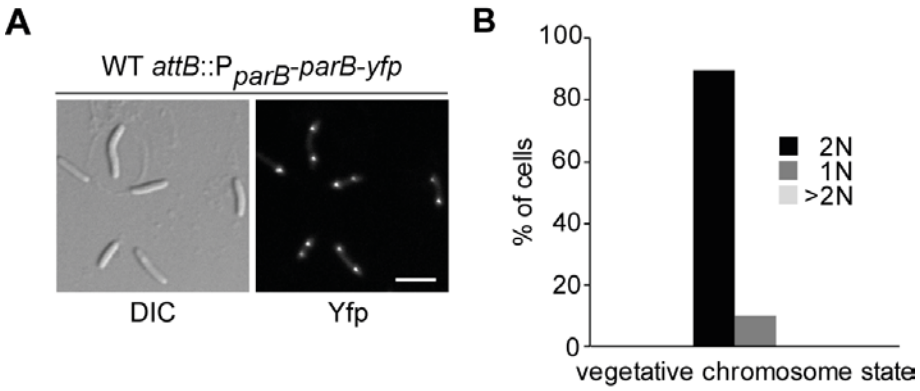

Fig. 2.36 Analysis of chromosome state of exponentially growing vegetative *M. xanthus* cells. A. Fluorescent microscope pictures. Cells of the WT *attB*::P$_{parB}$-*parB-yfp* strain were grown under vegetative broth conditions, harvested during the exponential growth phase and single cells (n≥ 100) were examined under the fluorescent microscope. The number of ParB-YFP foci per cell was quantified. B. Bar graph depicts the chromosome state of cells expressed as the percentage of the total cells analyzed. N, chromosome number. Scale bar, 5µm.

Having confirmed that the *parB-yfp* construct was working appropriately, cells were induced to develop in submerged culture, harvested and developmental subpopulations were separated at various time points. Dispersed cells of the two separated cell fractions were examined under a fluorescent microscope (Fig. 2.37) as described earlier.

With this assay, I was unable to evaluate the genome content of spores because of their auto fluorescent nature. Interestingly, however even very late in development (T=84), when one might expect peripheral rods to be present pre-dominantly in the non-aggregated fraction, most non-aggregated cells were also found to possess two origins of replication suggesting that they contain two copies of the chromosome.

To conclude, my results suggested that the peripheral rods might also possess two copies of the genome instead of one and demonstrated that the

chromosome state of a cell cannot be used as a marker to distinguish between subpopulations of cells.

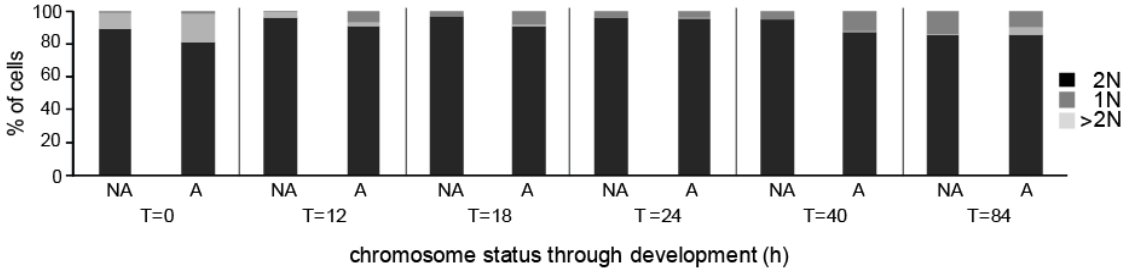

Fig. 2.37 Analysis of chromosome state of developmental subpopulations. Cells of the WT *attB*::P_{parB}-*parB-yfp* strain were developed in 16 ml submerged culture format, harvested and subjected to a low-speed centrifugation-based cell population separation assay through a developmental time course. Single cells (n≥ 100) of the two developmental populations were examined for Yfp foci at various time points as in Fig. 2.36A. NA, non-aggregated cells; A, aggregated cells. The column graph depicts the chromosome state of the separated cell populations expressed as the percentage of the total cells analyzed; N, chromosome number.

3. DISCUSSION

In the past, bacterial populations were always regarded as groups of identical cells with the same genetic make-up. However, gradually over these years, we have increasingly become aware that phenotypic heterogeneity exists in isogenic bacterial populations (Cozy & Kearns, 2010). Generation of different cell types is the characteristic of development in complex multicellular organisms (Robert *et al*., 2010). The challenge however, is to understand how cells of a genetically homogeneous population adopt distinct fates- as to whether cell fate decisions are stochastic by virtue of the feedback architecture of genetic networks or deterministically linked to the cell cycle or even a combination of both.

Myxococcus xanthus is an excellent model system for multicellular prokaryotic behaviour and Gram-negative differentiation. During the starvation induced developmental program, cells of the population undergo distinct fates- sporulation within multicellular fruiting bodies, differentiation into persister-like peripheral rods, cell clusters and cell lysis (Lee *et al*., 2012). The multicellular developmental program is tightly regulated by several positive feedback loops (refer section 1.2.2) that allow an orderly gene expression controlled both in space and time. These feedback loops may be involved in governing cell fate heterogeneity owing to the phenomenon of bistability (Dubnau & Losick, 2006; Smits *et al*., 2006) but not much is known precisely about how differentiation into the distinct cell types is regulated in our model organism.

At the start of this study, we hypothesized that MrpC, a key developmental transcriptional regulator, which is necessary for inducing aggregation and sporulation (Sun & Shi *et al*., 2001a) and had been implicated in mediating cell lysis (Nariya & Inouye, 2008) may act as a master cell fate regulator in *M. xanthus*. MrpC has been shown to accumulate heterogeneously in developmental subpopulations (Fig. 1.13, Lee *et al*., 2012) and its misaccumulation results in perturbed cell fate segregation (Fig. 1.16 & Fig. 1.17, Lee, PhD Thesis 2009). MrpC is known to be highly regulated. The accumulation if MrpC is controlled by at least three distinct signalling systems (EspAC, RedC-F and TodK). It has previously been proposed that MrpC positively regulates its own expression (Sun & Shi *et al*., 2001a). The activity of MrpC is also proposed to be regulated- it is inactivated by phosphorylation and activated by proteolytic processing to the shorter isoform MrpC2 (Nariya & Inouye, 2006) (refer section 1.3 for details). In the presented thesis, an attempt was made to characterize the role of MrpC in developmental cell fate determination in our model organism.

3.1 MrpC is a negative autoregulator and is regulated at the post-transcriptional level

The key transcription factor MrpC accumulates to different levels in the non-aggregated and aggregated developmental subpopulations (Lee *et al*., 2012) and the accumulation of MrpC can be correlated to cell fate segregation (Lee, PhD thesis, 2009). Thus, I wanted to investigate if this differential MrpC accumulation was regulated at the level of transcription. To address this question, a fluorescent promoter-reporter fusion (P_{mrpC}-*mCherry*) was generated for the analysis of *mrpC* promoter activity in developmental subpopulations.

Previously, Shi *et al*. proposed MrpC to be a positive regulator of its own expression as no *mrpC* expression was observed in a *ΔmrpC* background (Sun and Shi 2001a). Before using the *mrpC* reporter system for the intended analysis, it was first tested if the reporter was working appropriately. To our surprise, the reporter was over-expressed in the *ΔmrpC* background (Fig. 2.1). This data suggested that MrpC is a negative regulator of its own expression.

Since this observation had fundamental implications for the proposed model of MrpC's regulation, it needed further investigation. It became crucial to understand the reason for the discrepancy between the two results. The differences between the former and the presented study are as follows: 1) In the Sun & Shi study, the reporter was placed at the *mrpC* locus. In contrast, my reporter was placed at a secondary site (*att* site) in the genome. It is possible that there is a regulatory element upstream of the *mrpC* gene, *i.e.* between *mrpB* and *mrpC* which is lacking in my reporter system. 2) The Sun & Shi reporter contained 97 *mrpC* codons fused to the *lacZ* gene while my reporter contained 1 *mrpC* codon fused to the mCherry gene. It is possible that there is a regulatory element in the 5' end of the *mrpC* gene which is missing in my reporter system. 3) The Sun & Shi study was performed in the DK1622 wild type background while the presented study was carried out in the DZ2 wild type strain. Both these strains differ in their timing of development. 4) The Sun & Shi *ΔmrpC* strain contained the first 72 amino acids fused to the last 20 amino acids of *mrpC* while our *ΔmrpC* strain is more complete, containing the first 11 amino acids fused to the last 20 amino acids. 5) The two reporters are based on different detecting methods. The Sun & Shi group used a β-galactosidase enzymatic assay to detect *mrpC-lacZ* expression, while I used fluorescence as a measure of *mrpC* promoter activity.

Translational reporter fusions may sometimes be misinterpreted. The site at which a fusion is made can be important for mRNA stability or initiation of translation. For example, in case of the *arcDABC* operon of *Pseudomonas*

aeruginosa encoding enzymes involved in the arginine deaminase pathway, the more stable *arcA* mRNA is expressed in much higher amounts compared to the *arcD* mRNA as measured by Northern blot analysis but an *arcA-lacZ* fusion is expressed at much lower levels than an *arcD-lacZ* fusion. This discrepancy is due of the presence of an RNaseE-like cleavage at the farthest end of *arcD* mRNA that is excluded in the *arcD-lacZ* fusion resulting in greater stability and expression of the *arcD-lacZ* mRNA than the native *arcD* mRNA. Alternatively, the insertion of a *lacZ* reporter could destabilize an otherwise stable, highly expressed mRNA by lowering its half-life or disrupting a secondary structure important for translational regulation thus, leading to reduced or no expression (Pessi *et al*., 2001 & references therein). There could be such a problem with our fluorescent reporter fusion also, in addition to the fact that it was placed at a secondary site in the genome.

It was important to distinguish which of the two reporter systems were correct. Therefore, the *mrpC* mRNA levels were directly assessed by quantitative real-time PCR (qRT-PCR) using primers specific to the 5' UTR of the *mrpC* gene that is still present in the *ΔmrpC* strain (Fig. 2.3). In line with our fluorescent reporter analysis, *mrpC* was found to be over-expressed in the *ΔmrpC* background while no expression was observed in the *ΔmrpB,* $mrpB_{D58A}$ and $mrpB_{D58A}$ *ΔmrpC* strains. All the strains failed to aggregate and sporulate (Fig. 2.2). This result was consistent with the previously published analysis in the DK1622 wild type background in which no *mrpC* expression was observed in a *ΔmrpB* strain that failed to aggregate and sporulate as the $mrpB_{D58A}$ strain further confirming that *mrpB* phosphorylation at D58 was necessary for *mrpC* expression and hence, MrpC-mediated aggregation and sporulation (Sun and Shi 2001a). Taken together, my results revealed that *mrpC* levels are higher in a *ΔmrpC* strain suggesting that *mrpC* negatively regulates its own expression. It has been shown by *in-vitro* DNA binding assays that MrpC binds to at least eight sites in the upstream region of its promoter (Nariya & Inouye, 2006). Importantly, one of these binding sites overlaps with the putative -24 box of the σ^{54} driven *mrpC* promoter suggesting that MrpC can as well be a negative regulator of its own expression (Nariya & Inouye, 2006). A final step to confirm this result would be to complement the DK1622 *ΔmrpC* strain and check if the expression of *mrpC* is restored or alternatively, to complement the DZ2 *ΔmrpC* strain and check if the negative regulation on *mrpC* is relieved.

Based on the genetic analysis of the *mrp* locus by Sun & Shi (Sun and Shi 2001a) (Fig. 1.15), it is very well accepted that MrpC positively regulates its own expression. However, my results add information to the feedback-based regulatory network of *Myxococcus* development by revealing a previously unknown negative feedback loop on *mrpC* expression exerted by the master regulator itself. Apart from the known positive feedback loops [DevT on *fruA*

expression (Boysen *et al*., 2002)*;* C-signal amplification and FruA activation (Gronewold & Kaiser, 2001)] that could contribute to bistability, a negative feedback on *mrpC* could instead be involved to suppress the noise that could lead to population bifurcation (Davidson & Surette, 2008 and references therein).

After confirming that the *mrpC* fluorescent reporter was an appropriate reflection of its promoter activity, this reporter was employed to test if the differential MrpC accumulation in developmental subpopulations was regulated at the level of transcription. Cell populations were separated based on a low spin centrifugation assay into non-aggregated and aggregated cell fractions (Lee *et al*., 2012). It was known already that at 18 hours of development, the non-aggregated fraction is enriched in MrpC while in the aggregated fraction, MrpC levels are low and by the end of 36 hours, MrpC is specifically enriched in the aggregated cell fraction compared to the non-aggregated cell fraction. From the immunoblot and fluorescence results (Fig. 2.4), it was clear that early during development (18 hours), transcriptional differences did not account for the observed heterogeneity in MrpC accumulation in the non-aggregated and aggregated cell fractions as evident from the equal mCherry signal between the two cell fractions. However, later in development (36 hours), there was indeed an upregulation of transcription specifically in the aggregated cell fraction as seen from the increased mCherry signal in this fraction. This accounted for the higher MrpC levels compared to the non-aggregated cell fraction. Also, MrpC2 could be detected only in this late aggregated cell fraction which corresponds to cells being present in mounds by this time in development.

One of the caveats of this fluorescent reporter system was that the DZ2 *attB*::P_{mrpC}-*mCherry* strain employed for this analysis developed ~3 hours earlier than the wild type (Fig. 2.2) and displayed a slightly early MrpC accumulation (data not shown). This could be due to the presence of an extra copy of the *mrpC* promoter in this strain but since MrpC accumulated heterogeneously in the developmental populations as for the wild type, this strain could still be employed for our cell population analysis. However, the result of the fluorescent reporter analyses was additionally confirmed by measuring *mrpC* mRNA levels by qPCR on the separated cell populations of the native wild type strain so as to rule out any artefacts due to the presence of an extra copy of the promoter in the fluorescent reporter strain (Fig. 2.6). Another caveat of the fluorescent reporter system could be the half-life of mCherry. The mCherry fluorescence from P_{mrpC}-*mcherry* was found to be specifically increased in the aggregated cell fraction late during development; however, in the late non-aggregated fraction containing the peripheral rods, the fluorescence was observed to plateau after 24 h (Fig. 2.4). In the peripheral rod fraction, it could not be clearly distinguished if the transcription of *mrpC*

appeared to be constant due to the accumulation of mCherry in the cells or if it was even downregulated to account for the reduced MrpC levels in the non-aggregated cells.

Although an equal average expression of *mrpC* was observed between the two developmental populations of the aggregated and non-aggregated cells, it was possible that the expression levels were distributed across a population such that subpopulations existed at the single cell level. An advantage of the fluorescent reporter system was that it allowed monitoring expression in single cells. No significant difference in *mrpC* expression was observed between the non-aggregated and aggregated cell population at 18 hours of development (Fig. 2.5) although the protein accumulation was found to be significantly different. The broadly heterogeneous distribution of the fluorescent signal in single cells of both the populations suggested that at least the expression of *mrpC* was not the basis of bimodality or cell fate segregation during *Myxococcus* development. In conclusion, these results pointed towards a post-transcriptional level of regulation for the differential accumulation of the transcription factor in the developmental subpopulations.

3.2 MrpC's differential accumulation is likely not due to translational differences but due to a turnover event

The amount of total protein present in a cell at any given time is controlled by three fundamental processes- transcription, translation and protein degradation. Translational regulation allows cells to respond faster to physiological changes than transcriptional regulation (Brenneis & Soppa, 2009). Translational regulation in prokaryotes can be achieved in various ways for example via mRNA silencing by small non-coding RNA's (Waters and Storz, 2009), by regulatory elements in the 5' UTRs, or by the modulation of translational efficiency by regulatory RNA binding proteins (Brenneis & Soppa, 2009). For example, the major transcription regulator RpoS (σ^S), the master regulator of the general stress response in *E. coli,* is translationally stimulated by two *trans*-encoded sRNAs- DsrA and RprA that bind to *rpoS* mRNA and stabilize it. On the other hand, the sRNA MicF inhibits the translation of the mRNA encoding the major outer membrane porin OmpF in *E.coli* (Kaberdin & Bläsi, 2006).

With the result that MrpC's differential accumulation in the two developmental subpopulations early during development was not regulated at a transcriptional level, I generated a reporter system to measure the relative level of translation versus transcription of *mrpC* in the non-aggregated and aggregated cell fraction *in vivo*. This reporter system combines a translational and a transcriptional fusion construct to address the question if MrpC's heterogeneous accumulation is subject to a translational regulation. The strategy was to compare the

mCherry to Gfp signal ratios (representing translation and transcription respectively) at an average and single cell level between the two cell populations. At 18 hours of development, MrpC levels were found be higher in the non-aggregated fraction compared to the aggregated cell fraction. In case of a translational upregulation in the non-aggregated cell fraction (or a translational repression in the aggregated cell fraction) one would expect the mCherry to Gfp signal ratio to be higher in the non-aggregated cell fraction relative to the aggregated cell fraction. In case of no translational regulation, this ratio would be equal between the two cell populations. The two control reporters- one with the start codon of *mrpC* (or *mrpC-mCherry*) mutated and the other with the ribosome binding site (*rbs*) of Gfp mutated convincingly showed that the Gfp protein production was independent of mCherry. Mutation of the start codon of *mrpC* abolished mCherry protein production without affecting Gfp protein production while mutation of the rbs_{pilA} responsible for the translation of Gfp resulted in diminished Gfp production without altering mCherry production (Fig. 2.7). Therefore, I could show that the system worked as expected.

Using the translational-transcriptional reporter system, the comparison of the mcherry to Gfp ratios on a population level with immunoblot and fluorescence analysis (Fig. 2.9) as well as on a single cell level (Fig. 2.10) revealed no difference between the non-aggregated and aggregated cell populations suggesting that the heterogeneous MrpC accumulation early during development is not regulated at the level of translation. However, one of the caveats to this analysis was that the heterogeneous distribution of MrpC between the non-aggregated and aggregated subpopulations early during development (18 hours) was slightly perturbed in the reporter strain. This could be attributed to the presence of an extra copy of the *mrpC* promoter and a part of the *mrpC* sequence fused to mCherry protein. The fusion protein produced from this construct could interfere with the promoter binding activity of MrpC and thus, alter MrpC production. This observation further hints that the regulation of *mrpC* is delicately controlled in the cell and any alteration with the same affects the protein production and probably also its distribution within the two cell populations. Also, a degradation product of the $MrpC_{180}$-mCherry fusion was detected on the mCherry western blots, which corresponded to the native mCherry protein. This clipped product was detected in equal proportions in both the cell populations- the non-aggregated *vs* aggregated cell fraction signal intensity of the clipped product was similar to that of the full-length fusion protein, but it could interfere with the fluorescence analysis. Lastly, this reporter system relies on the fact that the mCherry and Gfp synthesis and degradation rate are comparable in the cell. A discrepancy would prevent from measuring correctly the translation and transcription rates simultaneously at any given time in a cell. Assuming that all the factors addressed above did not alter the

interpretation of my data, it seemed more likely that the differential MrpC accumulation was regulated at the level of protein degradation.

Proteolysis is yet another level of post-translational control that plays an important role in many regulatory systems, allowing the basal levels of regulatory proteins to be kept low and ensuring a rapid removal when they are no longer needed in the cell (Gottesman, 2003). Regulated protein degradation can be used by a cell to efficiently and robustly control key processes like cell division, stress responses, or cellular differentiation. For instance, the *E. coli* general stress response sigma factor RpoS, is rapidly degraded in exponentially growing cells by the ClpXP protease (and the adaptor RssB) but allowed to accumulate during the stationary phase or stress conditions (Hengge, 2009). The master transcriptional regulator CtrA in *C. crescentus* is degraded by the ClpXP protease to allow the swarmer-to-stalked cell transition during each cell cycle (Laub *et al*., 2007), and the transcriptional regulator ComK, required for competence development in *B. subtilis* is also known to be regulated by proteolysis to keep its basal levels low during exponential growth (Turgay *et al*., 1998).

It was recently shown in our lab that MrpC is controlled by proteolysis in the total cell population (Schramm *et al*., 2012). Therefore, I wanted to investigate if the differential MrpC accumulation in the two developmental subpopulations was subject to a protein turnover event. In our initial analysis, a strong turnover was observed in the aggregated cell fraction compared to the non-aggregated cell fraction at 18 hours in development (Fig. 2.11) suggesting that MrpC accumulates heterogeneously owing to a protein turnover specifically in the aggregated cell fraction. An MrpC half-life of ~41 minutes in the aggregated cell fraction was similar to that observed previously of MrpC (30±8 minutes) (Schramm *et al*., 2012) supporting the idea that the assay worked in principle. However, a drawback of this analysis was the reproducibility of the assay owing to the time required for the cell separation and the subsequent manipulation of samples (See appendix Table 5.1 for the variation between biological replicates). It seems that this assay was technically not the best to address the question of MrpC's turnover in the separated cell fractions. An alternate *in vitro* strategy to address the turnover of MrpC would be to add purified MrpC protein to 18 hour-old developmental cell lysates of the non-aggregated and aggregated cell fractions and subject them to immunoblot analysis to specifically detect the recombinant protein. In case MrpC is proteolysed specifically in the aggregated cell fraction, we would expect to detect less MrpC protein in the corresponding lysate. However, a disadvantage of this approach would be in the case if the recombinant MrpC protein lacks a post-translational modification- for example, phosphorylation, which might be a signal for specific degradation in the cell. No proteolysis would be observed in this scenario.

From my analysis, *mrpC* expression and probably also translation is not different in the developmental cell populations. It appears to be more likely that MrpC is regulated by a turnover event in the aggregated cell fraction leading to the observed heterogeneity in protein accumulation early during development. It still remains to be elucidated how this turnover of MrpC is mediated.

3.3 Tagging MrpC at the C- or N- terminus with mCherry alters its activity and/or turnover

We hypothesized that early during development (18 hours), the non-aggregated cell population, which is enriched in MrpC, is a heterogeneous population consisting of cells that will later aggregate, become peripheral rods or lyse. Later, as cells of this population progress through development to become true peripheral rods, the MrpC levels drop by the end of 36 hours. Therefore, I wanted to investigate the single cell distribution of MrpC to assess how levels of MrpC at a single cell level influenced cell fate segregation. Tagging a protein by fusing it with a fluorescent protein is a well known technique to assess the localization or distribution of a protein in a cell. To look at the single cell distribution of MrpC, strains bearing an MrpC protein fusion construct (promoter of *mrpC* including full length *mrpC* fused to the fluorescent protein mCherry at the N- or C-terminus) at the *att* site or at the endogenous locus were generated and analyzed. There were several problems with these constructs. Strains bearing the protein fusion construct displayed an early developmental phenotype- the WT *attB*::P_{mrpC}-*mrpC-mCherry* strain developed ~3 hours earlier while the *ΔmrpC attB*::P_{mrpC}-*mrpC-mCherry* strain developed ~7 hours earlier than the wild type (Fig. 2.12). The early developmental phenotype was also associated with an early production of an unstable fusion protein (Fig. 2.13). The tagging of mCherry to MrpC likely interfered with its normal function as a repressor resulting in an early accumulation. Alternatively, proteins that are specifically targeted for degradation in a cell usually contain intrinsic protease recognition signals at their N- or C- terminus (Gottesman, 2003) and masking them in this case could have adversely affected the turnover of MrpC. The instability of the chimeric product might have resulted in the cleavage of the fusion protein (Yewdell *et al*., 2011). Furthermore, when a differential MrpC-mCherry fusion protein accumulation was observed in the separated cell fractions on the immunoblots (Fig. 2.14), no difference in mCherry fluorescence signal was detected in the two cell fractions (Fig. 2.15). Such a non-correlation between immunoblot and fluorescence results could be either due to the quenching of fluorescence or due to the degradation of the fusion protein resulting in an altered mCherry fluorescence.

Taking into account all the above facts, it is evident that an alternate tool for single cell analysis of MrpC accumulation needs to be developed. MrpC levels

could be specifically detected at the single cell level by immunofluorescence with α`-MrpC antibodies. A problem with this technique is that signal detection relies on how each single cell is treated through the process of permeabilization and staining. However, our preliminary results suggest that this might be promising. A quantitative signal detection test could be performed by inducing MrpC under an inducible promoter to detect an increase in signal upon an increased induction. Alternatively, another strategy could be to tag MrpC with a smaller fluorescent tag which does not interfere with its degradation and folding.

3.4 Induction of MrpC under the vanillate/ IPTG inducible promoter might help to achieve over-expression to dissect cell fate decisions

As mentioned earlier, the levels of MrpC appear important in development and perhaps cell fate segregation (Lee, PhD Thesis 2009). I needed a tool to uncouple MrpC production from its own regulation and constitutively induce or over-express MrpC. I predicted to observe an early aggregation phenotype, probably also differences in developmental cell lysis and the proportions of cell populations to be altered. Conditional expression of a gene of interest is a powerful genetic tool to assess its function and is typically achieved by placing the gene under the control of an inducible promoter. The first choice was to test MrpC induction under the well-characterized *pilA* promoter since it is constitutively expressed at high levels during vegetative growth as well as development (Wu & Kaiser, 1997). The *pilA* promoter has been successfully used in the past to complement deletion mutants of various *M. xanthus* genes such as *csgA* (Lobedanz & Søgaard-Andersen, 2003), *crdS* (Willett & Kirby, 2012), *bacM* (Koch *et al*., 2011), and *romR* (Leonardy *et al*., 2007). Interestingly, however, a *ΔmrpC attB*::P_{pilA}-*mrpC* strain failed to develop and produced no MrpC protein. In contrast, the control strain *ΔmrpC attB*::P_{mrpC}-*mrpC* developed like the wild type and also produced MrpC at levels similar to the wild type (Fig. 2.16, Fig. 2.17). This result indicated that inducing MrpC under its native promoter from the *att* site was no problem in comparison to its induction under the *pilA* promoter. To add, Pkn14 could be successfully induced under the *pilA* promoter from the *att* site as evident from the complemented phenotype of a *Δpkn14 attB*::P_{pilA}-*pkn14 strain* (Fig. 2.25). Interestingly, the *mrpC* mRNA levels in the *ΔmrpC attB::*P_{pilA}-*mrpC* strain were found to be half in comparison to the wild type (Fig. 2.18). This observation suggested that *mrpC* was indeed expressed from the *pilA* promoter. The reason for not detecting any protein in this strain could be: (1) the levels of the induced transcript were not enough to produce detectable amounts of protein, and/or (2) the induced protein was subject to a rapid turnover in line with the result of the *in vivo* MrpC turnover assay performed in this study and also as reported previously (Schramm *et al*., 2012).

The first possibility could be addressed either by loading an excess amount of cell lysate for immunoblot analysis or by comparing the induced *mrpC* mRNA levels under starvation conditions because in comparison to vegetative conditions, *pilA* expression is upregulated ~1.3 to 1.75 fold around 12-15 hours in development (Wu & Kaiser, 1997) and also MrpC is easily detectable in the wild type. To rule out the second possibility of a turnover, we need information about the protease responsible to degrade MrpC and this is currently unknown. However, it might be possible to check MrpC induction by inducing MrpC from the same construct in a *ΔmrpC ΔespAC* background under developmental conditions. If the EspAC system regulates the protease responsible for the degradation of MrpC, one could expect to see some induced MrpC protein. We cannot rule out that induced *mrpC* transcript was for some reason not translated well in the *ΔmrpC* strain due to the lack of MrpC itself which might be involved directly/indirectly to stabilize/translate its own mRNA. To summarize, these results suggested that a stronger promoter was needed to achieve MrpC induction.

Therefore, the second choice was to test MrpC induction under the inducible multicopper oxidase *cuoA* promoter under the effect of copper. The expression from the copper promoter was found to increase linearly in a concentration-dependent manner (Gómez-Santos et al, 2012). It was recently reported that copper concentrations of up to 500 µM during vegetative growth and 60 µM during development did not affect the physiology of the wild type DK1622 strain. Also, a copper concentration of 120 µM was successfully used under vegetative conditions to achieve wild-type level of expression of the *pilB* gene, encoding the ATPase essential for social motility in *M*. *xanthus* (Gómez-Santos et al, 2012). In contrast, in the presented study, it was observed that a copper concentration as low as 40 µM prevented the wild type DZ2 cells from aggregating during development (Fig. 2.19). No induced MrpC protein could be detected in *ΔmrpC attB*::P_{cuoA}-*mrpC* strain under developmental conditions and also under vegetative conditions upon induction with different copper concentrations (data not shown). Furthermore, MrpC induction was additionally tested using the P_{cuoA}-$_{(+1)}$*mrpC* construct, in which *mrpC* was cloned until its predicted transcriptional start under the *cuoA* promoter. In this case, the native *mrpC* transcript would be expressed from the copper promoter. This was to exclude the possibility of a regulatory element (in the region upstream of the *mrpC* ORF) which might be required for the expression of the *mrpC* mRNA under native conditions. However, in total, MrpC could not be over-expressed using the copper inducible system.

So far, several systems for conditional expression of genes have been described in *M*. *xanthus*. Two of them are light-based inducible systems. The

first employs the P_{carQRS} promoter, which has a very low activity in dark but is expressed ~60 fold upon induction by light (Letouvet-Pawlak *et al*., 1990). The second uses the *M*. *xanthus* P_B promoter, which is repressed in the dark by vitamin B_{12} but is activated upon exposure to light (Garcia-Moreno *et al*., 2009). A limitation of both of these systems is their dependence on light for induction. Light exposure has been reported to impede multicellular fruiting body development (Li *et al*., 1992). Another inducible system is an IPTG-based system which employs the *M*. *xanthus pilA* promoter (P_{pilA}) in combination with a *lac* operator (*lacO*). It is inserted at the *pilA* chromosomal locus and the gene for the *E*. *coli* LacI repressor is supplied from the Mx8 *attB* site (Jelsbak & Kaiser, 2005). The limitations with the use of this system were a high level of basal expression and the need for chromosomal integration of two plasmids requiring both the available antibiotic selection markers in *M*. *xanthus*. Additionally, it is unsuitable because MrpC could not be induced under the *pilA* promoter as reported in this study (Fig. 2.16, Fig. 2.17). Importantly, very recently, two additional systems to achieve conditional expression in *M*. *xanthus* have been described (Iniesta *et al*., 2012). The first is an IPTG-inducible system with two *lac* operator sequences flanking one of the tandem *rrnD* (16 S rRNA) promoters of *M*. *xanthus* and a *lacI* gene to constitutively express the LacI repressor. The second is a vanillate-inducible system. It contains the vanillate-inducible P_{van} promoter including the operator and a gene for the constitutive expression of a repressor, VanR. Expression of the system is suppressed when VanR is bound to the operator but induced in the presence of vanillate. Both these systems are tightly controlled with essentially no expression in the absence of the inducer. Depending on the amount of the inducer, expression levels can be modulated such that either system can be used to conditionally express genes, for example, essential genes like *dksA*, *cdnL*, *ftsZ* have been demonstrated to be successfully induced under both of these promoters. The two systems operate during vegetative growth as well as during development and can serve as useful tools to achieve simultaneous induction of different genes in the cell. Thus, the new IPTG-based and the vanillate-based inducible systems might prove useful to achieve MrpC/MrpC2 induction to dissect its role in regulating cell fate decisions.

3.5 MrpC2 and MrpC-P may have a different role *in vivo* than proposed earlier based on *in vitro* data

A next step was to gain some information about the effect of MrpC activity on cell fate segregation by generating strains that only produced the proposed isoforms of MrpC. The previously proposed model for the regulation of *mrpC* by its various isoforms is described below (Fig. 3.1).

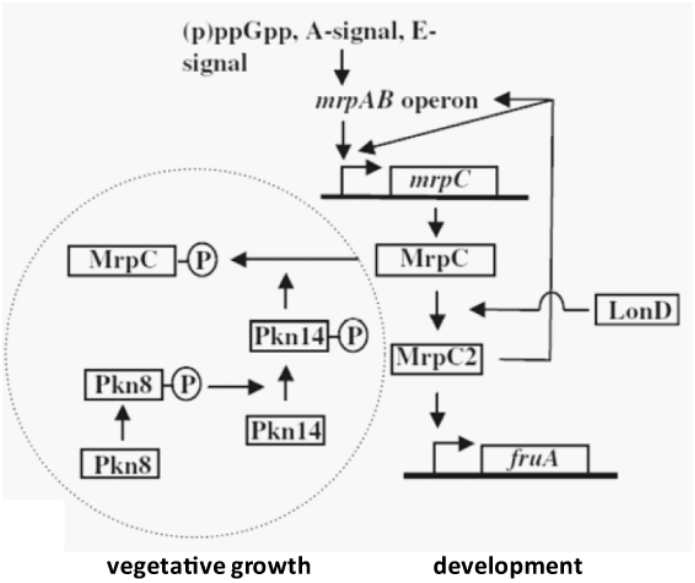

Fig. 3.1 A proposed model for regulation of *mrpC* expression during *M. xanthus* development (Figure modified from Ueki & Inouye, 2006)

It was proposed that under vegetative conditions, *mrpC* is expressed at low levels and the MrpC produced is phosphorylated by Pkn14, which is in turn activated by Pkn8 (Nariya & Inouye, 2005). It was suggested that the Pkn8-Pkn14 kinase cascade negatively regulates *mrpC* expression by phosphorylating MrpC during vegetative growth as the *Δpkn8* and *Δpkn14* strains display an early developmental phenotype with the production of highly elevated levels of MrpC/MrpC2 and FruA both during vegetative growth and development in comparison to the parent strain DZF1 (Nariya & Inouye, 2005, 2006). It was shown by *in vitro* DNA binding assays that the DNA binding activity of MrpC is greatly reduced upon its phosphorylation by Pkn14 (Nariya & Inouye, 2006). It is thought that early during development, *mrpC* is induced in an MrpAB dependent manner (Sun and Shi, 2001a). The newly synthesized MrpC is most likely unphosphorylated as Pkn14 expression is downregulated during development (Nariya and Inouye, 2005). It was proposed that during development, MrpC is clipped into a shorter isoform called MrpC2 which lacks the N-terminal 25 residues of MrpC. From previous literature, it is not really clear what exactly is the isoform MrpC2. It was initially identified as the *fruA*-promoter binding protein (FBP) and purified from developmental cell extracts (Ueki & Inouye, 2003). From the N-terminal sequence, FBP was found to be identical to the proposed sequence of MrpC (Sun & Shi, 2001a) from residues 33 to 53. A methionine residue is present seven bases upstream from the residue 33 (Leucine) in MrpC, therefore, a recombinant MrpC2 lacking the N-terminal 25 residues of MrpC was purified and shown to bind the *fruA* promoter with the same affinity as the FBP (Ueki & Inouye, 2003). It is thought that MrpC is likely proteolytically processed to MrpC2 by the protease LonD because MrpC2 was not detected in a *lonD* mutant in which *fruA* expression was also found to be low

(Nariya & Inouye, 2006). It was shown by *in-vitro* DNA binding assays that MrpC2 has a higher affinity for *mrpC* and *fruA* promoter regions than MrpC itself. Thus, it was suggested that MrpC2 is a positive regulator of *mrpC* and *fruA* expression (Nariya & Inouye, 2006). It was demonstrated that Pkn14 does not phosphorylate MrpC2 but phosphorylates MrpC at Thr residue(s) *in vitro*. Therefore, it was proposed that Thr-21 and/or Thr-22 is (are) the likely site(s) of MrpC phosphorylation (Nariya & Inouye, 2006). Furthermore, it is thought that phosphorylation of MrpC (MrpC-P) inhibits its proteolytic processing to MrpC2 as it was found to be present at high levels during vegetative growth in the *Δpkn8* and *Δpkn14* strains (Nariya & Inouye, 2006).

First, the role of the isoform MrpC2 was addressed by generating an $mrpC_{\Delta 1\text{-}25}$ strain that expresses only the proposed more active form of the transcription factor, MrpC2 (Nariya & Inouye, 2006). It should be mentioned that the $mrpC_{\Delta 1\text{-}25}$ strain was generated at a frequency of 1/100 recombinants; most of them were wild type. It is possible that the constitutive production of MrpC2 is toxic to the cells and this strain is a suppressor of a gene involved in cell death. The observation that this strain failed to develop (Fig. 2.20) was contrary to the prediction that MrpC2 is an inducer of *mrpC* expression (Nariya & Inouye, 2006). We predicted this strain to have an early developmental phenotype. The $mrpC_{\Delta 1\text{-}25}$ strain produced MrpC2 at levels comparable to the wild type, but only basal levels of FruA (P. Mann, data not shown). The increased *mrpC* expression (Fig. 2.21) and the lack of FruA in this strain background suggest that the MrpC2 produced in this strain is inactive and not efficiently binding to its own and *fruA* promoter *in vivo*. Interestingly, however, EMSA assays with MrpC and MrpC2 indicate that MrpC2 binds with equal affinity as MrpC to the *mrpC* promoter (Mann & Higgs, data not shown). This discrepancy could be attributed to the presence of affinity tags on the recombinant protein used for the *in vitro* analysis. It is also possible that the cleavage of the N-terminal 25 amino acid residues from MrpC to produce MrpC2 is designed to render the protein inactive. Therefore, the binding of MrpC2 to target promoters *in vivo* needs to be investigated further by ChiP (chromatin immunoprecipitation) analysis, for example.

The $mrpC_{\Delta 1\text{-}25}$ strain displayed a growth defect as evident from the round cells observed in developmental samples (Fig. 2.23) and the instability of freezer stocks. Furthermore, it mimicked the *ΔmrpC* strain in terms of its inability to form glycerol induced spores (Fig. 2.22). Another caveat to this analysis was that the isoform MrpC2 is not well defined (explained above), although we employed the same isoform that has been used previously in studies by various other groups.

In light of the aforementioned facts, it becomes important in the future to investigate the true biological role of MrpC2. MrpC2 is required for the activation

of several target genes, for example, *fruA*, *mazF*, *dev*, *fmgA*, *fmgBC* and some of these are late developmental genes having a role in aggregation and sporulation (Kaiser *et al*., 2010). MrpC2 binds with FruA cooperatively to the promoters of *fmgA* (Mittal & Kroos, 2009a), *fmgBC* (Mittal & Kroos, 2009b) and *dev* (Mittal & Kroos, 2009a, as unpublished data). The *dev* locus is known to be expressed at high levels only in cells present in nascent fruiting bodies (Julien *et al*., 2000). Additionally, from the results obtained in this study, MrpC2 was found to be present specifically in the aggregated cell fraction at the end of 36 hours when the cells are already in mounds (Fig. 2.4) consistent with a role late during development. Therefore, another approach to understand how MrpC2 might influence gene expression (its own and other targets) and cell fate decisions would be to alter the timing of MrpC2 production at various stages during development by expressing it under an inducible promoter as explained in detail in section 3.4.

The next attempt was to analyse the effect of the phosphorylated state of MrpC. Results obtained earlier in our lab showed that a *Δpkn14* strain in the DZ2 background displays a delayed developmental phenotype (P. Mann) contrary to previously published data (Nariya & Inouye, 2005). Furthermore, the various MrpC phosphorylation point mutants (*mrpC*$_{T21A}$, *mrpC*$_{T22A}$ and *mrpC*$_{T21-22A}$), in which the proposed phosphorylation sites (Thr-21/22) have been mutated to an alanine, did not exhibit a significantly altered developmental phenotype (Mann & Bhardwaj, data not shown). All these observations together initiated an in-depth analysis of the phosphorylated state of MrpC.

In the presented study, as a first step, I analyzed the developmental phenotype and the MrpC accumulation pattern of the *Δpkn14*, *pkn14*$_{K48N}$ and mrpC$_{T21-22A,S23-24A}$ quadruple phosphorylation mutants in the DZ2 background (Fig. 2.24). Intriguingly, the *Δpkn14* strain developed ~6 hours later than the wild type and accumulated MrpC at levels comparable to the wild type. This observation was contradictory to the published early developmental phenotype of the *Δpkn14* strain (DZF1 background) which accumulated MrpC/MrpC2 earlier and at elevated levels than the parent DZF1 wild type (Nariya & Inouye, 2005). However, the Pkn14 auto-phosphorylation deficient mutant, *pkn14*$_{K48N}$, displayed a wild-type phenotype along with wild-type MrpC accumulation levels. Previously, the constitutive expression of Pkn14$_{K48N}$ in the DZF1 background was shown to result in an early developmental phenotype (Nariya & Inouye, 2005). Therefore, these two contrasting observations put the role of Pkn14 under question. The discrepancy between previously published data and the presented results could be attributed to the difference in the wild type backgrounds. Previous analysis was performed in the mutant DZF1 (DK101) background that carries a *pilQ1* mutation and is partially deficient in social motility (Wall *et al*., 1999) while the presented study was performed in the DZ2

background. Previously, the reported phenotype for the deletion of the gene *mazF*, encoding an endoribonuclease thought to be involved in programmed cell death in the DZF1 background (Nariya & Inouye, 2008) was also found to not hold true in the other two wild type strains DZ2 and DK1622 (Lee *et al*., 2012; Boynton *et al*., 2013). The observation that the *Δpkn14* strain (DZ2 background) can be complemented (Fig. 2.25) supported the idea that the observed delayed phenotype was indeed due to the absence of the kinase. Hence, the early developmental phenotype of the *pkn14* mutants in the DZF1 background might be an adaptation in this mutant strain.

The *mrpC*$_{T21\text{-}22A,S23\text{-}24A}$ quadruple phosphorylation mutant exhibited a strong delayed developmental phenotype but produced MrpC slightly earlier and at higher levels than the wild type. This suggested that the phenotype was not a result of the absence or instability of the mutant protein, although it was possible that it indeed resulted from the loss of activity of MrpC in this strain. However, this was ruled out by the fact that the target of MrpC, FruA was produced in this strain at levels comparable to the wild type (data not shown), further suggesting that the phosphorylation of MrpC was not necessary for the induction of *fruA*.

Analysis of sporulation efficiency in the aforementioned mutant strains at the end of development was also noteworthy (Fig. 2.24). The *Δpkn14* and *pkn14*$_{K48N}$ strains were reduced in sporulation to ~60% of the wild type while the *mrpC*$_{T21\text{-}22A,S23\text{-}24A}$ mutant was significantly reduced in sporulation to ~20% of the wild type. These interesting observations prompted us to additionally analyse the sporulation of the *mrpC* single/double phosphorylation point mutants that were available in the lab. Importantly, an *mrpC*$_{S23\text{-}24A}$ mutant produced spores at levels comparable to the wild type, however, an *mrpC*$_{T21\text{-}22A}$ mutant was also reduced in sporulation like the *Δpkn14* and *pkn14*$_{K48N}$ strains (data not shown). The drastic reduction in sporulation in the *mrpC*$_{T21\text{-}22A,S23\text{-}24A}$ quadruple phosphorylation mutant (~20% of the wild type) and the strong developmental phenotype could be attributed to the fact that in addition to the proposed phosphorylation sites (T21-22A), two additional residues (S23-24A) are mutated in this strain which could affect the binding of the protein to the kinase (explained below). However, in conclusion, these results together suggested that that the presence of an active Pkn14 kinase and MrpC phosphorylation at the Thr-21/22 residue(s) might be important for sporulation during development. In line with this result, a number of other protein Ser/Thr kinases (PSTKs) are known to play a role during fruiting body development and sporulation in *Myxococcus*. The deletion of the PSTK Pkn1, which is expressed only during development, leads to premature fruiting body formation and a poor spore yield (Munoz-Durado *et al*., 1991). The deletion of the kinase Pkn9 leads to delayed development and also poor spore production (Hanlon *et al*., 1997). The deletion

of the kinases PktA5 and PktB8, results in the formation of translucent mounds and low spore yields during development (Stein *et al*., 2006).

In addition to the generation and analysis of various mutant strains for the *in vivo* analysis of the activity of phosphorylated MrpC, I tried to reproduce the results of the published *in vitro* analysis (Nariya & Inouye, 2005) to confirm the phosphorylation of MrpC by Pkn14 (Fig. 2.26) and to further link it with the observed phenotypes of the Pkn14 and MrpC phosphorylation mutants. My analysis confirmed that Pkn14 autophosphorylates and phosphorylates MrpC. $Pkn14_{K48N}$ was incapable of autophosphorylation and did not phosphorylate MrpC. These observations were consistent with the previously published analysis (Nariya & Inouye, 2005). Further, I additionally tested various MrpC mutants for phosphorylation by Pkn14 to address the exact phosphorylation site in MrpC. It was revealed that Thr-21 is the preferred phosphorylation site in MrpC as the signal observed for the phosphorylation of $MrpC_{T22A}$ mutant protein by Pkn14 was lost in case of the $MrpC_{T21\text{-}22A}$ mutant protein. A confirmatory step in this direction would be to additionally test the $MrpC_{T21A}$ mutant protein for phosphorylation by Pkn14. We would expect that it is not phosphorylated by Pkn14. A surprising result was that the truncated form of MrpC, MrpC2 was also found to be phosphorylated by Pkn14 suggesting that Thr-21 might not be the only site of phosphorylation in MrpC. Contrarily, it was shown earlier that the N-terminal 25 residues of MrpC are required for phosphorylation by Pkn14 as MrpC2 cannot be phosphorylated by Pkn14 even though it interacts with Pkn14 (Nariya & Inouye, 2006). We cannot rule out that the variability in the two results could be due to the difference in the recombinant proteins. In the Nariya & Inouye study, MrpC2 was expressed with 12 amino acid N-terminal additions containing 10x histidine tags while in this study, MrpC2 was expressed with 28 amino acid N-terminal additions containing 6x histidine tags. It is possible that having a different N-terminus exposed new phosphorylation site(s) for Pkn14 due to a different configuration of MrpC2. However, I could not detect the quadruple phosphorylation mutant protein $MrpC_{T21\text{-}22A,S23\text{-}24A}$ to be phosphorylated by Pkn14. It was likely that the kinase-substrate recognition was lost in this case as the residues situated immediately at the N- and C-terminal to the phosphorylation site (T21-22) are also mutated in this version of MrpC. It is known that up to three residues situated on either side of the phosphorylation site act as consensus sequences to often contribute substantially to kinase-substrate recognition (Ubersax & Ferrell, 2007). In this analysis, a random protein molecule that lacked a kinase/phosphatase activity and carried the same N-terminus as all the other recombinant proteins was used as a control for the non-specific phosphorylation of the tag. Bovine serum albumin (BSA) was used as another control protein to test the ubiquity of phosphorylation by the kinase Pkn14. Both these control proteins were not phosphorylated by Pkn14 (see

appendix Fig. 5.1) consistent with the fact that the above results were not an artefact of non-specific phosphorylation by the kinase.

My results revealed that a *Δpkn14* strain and a strain that produces only the autophosphorylation deficient form of Pkn14, *pkn14*$_{K48N}$ do not display an early developmental phenotype contradictory to the proposed role of Pkn14 to phosphorylate MrpC and down regulate its expression (Nariya & Inouye, 2005). In addition to the result that the activity of Pkn14 and MrpC phosphorylation appears to be important during development for sporulation, it also appears likely that the phosphorylation of MrpC can be achieved alternatively without the presence of an active Pkn14. I speculate that the kinase Pkn8 of the Pkn8/Pkn14 kinase cascade could interact with MrpC and phosphorylate it. Previously, a Pkn8 autophosphorylation deficient mutant (Pkn8$_{K116N}$) could not be phosphorylated by Pkn14 *in vitro* and thus, Pkn8 was placed upstream in the kinase pathway (Nariya & Inouye, 2005) but the interaction of Pkn8 with MrpC has not been tested so far. The fact that Pkn14 expression is upregulated only during the mid-log to late-log phase during vegetative growth while Pkn8 expression is upregulated during vegetative growth as well as starvation (Nariya & Inouye, 2005) further supports the idea of the involvement of Pkn8 in MrpC phosphorylation during starvation. The expression of the kinases Pkn14 and Pkn8 could also be investigated in the DZ2 background to link their exact role to the regulation of *mrpC* expression. From the results obtained earlier in our lab, a *Δpkn8* mutant could not be generated in the DZ2 background (P. Mann).

The biological significance of the phosphorylation of MrpC/MrpC2 by Pkn14 is not yet clear. To address this, the first step is to determine the exact phosphorylation sites in MrpC by mass-spectrometric analysis of the *in vitro* non-radioactively phosphorylated protein samples. Furthermore, the phosphorylation of MrpC2 needs to be confirmed *in vivo*. This can be done by immunoprecipitation of MrpC2 *in vivo* and subsequent analysis by mass-spectrometric analysis. This is partly in progress. Moreover, the expression of important developmental regulators like *mrpC* and *fruA* could be analysed in the various *mrpC* phosphorylation mutant strains in order to understand how the phosphorylated isoform of MrpC regulates the expression of target promoters. Last but not the least, *in vitro* DNA binding assays could be performed with the various mutated versions of MrpC in the presence and absence of the kinase Pkn14 to study the effect of phosphorylation on the DNA binding ability of MrpC/MrpC2 to its target promoters e.g. *mrpC* and *fruA*.

3.6 Mxan_5126 does not play a significant role during development

It is not uncommon that some accessory proteins can alter the activity of important regulatory proteins. For example, the master transcriptional activator

ComK, responsible for the development of competence in *B. subtilis*, is bound by the adapter protein MecA and targeted to the ClpC-ClpP protease for degradation (Leisner *et al*., 2008); the anti-repressor protein SinI binds to the pleiotropic response regulator SinR and prevents it from binding DNA and thus, induces the expression of genes involved in matrix production (Chai *et al*., 2008). It was previously shown that the endoribonuclease MazF interacts with MrpC and prevents it from being phosphorylated (Nariya & Inouye, 2008). The gene Mxan_5126 was found to be present immediately downstream of MrpC. Interestingly, it contains a domain common to immunity proteins in bacterial toxin systems. It was plausible to think that this protein could be involved to modulate MrpC activity. Therefore, I began to analyze the hypothetical protein Mxan_5126. Reciprocal Blastp analysis and genome comparison revealed the gene to be present only in *M. xanthus* and the close relative *Anaeromyxobacter dehalogenans* (Fig. 2.27). The fact that MrpC and Mxan_5126 were found to be transcribed together (Fig. 2.28) led to further investigation of the role of Mxan_5126 by deleting this gene. I expected to observe a dramatic phenotype; however, the deletion of this gene had no effect on development and sporulation (Fig. 2.29). Lastly, to be able to assign a function to this gene and address its association with MrpC, I wanted to investigate if the protein was produced in the cell and how it localized within the cells. I generated a C-terminal fusion of mCherry to this gene at the endogenous locus and analyzed the accumulation of mCherry with immunoblot and fluorescence analysis (Fig. 2.30). Unfortunately, no mCherry could be detected in the immunoblot analysis and only a very weak fluorescence signal was observed in single cells that precluded analyzing its production and localization. These results suggested that either the protein fusion was non-functional and degraded rapidly or that Mxan_5126 is not a real protein.

To summarize, Mxan_5126 does not play a significant role in development or influence the activity of MrpC to affect cell fate decisions.

3.7 Targets of MrpC do not follow the differential accumulation of MrpC

At the start of this study, we correlated the levels of MrpC to a particular cell fate. A good assay based on differential centrifugation was also available to track the segregation of cells into the non-aggregated and aggregated cell populations through development. So far, based on our low-speed centrifugation assay, we can only separate cell clusters and peripheral rods from the rest of the population at 18 and 36 hours of development, respectively. As a second part of the project, I adopted a reverse approach to understand the role of MrpC in cell fate decisions. I wanted to identify transcriptional markers to be able to differentiate between developmental subpopulations and finally, look at the

levels of MrpC in a particular cell fraction. As a first step, I investigated the expression of two of the targets of MrpC/MrpC2.

fruA, a transcriptional target of MrpC (Ueki & Inouye, 2003), encodes a transcriptional regulator (FruA) which is required for the induction of aggregation (Ogawa *et al*., 1996) and accumulates heterogeneously in the non-aggregated and aggregated cell populations (Lee *et al*., 2012) as is true for MrpC. The rationale was that since MrpC accumulates differentially in the developmental subpopulations, its targets might be differentially expressed in the different cell populations. Given that FruA induces the transcription of several late genes involved in aggregation and sporulation (Vishwanathan *et al*., 2007, Licking *et al*., 2000), we thought that it could serve as a cell-specific marker for the aggregated cells. Hence, to monitor the expression of *fruA* in developmental subpopulations, I constructed a P_{fruA}-*mCherry* reporter. The expression of the P_{fruA}-*mCherry* reporter was first checked in the *ΔmrpC* background and no mCherry expression was detected (data not shown). This observation was consistent with the fact that MrpC is necessary for *fruA* induction (Ueki & Inouye, 2003) and further confirmed that the reporter was functioning appropriately. *fruA* expression observed using the fluorescent reporter system in this study was slightly different than reported previously by qRT-PCR on the wild type DZ2 (Higgs *et al*., 2008). In the former, expression was induced between 12-18 hours in development and peaked at 30 hours while in the latter, expression was induced as early as 2 hours in development and peaked at 24 hours. This difference was likely due to the different methods used to measure *fruA* expression. In the presented study, no significant difference in *fruA* expression was detected between the two developmental subpopulations at the average population level (Fig. 2.31) as well as at the single cell level (Fig. 2.32). These results suggested that the different accumulation levels of MrpC do not seem to significantly affect the expression of its target *fruA*. Given that FruA accumulates heterogeneously in developmental subpopulations (Lee *et al*., 2012), these results further suggested that *fruA* might be regulated at the post-transcriptional level. It has been published that *fruA* has a long 5' untranslated region (UTR) that is absolutely necessary for the induction of FruA synthesis during development (Ding & Zheng *et al*., 2008). It has also been suggested that this 5' UTR could influence FruA protein production by affecting its translation (Ding & Zheng *et al*., 2008). Therefore, it is possible that *fruA* is translationally regulated.
The second target of MrpC to be investigated was *mazF*, a gene encoding an endoribonuclease which at the time of this study had been implicated in mediating developmental lysis (Nariya & Inouye, 2008). It has been demonstrated that MrpC/MrpC2 binds the *mazF* promoter and activates its transcription (Nariya & Inouye, 2008). I wanted to investigate if *mazF* would serve as an exclusive transcriptional marker for the cell population that is destined to lyse during development. As for the P_{fruA}-*mCherry* reporter, the

expression of the P_{mazF}-*mCherry* reporter was checked in the *ΔmrpC* background and no mCherry expression was detected (data not shown). This observation was consistent with the fact that MrpC is required for *mazF* induction (Nariya & Inouye, 2008). Additionally, the *mazF* expression in the DZ2 wild type background was quite similar to that reported earlier in the DZF1 background using a P_{mazF}-*lacZ* fusion (Nariya & Inouye, 2008). This suggested that the reporter was an appropriate reflection of *mazF* expression. Also, the observed fluorescence signal was not very strong relative to that observed for *mrpC* or *fruA*, consistent with the idea that *mazF* is a toxin and is enough to be expressed at low levels to mediate its toxic effect. No significant differences could be observed for *mazF* expression in the non-aggregated and the aggregated sub-populations at the average population level (Fig. 2.33) as well as at the single cell level (Fig. 2.34).

To summarize, it was indeed intriguing that both the targets of MrpC, *fruA* and *mazF*, did not follow the heterogeneous accumulation pattern of MrpC in the two subpopulations. However, a caveat to such an analysis could be that the fluorescent reporter was not sensitive enough to reveal small changes in expression. Therefore, to rule out this possibility, *fruA* or *mazF* mRNA levels in the separated populations could be measured by qRT-PCR as done already for *mrpC*. Alternatively, as mentioned earlier, the expression of targets of MrpC could also be investigated in the various phosphorylation mutants of MrpC or the $mrpC_{\Delta 1\text{-}25}$ strain in order to assess how the activity state of MrpC influences target gene expression.

3.8 The aggregated population specific FibA metalloprotease is likely regulated at the post transcriptional level

As a last possibility, to assign a cell-specific transcriptional marker to one or more of the developmental subpopulations, I examined if FibA, the heterogeneously accumulating aggregated fraction-specific extracellular metalloprotease (Lee *et al*., 2011) could serve as a transcriptional marker exclusively for cell clusters to differentiate them from the rest of the population. Analysis of *fibA* expression using a fluorescent reporter revealed that the accumulation of FibA specifically in the aggregated cell fraction is not due to increased promoter activity in the aggregated cell fraction and that it was not a transcriptional marker for the cell clusters at the single cell level (Fig. 2.35). It is also likely that *fibA* is post-transcriptionally regulated. Intriguingly, a translation attenuator is predicted for *fibA* since both the predicted AGGAGG ribosome binding site and ATG start codon are predicted to be sequestered in a stable stem-loop structure (Lee *et al*., 2012).

3.9 Chromosome status cannot be used as a marker to distinguish between populations and peripheral rods might possess a 2N genome instead of 1N

As shown above, we could not differentiate between developmental subpopulations on the basis of a transcriptional marker. It is known that the replication of DNA in the early aggregation phase is necessary for development to proceed (Tzeng & Singer, 2006). Furthermore, it was reported, that all myxospores contained two copies of the genome while peripheral rods contained only one copy of the genome (Tzeng & Singer, 2005). Therefore, I wanted to investigate if I could differentiate specifically only the peripheral rods from the non-aggregated cell fraction, early during development. Such an idea was consistent with cell fate being linked to the cell cycle as in case of the swarmer and stalked cell differentiation in *Caulobacter* (section 1.1.4). For my analysis, I used a novel reporter system (Harms & Søgaard-Andersen, unpublished) which was based on the binding of the ParB-Yfp fusion protein to the origin of replication forming fluorescent foci, thus, indicating the chromosome status of a cell. I showed that the two developmental subpopulations *i.e.* the non-aggregated and aggregated cells did not differ in their chromosome status and both possess two copies of the genome (2N) (Fig. 2.37). My data also suggested that even peripheral rods are 2N instead of 1N as proposed. A reason for this discrepancy from the results of Tzeng & Singer might be that they used flow cytometry to quantitate the DNA content of myxospores and cells (peripheral rods) associated with fruiting bodies using *B. subtilis* endospores as a standard. In the Tzeng & Singer study, the DNA content of myxospores was verified by DAPI staining and fluorescence microscopy with *Bacillus* spores, however, it is possible that the chromosome status of peripheral rods was misinterpreted based on the flow cytometric data alone given that *Bacillus* spores and *Myxococcus* cells differ in their chromosome size (4.2 Mbp of *Bacillus vs* 9.2 Mbp of *Myxococcus*) (Kunst *et al*., 1997; Goldman, Nierman *et al*., 2006).

In addition to the presented experiments, the following could be done in the future with the ParB-Yfp tool to support the above results: (1) the chromosome state of stationary phase cells could also be analysed as for exponentially growing cells (Fig. 2.36). This would serve as an additional proof that the tool works appropriately. (2) True peripheral rods could be separated from the rest of the population late during development (at the end of 120 hours) using a sucrose-density gradient centrifugation for precision or even the low-speed centrifugation technique used in this study and analysed for their chromosome content. (3) Starvation spores could be partially germinated in the presence of the RNA polymerase inhibitor, rifampicin or the DNA replication inhibitor,

nalidixic acid and analysed for their DNA content as untreated myxospores were otherwise auto fluorescent making their analysis impossible in this study.

It still remains to be elucidated as to what extent and how the decisions relating to cell fate are influenced by the feedback loops in genetic networks involved in cell signalling and simultaneously coupled to the cell cycle that governs the chromosome state of cells.

3.10 Conclusion

In the presented work, I tried to understand the regulatory mechanism(s) behind cell fate differentiation in our model organism *Myxococcus xanthus*. I started with the detailed characterization of the transcription factor MrpC which we hypothesized as the master regulator of cell fate in this system.

As part of my analysis, we realized that so far, all our models regarding the regulation of *mrpC* by its various isoforms and its precise role in cell fate decisions have been based on previously published literature. However, as highlighted in some of the above sections, some of this data needs to be carefully interpreted and investigated in greater detail to re-build models involving the master regulator MrpC and aid in a better understanding of the regulation of cell fates. Therefore, based on the results obtained in this study, I propose the following model (Fig. 3.2) for the regulation of *mrpC*.

The genetic analysis performed in this study was consistent with the idea that the response regulator MrpB is essential for the induction of *mrpC* expression (Sun & Shi, 2001a) as no *mrpC* expression was observed in the *ΔmrpB* strain. However, my analysis revealed a novel negative feedback loop in the regulation of *mrpC* expression. *mrpC* was expressed at higher levels in the *ΔmrpC* strain suggesting it to be a negative regulator of its own expression. MrpC's negative regulation of its own expression can either be direct or indirect. It can either bind directly to its own promoter to repress the induction of its expression or indirectly, by repressing the *mrpAB* promoter. It is not yet clear if MrpC is also a positive regulator of its own expression as previously proposed (Sun & Shi, 2001a). My analysis further revealed that the differential accumulation of MrpC was not due to transcriptional or translational differences but likely due to stimulation of turnover of MrpC specifically in the aggregated cell fraction. This result was in line with the regulation of MrpC accumulation in the total population by the EspAC signalling system mediated proteolytic event (Schramm *et al*., 2012). The two mechanisms- negative regulation of *mrpC* expression and proteolysis of MrpC, represent a strategy to tightly control and fine tune MrpC levels in this system such that this important developmental regulator is allowed to accumulate only gradually during development. The gradual increase in MrpC

levels would ensure a proper coordination between mound formation and sporulation only within aggregates.

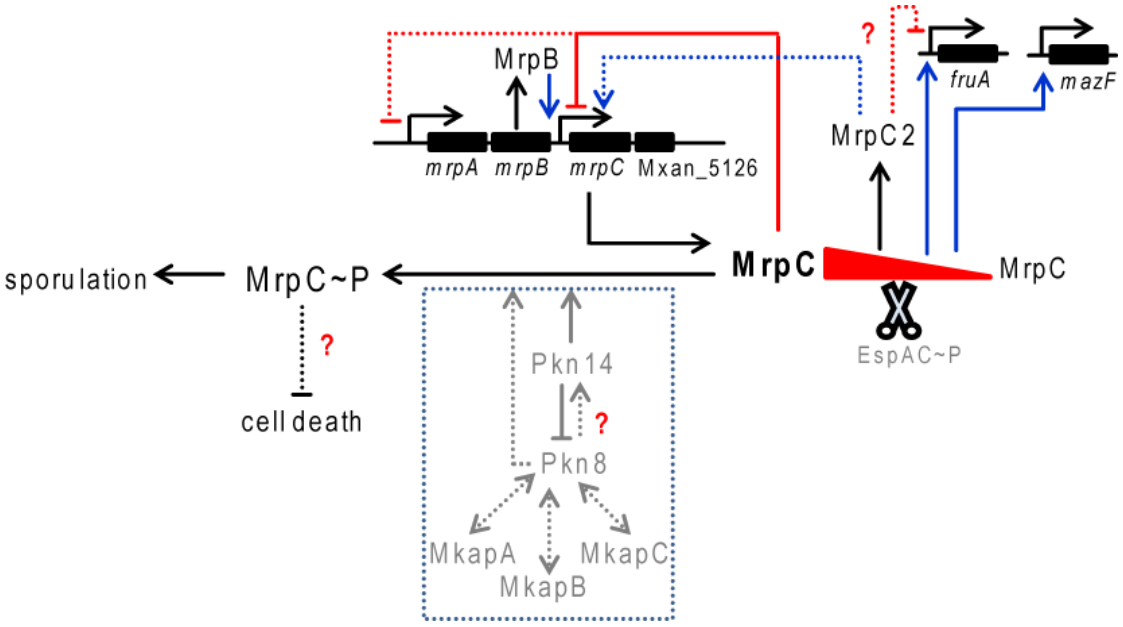

Fig. 3.2 Our current model for the regulation of *mrpC* expression during *M. xanthus* development. Red coloured T-bar, negative regulation; blue coloured arrow, positive regulation; coloured red triangle, MrpC levels; ?, yet unknown; ~P, phosphorylation; dotted lines, putative interaction.

The analysis of the phosphorylation state of MrpC revealed that it is phosphorylated by Pkn14 *in vitro* (preferentially at the Thr-21 residue). The phosphorylation of MrpC and the presence of active Pkn14 are important during development in sporulation as evident from the reduction in sporulation efficiency of the *Δpkn14*, *pkn14*$_{K48N}$ and the *mrpC*$_{T21-22A}$ mutants. I demonstrated that the *Δpkn14* and the *pkn14*$_{K48N}$ mutant strains do not display an early developmental phenotype and early MrpC accumulation contrary to the proposed role of Pkn14 to phosphorylate MrpC and down regulate its expression (Nariya & Inouye, 2005). I, therefore, speculate a possible involvement of the kinase Pkn8 to directly phosphorylate MrpC in the absence of Pkn14. It was shown that Pkn14 is incapable of phosphorylating the kinase deficient mutant of Pkn8 (Pkn8$_{K116N}$) *in vitro* (Nariya & Inouye, 2005). Hence, the Pkn8 kinase was placed upstream in the phosphorylation pathway. However, the interaction of Pkn8 and MrpC has never been tested. It was shown that Pkn8 can phosphorylate the kinase deficient mutant of Pkn14 (Pkn14$_{K48N}$) *in vitro* (Nariya & Inouye, 2005) but whether Pkn8 interacts with Pkn14 to phosphorylate it *in vivo* still needs to be tested. Furthermore, it is also speculated that some multikinase-associated proteins, MkapA, B and C, which were previously found to associate with Pkn8 in yeast two-hybrid assays, may play a role to modulate *mrpC* expression via the Pkn8-Pkn14 kinase pathway (Nariya & Inouye, 2006). It was not possible to generate a *Δpkn8* mutant in our

wild type background (DZ2) (Mann & Higgs) and it seemed that the constitutive production of MrpC2 was toxic to the cells (as reflected by the difficulty to generate the *mrpC*$_{\Delta 1\text{-}25}$ strain). This suggested that the phosphorylation of MrpC (at Thr-21/22) might be necessary to prevent cell death. The phosphorylation of MrpC does not seem to be important for the induction of *fruA* (and likely also *mazF*) given that FruA was produced in the quadruple MrpC phosphorylation mutant (*mrpC*$_{T21\text{-}22A,S23\text{-}24A}$) at levels comparable to the wild type (data not shown). Nevertheless, as mentioned earlier, more details on the activity of phosphorylated MrpC (MrpC~P) for the expression of *mrpC* as well as other targets require further investigation.

I envision two possibilities regarding the biological role of the isoform MrpC2. The increased expression of *mrpC* and lack of FruA production in the *mrpC*$_{\Delta 1\text{-}25}$ strain could mean that MrpC2 is a positive inducer of *mrpC* expression but a negative regulator of *fruA* expression. This would be consistent with the stronger binding ability of MrpC2 to its own and *fruA*'s promoter *in vitro* (Nariya & Inouye, 2006). Alternatively, it is speculated that MrpC, is designed to be clipped to MrpC2 during development such that the protein is rendered inactive to repress its own transcription. As a consequence, in both these scenarios, the negative feedback on *mrpC* expression would be relieved and MrpC would be allowed to accumulate late during development in the aggregated cell fraction to trigger the expression of the downstream genes involved in sporulation. One would then predict that the gene expression during development would be governed by the levels of MrpC in the cell and depend upon the threshold required by different target genes.

The analysis of expression of targets of MrpC revealed no difference in the expression of *fruA* and *mazF* in the developmental subpopulations although MrpC accumulates differentially in the developmental subpopulations. It seems likely that the threshold for MrpC activity is very low since the aggregated cell fraction which does not accumulate sufficient levels of MrpC early during development (18 hours) shows no difference in the expression of the targets tested. On similar lines, it is also plausible to think that at this point in development, the majority of the MrpC protein produced in the non-aggregated cell fraction, is rendered inactive: by phosphorylation or by interaction with another yet unknown factor.

Overall, the regulation of the master regulator MrpC resembles that of Spo0A, the master regulator for spore formation in *B. subtilis* (Fujita & Losick, 2005). Like MrpC, Spo0A is regulated at the level of transcription and post-translationally by phosphorylation. We haven't identified targets of MrpC that are expressed differentially in certain cell types. However, it is likely that differentiation into various cell types is regulated by a threshold mechanism

involving the balancing of the different activity states of MrpC within the different cell types.

Thus, the results obtained in this study have a fundamental implication on our understanding of the regulation of the developmental program by this key transcription factor MrpC and set the basis to further investigate the highlighted grey areas, thus, paving the path towards a better and correct understanding of the regulation of cell fate differentiation in this system. In addition, my analysis of transcriptional reporters in developmental subpopulations revealed that cell fate-specific transcriptional markers cannot be assigned to the different developmental cell types. The results of this study were different from the transcriptional reporter fusion analysis in a *Bacillus* population where, for example, a P_{comK}-*gfp* reporter was expressed at high levels only in competent cells while a basal level of expression was observed in the non-competent cells (Leisner *et al*., 2008); P_{sinI}-*gfp*, P_{yqxM}-*cfp* and P_{eps}-g*fp* reporter fusions were expressed only in a subpopulation of biofilm forming cells (Chai *et* al., 2008) and a P_{hag}-*gfp* reporter was expressed only in the subpopulation of motile cells (Kearns & Losick, 2005). Therefore, it is clear that this Gram-negative bacterium does not mimic the well-known model system for prokaryotic differentiation, *B. subtilis* where cell-specific gene expression is a common phenomenon for the different co-existing cell subtypes.

4. MATERIALS AND METHODS

4.1 Chemicals, equipment and software

4.1.1 Chemicals and reagents

All media components and pure chemicals were purchased from Carl Roth (Karlsruhe), Merck (Darmstadt), Difco (Heidelberg) and Sigma-Aldrich (München). Size standards for SDS-PAGE (Page Ruler™ Pre-stained Protein Ladder Plus) and agarose gel electrophoresis (MassRuler™ DNA Ladder Mix) were purchased from Thermo Scientific (Schwerte). Oligonucleotides were synthesized by Sigma-Aldrich (München). DNA sequencing was performed by Eurofins MWG Operon (Ebersberg). Anti-rabbit HRP-coupled antibody was purchased from Thermo Scientific (Schwerte), α-MrpC polyclonal rabbit antisera were purchased from Eurogentec (Belgium, Serain) and α-mCherry antibodies were sought from the research group of M. Thanbichler. Platinum® Pfx DNA polymerase was bought from Invitrogen (Darmstadt), *Taq* DNA-polymerase and DNA modifying enzymes (restriction endonucleases, T_4 DNA ligase, antarctic phosphatase) were purchased from Thermo Scientific (Schwerte) or New England Biolabs (Frankfurt am Main). Superscript™III reverse transcriptase for cDNA synthesis was purchased from Invitrogen (Darmstadt) and DnaseI (Rnase-free) was bought from Ambion (Huntington, UK). SYBR® Green PCR master mix was purchased from Applied Biosystems (Darmstadt). Proteinase K, Lysozyme were bought from Sigma-Aldrich (München). The Bradford reagent for protein assay was supplied by Bio-Rad, Munchen) and the BCA™ Protein Assay Kit was supplied by Thermo Scientific (Schwerte). PCR purification, plasmid isolation and gel extraction kits were purchased from Qiagen (Hilden) or Zymo Research (Freiburg). Strep-Tactin® Sepharose® beads, the over-expression plasmid carrying the Strep-tag II® and the Strep-tag II® purification kit were purchased from IBA BioTAGnology (Goettingen). His-trap FF affinity columns were purchased from GE Healthcare (Freiburg). [γ^{32}P]-ATP was purchased by Hartmann analytic (Braunschweig). Antibiotics kanamycinsulfate, ampicillin-sodium salt, oxytetracycline dihydrate, chloramphenicol and tetracycline hydrochloride were purchased from Carl Roth (Karlsruhe) and Sigma-Aldrich (München). All solutions were prepared using demineralised autoclaved water.

4.1.2 Equipment and software

All instruments and software used in this study are listed in Table 4.1 and 4.2 respectively. The particular setting or modification is described in the relevant sections.

Table 4.1 Instruments used in this study

Application	Device	Manufacturer
	RC 5B plus, ultra Pro 80	Sorvall / Thermo Scientific (Dreieich)
Centrifugation	Multifuge 1 S-R, Biofuge pico, Biofuge fresco	Heraeus / Thermo scientific (Dreieich)
PCR	Mastercycler Personal	Eppendorf (Hamburg)
Real time PCR	7300 Real time PCR system	Applied Biosystems (Darmstadt)
Cell disintegration	FastPrep® 24 cell and tissue homogenizer	MP Biomedicals (Illkirch, France)
	French® Pressure cell press	SLM instruments (Urbana, IL)
Sonification	Branson sonifier 250	Heinemann (Schwäbisch Gmünd)
Protein electrophoresis	Mini-PROTEAN® 3 Cell PROTEAN®II XI Cell	Bio-Rad (München)
Western blotting	TE42 Protein transfer tank	Hoefer (San Francisco, USA)
FPLC protein purification	Äktapurifier™	GE Healthcare Life science (München) München)
DNA illumination	UVT_20 LE UV table	Herolab (Wiesloch)
	2 UV Transilluminator LM20E with BioDoc-IT-system and Mitsubishi P93 thermal video printer	UVP (Upland, CA) Mitsubishi Digital Electronics (Irvine,USA)
Electroporation	Gene pulser Xcell	Bio-Rad (München)
DNA concentration	NanoDrop ND 1000	NanoDrop products (Wilmington,USA)
Spectrophotometry	Ultrospec 2100 pro	Amersham Bioscience (München)
Microscopy	Zeiss Axio Imager.M1	Carl Zeiss (Jena)
	Cascade 1K camera, HXP-120 Light Source for fluorescence illumination	Visitron Systems (Puchheim)
	MZ8 stereo microscope with DFC320 camera	Leica Microsystems (Wetzlar)
	DME light microscope	
Incubation of bacterial cultures	Innova 4000® and Innova 44® incubator shaker	New Brunswick Scientific (Nürtingen)
	B6420 incubator	
Reaction incubation	Thermomixer comfort	Eppendorf (Hamburg)
Fluorescence Quantitation	Infinite M200 plate reader	Tecan (Groeding, austria)
Cell counting	Multisizer™3 Coulter Counter®	Beckman Coulter, Inc.
	Helber counting chamber	Hawksley (Lancing, UK)
Phosphor autoradiography	StormTM 840 imager	GE Healthcare Life science (München)
	Storage phosphor screen	
Filter sterilization	0.2 µm pore size filters	Sarstedt (Nümbrecht)
Steam Sterilization	MLS-3751L	Sanyo (San Diego, USA)

Table 4.2 Software and web-based programs used in this study

Application	Program	Manufacturer
Fluorescence microscopic analysis	Metamorph® v.7.5	Molecular Devices (Union City, CA)
In silico cloning	Vector NTI Advanced™	Invitrogen (Karlsruhe)
Microscopy imaging	Leica Application Suite	Leica microsystems (Wetzlar)
Image Processing	Adobe Photoshop CS2 Adobe Illustrator CS5	Adobe Systems GmbH (München)
Äkta system management	UNICORN	GE Healthcare Life science (München)
Statistical analysis	Microsoft Excel 2007	Microsoft® (Redmond, USA)
	Origin v.6.1	Origin Lab (Northampton, MA, USA)
Phosphor autoradiography	Image Quant 5.2	GE Healthcare Life science (München)
Quantification of immunoblot	Image J	NIH (Maryland, USA)
Ortholog identification	ACT: Artemis Comparison Tool	Wellcome Trust Sanger Institute (Hinxton, UK); www.sanger.ac.uk
	BLASTp and tBLASTn	NCBI, www.ncbi.nlm.nih.gov

4.2 Media

All Media and solutions were autoclaved at 121°C for twenty minutes at 15 psi pressure. Antibiotics / additives were added at the desired concentration (Table 4.5) after cooling the media to ~60°C. Heat sensitive solutions were filter sterilized using 0.2 µm pore size filters (Millipore, Schwalbach).

Table 4.3 Media for *E. coli*

Medium	Composition
Luria-Bertani (LB) broth	1% tryptone, 0.5% yeast extract, 1% NaCl
Luria-Bertani (LB) agar	LB broth, 1% Difco™ agar
TSS	1% tryptone, 0.5% yeast extract, 1% NaCl, 10% PEG(MW 3350), 5% DMSO, 50 mM $MgCl_2$, pH 6.5

Table 4.4 Media for *M. xanthus*

Medium	Composition
Casitone yeast extract (CYE) broth	1% Bacto™ Casitone, 0.5% yeast extract,10 mM MOPS pH 7.6, 8mM $MgSO_4$
Casitone yeast extract (CYE) agar	CYE broth, 1.5% Difco™ agar
Casitone yeast extract (CYE) top agar	CYE broth, 1.0% Difco™ agar
CTT broth	1% Bacto™ Casitone, 10 mM Tris-HCl pH 8.0, 1 mM potassium phosphate buffer pH7.6, 8 mM $MgSO_4$
CTT agar	CTT broth, 1.5% Difco™ agar
MMC starvation buffer	10 mM MOPS pH 7.0, 4 mM $MgSO_4$, 2mM $CaCl_2$

Table 4.5 Antibiotics or Additives

Additive	Concentration for *M.xanthus*	Concentration for *E.coli*	Dissolved in
Kanamycinsulfate	100 µg/ml	50 µg/ml	water
Ampicillin sodium salt	n.a.	100 µg/ml	water
Tetracyclin hydrochloride	n.a.	5 µg/ml	methanol
Oxytetracyclin dihydrate	10 µg/ml	n.a.	methanol (fresh)
X-Gal	n.a.	40 µg/ml	DMF
IPTG	n.a.	1.67 mM/µl	water
Galactose	2.5%	n.a.	water
Chloramphenicol	34 µg/ml	34 µg/ml	99.9% ethanol

4.3 Microbiological methods

4.3.1 Bacterial strains

The *M. xanthus* and *E. coli* strains used in this study are listed in Table 4.6 and Table 4.7, respectively.

Table 4.6 *M. xanthus* strains used in this study

Strain	Genotype	Reference or Source
DZ2	wild type	Campos & Zusman, 1975
PH1100	DZ2 *attB*::pSL8-P_{mrpC}-*mCherry*, Km^R	This study
PH1101	DZ2 *attB*::pVG112, Tc^R	This study
PH1102	DZ2 *attB*::pBM002, Km^R	Mensch, Bachelor thesis (2009)
PH1019	DZ2 *attB*::pPH161, Km^R	Lee *et al*., 2011
PH1103	DZ2 *attB*::pVG102, Km^R	This study
PH1025	DZ2 Δ*mrpC*	Lee *et al*., 2012
PH1104	PH1025 *attB*::pSL8-P_{mrpC}-*mCherry*, Km^R	This study
PH1105	PH1025 *attB*::pVG112, Tc^R	This study
PH1106	PH1025 *attB*::pBM002, Km^R	This study
PH1107	DZ2 *attB*::pAH7, Tc^R	This study
PH1108	DZ2 $mrpC_{\Delta 1\text{-}25}$	P. Mann
PH1109	PH1108 *attB*::pVG112, Tc^R	This study
PH1110	DZ2 *attB*::pVG106, Km^R	This study
PH1111	DZ2 *attB*::pVG107, Km^R	This study
PH1112	PH1025 *attB*::pVG107, Km^R	This study
PH1113	DZ2 *attB*::pVG109, Km^R	This study
PH1114	PH1025 *attB*::pVG109, Km^R	This study
PH1115	DZ2 *attB*::pVG111, Km^R	This study
PH1116	PH1025 *attB*::pVG111, Km^R	This study
PH1117	DZ2 *attB*::pVG114, Km^R	This study
PH1118	PH1025 *attB*::pVG114, Km^R	This study

PH1119	DZ2 *attB*::pVG116, Km^R	This study
PH1120	DZ2 *attB*::pVG117, Km^R	This study
PH1121	DZ2 Δ*mrpB*	This study
PH1122	PH1121 *attB*::pSL8-P_{mrpC}-*mCherry*, Km^R	This study
PH1123	DZ2 $mrpB_{D58A}$	This study
PH1124	PH1123 *attB*::pSL8-P_{mrpC}-*mCherry*, Km^R	This study
PH1125	DZ2 $mrpB_{D58A}$ Δ*mrpC*	This study
PH1126	PH1125 Δ*mrpC attB*::pSL8-P_{mrpC}-*mCherry*, Km^R	This study
PH1127	DZ2 pVG120, Km^R	This study
PH1128	PH1025 *attB*::pVG124, Km^R	This study
PH1129	DZ2 ΔMxan_5126	This study
PH1130	DZ2 Δ*mrpC* ΔMxan_5126	This study
PH1131	DZ2 pVG123, Km^R	This study
PH1132	DZ2 Δ*pkn14*	P. Mann
PH1133	DZ2 $pkn14_{K48N}$	This study
PH1134	PH1132 *attB*::pVG126, Km^R	This study
PH1135	PH1132 *attB*::pVG127, Km^R	This study
PH1136	DZ2 $mrpC_{T21-22A}$	P. Mann
PH1137	DZ2 $mrpC_{S23A}$	P. Mann
PH1138	DZ2 $mrpC_{S23-24A}$	This study
PH1139	DZ2 $mrpC_{T21-22,S23-24A}$	This study

Table 4.7 *E. coli* strains used in this study

Strain	Genotype	Reference / Source
Top10	host for cloning F- *endA1 recA1 galE15 galK16 nupG rpsL* Δ*lacX74* Φ80*lacZ* Δ*M15 araD139* Δ*(ara, leu)7697 mcrA* Δ*(mrr-hsdRMS-mcrBC) λ-*	Life Technologies
BL21/ λDE3	host for over-expression F^- *ompT gal dcm lon* $hsdS_B$ (r_B^- m_B^-) λ(DE3)	Novagen

4.3.2 Growth conditions of bacteria

M. xanthus strains were grown under vegetative conditions on casitone yeast extract (CYE) agar plates at 32°C in the dark. Cells were inoculated in CYE broth using a sterile wooden stick and grown overnight in an orbital shaker at 32°C in the dark. The optical density of the cell suspension was measured at 550 nm (A_{550}) with a spectrophotometer using a 1 cm path length cuvette.

E.coli strains were grown aerobically on Luria-Bertani (LB) agar plates at 37°C. To prepare a broth culture, cells were inoculated and aerobically grown in LB broth in an orbital shaker at 37°C. The optical density of *E. coli* suspensions was

measured at 550 nm (A_{550}) with a spectrophotometer using a cuvette with a 1 cm path length.

4.3.3 Storage of bacterial cultures

For long term storage of *M. xanthus* strains, 900 µl of dimethylsulfoxide solution (DMSO; ≥ 99.5%) was added to a 25 ml vegetatively growing culture to induce sporulation overnight. Cultures were centrifuged at 4600 x g at room temperature for 15 minutes (Multifuge 1 S-R) and cell pellets were resuspended in 1 ml CYE broth. The cell suspension was mixed with 250 µl DMSO in a 2 ml screw cap tube and stored at -80°C. (The non-sporulating strains were grown vegetatively without DMSO, pelleted and stored in DMSO)

For long term storage of *E. coli* strains, 680 µl of an overnight culture was mixed with 320 µl of 50% (v/v) glycerol and stored at -80°C.

4.3.4 Development assays for *M. xanthus*

To induce development in submerged culture (16 ml Petri-dish or 24-well format), cells were grown vegetatively at 32°C overnight to achieve an optical density of 0.3-0.9 A_{550}. Cells were diluted to an A_{550} of 0.035 in CYE broth. 16 ml or 0.5 ml of the diluted culture was seeded in 85 mm Petri-dishes or 24-well tissue culture plates (Sarstedt), respectively. The plates were incubated at 32°C (without shaking) in the dark for 24 h, and CYE was replaced with an equivalent volume of MMC starvation buffer to induce development. Pictures were recorded at various time points over a period of 5 days using a Leica MZ8 stereomicroscope with an attached Leica DFC320 camera.

To enumerate starvation induced spores at 120 h of development, cells were harvested from 1 well of a 24-well plate in 2 ml screw cap tubes in biological triplicate experiments. Cells were pelleted down by centrifuging at 13,000 rpm at room temperature for 5 minutes (Biofuge pico) and the MMC was aspirated with a vacuum pump. Cells were resuspended in 1 ml daH_2O, heated to 50°C for 1 h and sonicated (output 3, 30% duty cycle, 2 x 20 pulses, Branson Sonifier 250). Phase-bright spherical spores were enumerated under a light microscope by placing 10 µl of sample on a Helber bacterial counting chamber (Hawksley, UK). The sporulation efficiency was calculated as a percentage of wild type spores.

To determine spore viability, a spore germination assay was performed. 100-fold serial dilutions of heat and sonicated spore samples were mixed in CYE top agar, plated on CYE agar plates and incubated at 32°C. The number of colonies

were counted after 5-6 days. The spore germination efficiency was also calculated as a percentage of the wild type spores that germinated.

4.3.5 Cell separation assay for developmental subpopulations

Cells were developed under submerged culture conditions in 16 ml Petri-dish format as described before. For cell subpopulation analysis, developing cells were harvested using a 20 ml pipette to flush the lawn of cells off the surface of the Petri-dish in a 50 ml Falcon tube and were dispersed in the tube by vigorously pipetting up and down 30 times. The two cell fractions were separated by centrifugation at 50 x g for 5 minutes at room temperature (Heraeus Multifuge 1S-R). The supernatant containing the non-aggregated cell fraction was carefully removed and transferred to a fresh 50 ml Falcon tube while the pellet containing the aggregated fraction was resuspended in an equivalent volume (16 ml) of MMC starvation buffer. Both fractions were dispersed at least three times at 5 m/s for 45 sec in a FastPrep® 24 cell and tissue homogenizer (MP Biomedicals) at 4°C to get single cells from cells in clusters / groups. The number of cells in each fraction was counted with a Beckman Coulter cell counter using a 20 µm cappillare. Counted cells in each fraction were pelleted at 4600 x g, 4°C for 10 min and resuspended in proportionate volumes of lysis buffer to have equal number of cells for immunoblots.

4.3.6 Glycerol-induction of sporulation in *M. xanthus*

Fresh *M. xanthus* cells (grown on CYE plates for about 3 days) were inoculated in 25 ml CYE broth in a 250 ml flask at 32°C at 220 rpm overnight in an orbital shaker. This pre-culture was mixed with fresh CYE (20 ml CYE in 250 ml flask; 1:12.5 ratio of liquid to flask volume) and incubated as above so as to get an optical density of 0.3 (A_{550}) cells after ~24 hours. Cells with 0.3 (A_{550}) were induced for sporulation with 1 ml of 10 M filter sterilized glycerol for 24 hours. For microscopy, the un-induced and the induced culture were pelleted down, resuspended in 1 ml of spent medium, vortexed and analyzed under the microscope as explained in section 4.8.

4.3.7 Copper-based MrpC induction assays

In the copper-based MrpC induction experiments, *M. xanthus* strains were grown on CTT plates supplemented with 40 µg/ml kanamycin, if needed. Only plastic ware was used at all times in order to avoid any copper contamination from glassware. To induce MrpC under vegetative conditions, strains were grown overnight in shaking liquid cultures as explained in section 4.3.2 and

induced overnight using varying concentrations of copper sulfate (100, 300 and 600 µM). After induction, the cell cultures were centrifuged at 4600 x g at 4°C for 10 min (Multifuge 1 S-R) to harvest cell pellets and cell lysates containing equal protein were subjected to anti-MrpC immunoblot as explained in section 4.5. To induce MrpC under starvation conditions, strains were developed under submerged conditions in the 16 ml format as explained in section 4.3.4 but with the difference that cells were plated in CTT broth for 24 hours in the presence or absence of copper sulfate (40 and 200 µM). To induce starvation *i.e.* at T=0, the CTT medium was respectively replaced with MMC starvation buffer with or without copper. Cell pellets were harvested at 0, 18 and 24 h of development to prepare protein samples for MrpC immunoblot as explained previously. For the copper induction experiments to reduce the copper exposure of cells during development, cells were plated in CTT medium and then induced to develop in MMC starvation buffer free of copper for 24 h. After 24 hours, the cultures were incubated in the absence or presence of 40 µM copper for 2 h. Finally, as explained above, cells were harvested after the 2 h induction period and lysates were subjected to MrpC immunoblot analysis.

4.4 Molecular biological methods

4.4.1 Oligonucleotides and plasmids

The oligonucleotides used for the construction of plasmids, qRT-PCR, cDNA synthesis or sequencing are listed in Table 4.8 and all the plasmids used in this study are listed in Table 4.9.

Table 4.8 Oligonucleotides used in this study

Plasmid/ type of primer	Sequence (5' - 3')	Name	Description
Sequencing	gtgaagacccgtgctgcggag	oPH 515	pSL8 f
	gggatgtgctgcaaggcg	oPH 516	pBJ114 f & pSL8 r
	ggatgtaccccgaggacg	oPH 517	*mCherry*
	ttcgctattacgccagctgg	oPH 553	M13 f
	ttagctcactcattaggcacc	oPH 554	M13 r
	gcggataacaatttcacac	oPH 344	M13 r
	tcgatctcgaactcg	oPH 623	mcherry 5' end r
	aggaggataacatgg	oPH 624	mcherry 5' end f
	cgcggcaccaacttc	oPH 625	mcherry 3' end f
	agggggatgtgctgc	oPH 626	pSL8 3' HindIII r
	caaccagatggagcagac	oPH 844	*pkn14*
	cacgcccagggagaagac	oPH 845	*pkn14*

qRT-PCR	gaacggtaacaggaagaagcttgct	oPH1129	*E. coli* 16sRNA f
	cgatggcaagaggcccgaag	oPH 1130	*E. coli* 16sRNA r
	ggaggccatcgacttcaagg	oPH 353	*mrpC* f
	ggccggacttcagcaggtag	oPH 354	*mrpC* r
	aactgttgtgcttgagtgccg	oPH 235	*M. x* 16sRNA f
	atctaatcctgtttgctccccac	oPH 236	*M. x*16sRNA r
	gttcgccgctgaagcagac	oPH 655	5' UTR of *mrpC* f
	tgaaaccgtgcatggcataa	oPH 656	5' UTR of *mrpC* r
att PCR	cggcacactgaggccacata	oPH 477	*attB* left
	ggaatgatcggaccagctgaa	oPH 478	*attB* right
	gggaagctctgggtacgaa	oPH 479	*attP* left
	gctttcgcgacatggagga	oPH 480	*attP* right
pVG102	gctctagactccgcgagcttccacagg	oPH 680	A
	cttgctcaccatgccctcggggtctcct	oPH 681	B
	gagggcatggtgagcaagggcgaggag	oPH 682	C
	gcagaagctttcacttgtacagctcgtccatgc	oPH 615	D
pVG104	cgagatcatatgcagtggtaccgtgagcaagggcgaggag	oPH 906	*mcherry* f
	gctggatcctcatcatcacttgtacagctcgtccatgcc	oPH 913	*mcherry* r
pVG106	gcagatcatatgtcttgcacagagccagagc	oPH 908	P_{mrpC} f
	gcaggtacccgcttcaaccagggtgagcag	oPH 910	$mrpC_{180a.a.}$r
pVG107	gcagatcatatgtcttgcacagagccagagc	oPH 908	P_{mrpC} f
	gcggtaccacccgagccacccccgcccttctccttgccggcgatcttcc	oPH 911	$mrpC_{248a.a._}$ linker r
-	gctggatcccccgttgcaaccttctctg	oPH 504	rbs_{pilA} *gfp* f
-	gcagaagctttcacttgtacagctcgtccatg	oPH 505	*gfp* r
pVG109	gctctagaatgcacggtttcaaccgcccc	oPH 948	A
	cgataagcttctacttctccttgccg	oPH 947	B
pVG111	atggatccgctgatcgacagttatcgtc	oPH 944	A
	gaaaccgtgcatgggggtcctcagagaag	oPH 945	B
	cacggtttcaaccgccccctc	oPH 946	C
	cgataagcttctacttctccttgccg	oPH 947	D
pVG114	gcggaattccacctccgcccaccacac	oPH 487	A
	cgataagcttctacttctccttgccg	oPH 947	D
pVG116	gcagatcatatgtcttgcacagagccagagc	oPH 908	A
	gaaaccgtgatgggcataactcc	oPH 1078	B
	ggagttatgcccatcacggtttcaaccg	oPH 1079	C
	gcaggtacccgcttcaaccagggtgagcag	oPH 910	D
pVG117	gagctcggcgcgggtaccgtgagcaagggc	oPH 1074	A
	ctagacatgggggggaggcagagaaggttgc	oPH 1080	B
	gcaaccttctctgcctccccccatgtctag	oPH 1081	C
	gcagaagctttcacttgtacagctcgtccatg	oPH 505	D
pVG118	gcgaattcgagcgcatgctctggctcctctcc	oPH 1123	A
	ggtgtgcacgacgatgagaagggtctccatggc	oPH 1097	B
	ctcatcgtcgtgcacaccttccctgtgaaggatgcg	oPH 1098	C

	atacaagcttggacttcagcaggtagacgcggtcgg	oPH 1127	D
	tcagccacgagattcgcaac	oPH 1128	E
	gcaggtacccgcttcaaccagggtgagcag	oPH 910	F
pVG119	gcgaattcgagcgcatgctctggctcctctcc	oPH 1123	A
	catggcgaggatgaccacgctgggc	oPH 1124	B
	ctcgccatgatgctcccggaccgc	oPH 1125	C
	atagaagcttgcagcgtgtcgacgatggccg	oPH 1135	D
	gcggtccgggagcatcatgt	oPH 1179	wt *mrpB*$_{D58A}$
	gcggtccgggagcatcatgg	oPH 1180	mutant *mrpB*$_{D58A}$
pVG120	gctctagaatgcacggtttcaaccgcccc	oPH 948	A
	gctggatcctcatcatcacttgtacagctcgtccatgcc	oPH 913	B
	gcggaattccacctccgcccaccacac	oPH 487	E
pVG121	gcgaattccagcacccgctccgtggtgtcc	oPH 1204	A
	gtccttctcgccacgcggcatgcgc	oPH 1205	B
	ccgcgtggcgagaaggactgggggc	oPH 1206	C
	atagaagcttgtgctggagatgctcgc	oPH 1207	D
	agcgccgggatgatggtcaccgccaac	oPH 598	E
	gcgcggaccgtcaatcacctgg	oPH 1260	F
pVG122	gcggaattccacctccgcccaccacac	oPH 487	A
	gtccttctcgcggttgaaaccgtgcatg	oPH 1208	B
	ttcaaccgcgagaaggactgggggc	oPH 1209	C
	atagaagcttgtgctggagatgctcgc	oPH 1207	D
	aactggagaacgtgctcacc	oPH 555	E
	gcgcggaccgtcaatcacctgg	oPH 1260	F
pVG123	gcgaattcctgaccatgcgcatgccgcgtg	oPH 1210	A
	acccccgccgcgcccccagtccttctc	oPH 1211	B
	tgggggcgcggcgggggtggctc	oPH 1212	C
	gctggatcctcatcatcacttgtacagctcgtccatgcc	oPH 913	D
pVG124	gcgaattcggccatgaacggcacttcacg	oPH 1215	A
	gcggcgaaccatgaagcctcttcacgaatg	oPH 1216	B
	ggcttcatggttcgccgctgaagcagacg	oPH 1217	C
	cgataagcttctacttctccttgccg	oPH 947	D
pVG125	cgggatcctccttcgacatcgtcatc	oPH 785	A
	gcggttgatgacgacgggagactc	oPH 786	B
	atcaaccgcatccgcccgcatctg	oPH 787	C
	gcagaagcttagggagaagacgtcgctg	oPH 788	D
	acagatgcgggcggatgcgc	oPH 841	wt *pkn14*$_{K48N}$
	acagatgcgggcggatgcgg	oPH 842	mutant *pkn14*$_{K48N}$
pVG126	atggatccgctgatcgacagttatcgtc	oPH 944	A
	ggcgggaggcatgggggtcctc	oPH 1235	B
	acccccatgcctcccgccgcc	oPH 1236	C
	ccataagcttccttcgtattcgagcgtcagc	oPH 1244	D
pVG127	cgggatcctccttcgacatcgtcatc	oPH 785	A

	ccataagcttccttcgtattcgagcgtcagc	oPH 1244	D
pVG128	gcggaattccacctccgcccaccacac	oPH 487	A
	cccggcggcggccgcctgcagc	oPH 1233	B
	gccgccgccgggatgatggtcacc	oPH 1234	C
	gcgggatccagcgtggacacgaaggag	oPH 493	D
pVG129	gcggaattccacctccgcccaccacac	oPH 487	A
	tgaccatcatcccggcggc	oPH 1245	B
	gccgccgccgggatgatggtcacc	oPH 1234	C
	gcgggatccagcgtggacacgaaggag	oPH 493	D
pVG130	ggaattcatgcctcccgccgccccgcag	oPH 833	A
	ccataagcttccttcgtattcgagcgtcagc	oPH 1244	D
pVG131	catggatcccacggtttcaaccgccccctc	oPH 485	pET 28a+ *mrpC* f
	ggctcgagctacttctccttgccggcgatc	oPH 486	pET 28a+ *mrpC* r
MrpC &	tggttgaagcgcacggcg	oPH 1174	D (*mrpC*)
Mxan_5126	atgcgcatgccgcgtgg	oPH 1176	C (Mxan_5126 f)
cDNA	gccaccggcgtgagcgac	oPH 1191	B (Mxan_5126 r)
synthesis	acgtaggcctggggaagcagc	oPH 1178	A (cDNA)
	tgctggagtggggcgaggag	oPH 840	*Δpkn14* E
	gacgtgccttccaccgccag	oPH 843	*Δpkn14* F
	aactggagaacgtgctcacc	oPH 555	Δ*mrpC* E primer

Note: f, forward; r, reverse; A,B,C,D; primers used to generate AB and CD fragments that were later used to generate AD fragment by an overlap PCR, E and F primers are primers used for screening of a deletion/integration.

Table 4.9 Plasmids used in this study

Plasmid	Description	Reference or Source
pSL8-P_{mrpC}-*mCherry**	P_{mrpC}-*mCherry*, Km^R	P. Higgs
pBM001*	P_{mrpC}-*mCherry-Gfp*, Km^R	Mensch, Bachelor thesis (2009)
pBM002*	P_{fruA}-*mCherry*, Km^R	Mensch, Bachelor thesis (2009)
pFM18*	Mx8 *attP* backbone vector, Km^R	Mueller *et al*., 2010
pSWU30*	Mx8 *attP* backbone vector, Tc^R	Wu and Kaiser, 1996
pBJ114	suicide plasmid with Km^R and *galK*	Julien *et al.*, 2000
pAH7*	P_{parB}-*parB-Yfp*, Tc^R	Harms & Søgaard-Andersen, unpublished
$pMAT_1$*	P_{cuoA}-*pilB*, Km^R	Gómez-Santos *et al.*, 2012
pVG102*	P_{mazF}-*mCherry*, Km^R	This study
pVG104*	*mCherry-Gfp*, Km^R	This study
pVG106*	P_{mrpC-} $mrpC_{180}$-*mCherry-Gfp*, Km^R	This study
pVG107*	P_{mrpC-} $mrpC_{248}$-*mCherry-Gfp*, Km^R	This study

pVG109*	P_{cuoA}-*mrpC*, Km^R	This study
pVG111*	P_{pilA}-*mrpC*, Km^R	This study
pVG112*	P_{mrpC}-*mCherry*, Tc^R	This study
pVG114*	P_{mrpC}-*mrpC*, Km^R	This study
pVG116*	P_{mrpC}-*mrpC*$_{180}$-$_{CAT}$*mCherry-Gfp*, Km^R	This study
pVG117*	P_{mrpC}-*mrpC*$_{180}$-*mCherry*-$_{CCTCCC}$*Gfp*, Km^R	This study
pVG118	pBJ114 *ΔmrpB*	This study
pVG119	pBJ114 *mrpB*$_{D58A}$	This study
pVG120	pBJ114 *mrpC-mCherry*	This study
pVG121	pBJ114 ΔMxan_5126	This study
pVG122	pBJ114 *ΔmrpC* ΔMxan_5126	This study
pVG123	pBJ114 Mxan_5126-*mCherry*	This study
pVG124*	P_{cuoA}-$_{(+1)}$*mrpC*, Km^R	This study
pVG125	pBJ114 *pkn14*$_{K48N}$	This study
pVG126*	P_{pilA}-*pkn14*, Km^R	This study
pVG127*	P_{pkn14}-*pkn14*, Km^R	This study
pVG128	pBJ114 *mrpC*$_{S23-24A}$	This study
pVG129	pBJ114 *mrpC*$_{T21-22A,S23-24A}$	This study
pASK-IBA15	Tet-promoter, N-term StrepII® tag, ColE1 *ori*, Amp^R	IBA BioTAGnology
pET-28a+	T7-promoter, His_6-tag (N & C terminal), Km^R	Novagen
pVG130	pASK-IBA15-*pkn14*$_{K48N}$	This study
pVG131	pET-28a+ *mrpC*$_{T21-22A,S23-24A}$	This study
pPH158	pET-28a+ *mrpC*	P.Higgs
pPH166	pASK-IBA15-*pkn14*	Mei X.
pPH167	pET-28a+ *mrpC2*	Schramm A.
pPH168	pET-28a+ *mrpC*$_{T22A}$	P. Mann
pPH169	pET-28a+ *mrpC*$_{T21-22A}$	P. Mann
pPH170	pBJ114 *mrpC*$_{Δ1-25}$	P. Mann

*, Mx8 *attP* backbone vectors; Km^R, Tc^R, and Amp^R, resistance to kanamycin, tetracyclin and ampicillin respectively.

4.4.2 Construction of plasmids

The various mutagenesis plasmids were created by amplifying overlapping fragments ~500 bp upstream and downstream of the genomic region to be mutated or deleted. Purified *M. xanthus* genomic DNA was used as a template to amplify the chromosomal regions and the respective A and B or C and D oligonucleotides (as listed in Table 4.8) were used to generate the overlapping AB (upstream) and CD (downstream) fragments. Following the purification of these fragments, an overlap PCR was performed using 40ng each of both AB and CD fragments as a template and the respective A and D primers to generate the fused ~1 Kb AD fragment. This fragment was then cloned into the multiple cloning sites of the plasmid pBJ114. The resulting plasmid was transformed into *E. coli* and clones were selected on LB plates containing the desired antibiotic. The plasmid was isolated and sequenced to be error-free. Further, in-frame deletion or point mutants in *M. xanthus* were created using these plasmids as described in section 4.4.3.

The various Mx8 *attB* site integration plasmids were also created following the approach of an overlap PCR as described above. The desired fragment generated was then cloned into the multiple cloning site of a plasmid bearing the Mx8 *attP* site. Finally, the resulting error-free sequenced plasmid was transformed into *M*. *xanthus* and the integration was confirmed as described in section 4.4.7.

The various over-expression plasmids were constructed by amplifying the gene or region of interest using specific oligonucleotides (Table 4.8) and *M*. *xanthus* genomic DNA as template. Following purification, the resulting fragments were cloned into the multiple cloning site of the respective over-expression plasmid. Subsequently, the resulting error-free sequenced plasmid was used for over-expression.

pVG102

The plasmid pVG102 was generated by PCR amplifying and fusing the putative *mazF* promoter (597 bp upstream of and including the *mazF* start codon) and the second codon of *mCherry* using *M*. *xanthus* genomic DNA and pBM001 as templates, respectively. The P_{mazF}-*mCherry* insert was cloned into the XbaI and HindIII restriction sites of pFM18.

pVG104

The plasmid pVG104 was used a template for the construction of plasmids pVG106 and pVG107. It was generated by PCR amplifying *mCherry* (starting with its second codon; using the PCR template pBM001) and cloning it into the NdeI and BamHI restriction sites of pBM001.

pVG106

The Mx8 *attB* site integration plasmid pVG106 was generated by PCR amplifying the *mrpC* promoter (331 bp upstream of the *mrpC* start codon; P_{mrpC}) including 540 bp (180 amino acids) of the *mrpC* ORF. The P_{mrpC}-$mrpC_{180}$ insert was cloned into the NdeI and KpnI restriction sites of pVG104.

pVG107
The Mx8 *attB* site integration plasmid pVG107 was generated by PCR amplifying the *mrpC* promoter (331 bp upstream of the *mrpC* start codon; P_{mrpC}) including the 744 bp (248 amino acids) long *mrpC* ORF ending in a Gly-Gly-Gly-Gly-Ser-Gly-Gly-Thr linker. The P_{mrpC}-$mrpC_{248}$-linker insert was cloned into the NdeI and KpnI restriction sites of pVG104.

pVG109
The Mx8 *attB* site integration plasmid pVG109 was generated by PCR amplifying the *mrpC* gene and cloning it into the XbaI and HindIII site of $pMAT_1$ (Gómez-Santos *et al*., 2012).

pVG111
The Mx8 *attB* site integration plasmid pVG111 was generated by PCR amplifying and fusing the *pilA* promoter (189 bp upstream of and including the *pilA* start codon; P_{pilA}) to the second codon of the *mrpC* gene. The P_{pilA}-*mrpC* insert was cloned into the BamHI and HindIII restriction sites of pFM18.

pVG112
The Mx8 *attB* site integration plasmid pVG112 was generated by digesting the plasmid pBM001 with the restriction enzymes EcoRI and BamHI and ligating the excised insert (P_{mrpC}-*mCherry*) into pSWU30.

pVG114
The Mx8 *attB* site integration plasmid pVG114 was generated by PCR amplifying the *mrpC* promoter (331 bp upstream of the *mrpC* start codon; P_{mrpC}) including the *mrpC* ORF. The P_{mrpC}-*mrpC* insert was cloned into the NdeI and HindIII restriction sites of pBM001.

pVG116
The Mx8 *attB* site integration plasmid pVG116 was generated by PCR amplifying and fusing AB and CD fragments of the *mrpC* promoter including 540 bp (180 amino acids) of the *mrpC* ORF such that in the resulting overlapping fragment, the start codon of *mrpC* is mutated (ATG to CAT). The fragment was inserted into the NdeI and KpnI restriction sites of pVG106.

pVG117

The Mx8 *attB* site integration plasmid pVG117 was generated by PCR amplifying and fusing the ribosome binding site of *pilA* gene (31 bp upstream of and including the start codon of *pilA*; rbs_{pilA}) and the gene *gfp* such that in the resulting overlapping fragment, the rbs_{pilA} is mutated (AAGAAC to CCCTCC). The plasmid pVG106 was used as a template for amplifying the AB and CD fragments. The resulting overlap fragment was inserted into the KpnI and HindIII restriction sites of pVG106.

pVG118
The deletion plasmid pVG118 was generated by PCR amplifying and fusing two fragments spanning -499 to 21 bp and 1435 to 1957 bp, respectively, from the start of the *mrpB* gene. The resulting overlap fragment was cloned into EcoRI and HindIII restriction sites of pBJ114.

pVG119
The mutagenesis plasmid pVG119 was generated by PCR amplifying and fusing two fragments spanning -499 to 177 bp and 169 to 469 bp, respectively, from the start of the *mrpB* gene such that the overlap fragment harbors a mutation in the codon 58, GAC (Asp) to GCC (Ala). The resulting overlap fragment was cloned into EcoRI and HindIII restriction sites of pBJ114.

pVG120
The mutagenesis plasmid pVG120 was generated by PCR amplifying the promoter region of *mrpC* including the *mrpC* ORF linked to *mCherry* by a Gly_4-Ser-Gly_2-Thr linker using pVG107 as the PCR template. The resulting insert was cloned into the XbaI and BamHI restriction sites of pBJ114.

pVG121
The deletion plasmid pVG121 was generated by PCR amplifying and fusing two fragments spanning -548 to 18 bp and 634 to 1249 bp, respectively, from the start of the gene Mxan_5126. The resulting overlap fragment was cloned into EcoRI and HindIII restriction sites of pBJ114.

pVG122
The deletion plasmid pVG122 was generated by PCR amplifying and fusing two fragments- one spanning -529 to 18 bp from the start of the *mrpC* gene and the other spanning 634 to 1249 bp from the start of the gene Mxan_5126. The resulting overlap fragment was cloned into EcoRI and HindIII restriction sites of pBJ114.

pVG123
The insertion plasmid pVG123 was generated by PCR amplifying and fusing two fragments- one spanning -6 to 651 bp from the start of the gene Mxan_5126 and

the other containing a Gly_4-Ser-Gly_2-Thr linker fused to *mCherry* using genomic DNA and plasmid pVG107 as templates, respectively. The resulting overlap fragment was cloned into EcoRI and BamHI restriction sites of pBJ114.

pVG124
The Mx8 *attB* site integration plasmid pVG124 was generated by PCR amplifying and fusing the *cuoA* promoter (824 upsteam of and including the *cuoA* start codon; P_{cuoA}) to the transcriptional start of the *mrpC* gene (-58 bp from the start of the *mrpC* gene). The P_{cuoA}-$_{(+1)}$*mrpC* insert was cloned into EcoRI and HindIII site of pVG109.

pVG125
The mutagenesis plasmid pVG125 was generated by PCR amplifying and fusing two fragments spanning -385 to 147 bp and 139 to 647 bp, respectively, from the start of the *pkn14* gene such that the overlap fragment harbors a mutation in the codon 48, AAG (Lys) to AAC (Asn). The resulting overlap fragment was cloned into BamHI and HindIII restriction sites of pBJ114.

pVG126
The Mx8 *attB* site integration plasmid pVG126 was generated by PCR amplifying and fusing the *pilA* promoter (189 bp upstream of and including the *pilA* start codon; P_{pilA}) to the second codon of the *pkn14* gene. The P_{pilA}-*pkn14* insert was cloned into the BamHI and HindIII restriction sites of pFM18.

pVG127
The Mx8 *attB* site integration plasmid pVG127 was generated by PCR amplifying the putative *pkn14* promoter (385 bp upstream of the *pkn14* start codon; P_{pkn14}) followed by the *pkn14* gene (1265 bp downstream including the start codon). The P_{pkn14}-*pkn14* insert was cloned into the BamHI and HindIII restriction sites of pFM18.

pVG128
The mutagenesis plasmid pVG128 was generated by PCR amplifying and fusing two fragments spanning -529 to 75 bp and 64 to 644 bp, respectively, from the start of the *mrpC* gene. The genomic DNA of the DZ2 $mrpC_{S23A}$ strain (PH1137) was used as the template for this PCR. The resulting overlapping fragment that harbors a mutation in the codons 23, AGC (Ser) to GCC (Ala) and 24, TCC (Ser) to GCC (Ala) of *mrpC* was cloned into EcoRI and BamHI restriction sites of pBJ114.

pVG129
The mutagenesis plasmid pVG129 was generated by PCR amplifying and fusing two fragments spanning -529 to 85 bp and 64 to 644 bp, respectively, from the

start of the *mrpC* gene. The genomic DNA of the DZ2 *mrpC*$_{S23-24A}$ strain (PH1138) was used as the template for this PCR. The resulting overlapping fragment that harbors a mutation in the codons 21, ACG (Thr) to GCG (Ala); 22, ACC (Thr) to GCC (Ala); 23, AGC (Ser) to GCC (Ala) and 24, TCC (Ser) to GCC (Ala) of *mrpC* was cloned into EcoRI and BamHI restriction sites of pBJ114.

pVG130

The over-expression plasmid pVG130 was generated by PCR amplifying a region spanning 1265 bp including the start of the *pkn14* gene using the genomic DNA of the DZ2 *pkn14*$_{K48N}$ strain as the PCR template. The resulting fragment containing the entire *pkn14* gene with a mutation in the codon 48, AAG (Lys) to AAC (Asn) was cloned into the EcoRI and HindIII restriction sites of the plasmid pASK-IBA15.

pVG131

The over-expression plasmid pVG131 was generated by PCR amplifying a region spanning 4 to 744 bp from the start of the *mrpC* gene using the genomic DNA of the DZ2 *mrpC* $_{T21-22A,S23-24A}$ strain (PH1139) as the PCR template. The insert was cloned into the BamHI and XhoI restriction sites of pET28a+ (Novagen).

4.4.3 Construction of in-frame deletion / point mutants in *M. xanthus*

In-frame deletion and site-specific point mutants were generated by homologous recombination of a suicide plasmid followed by counter selection based on a previously reported method (Ueki *et al.*, 1996). Approximately 500 bp upstream and downstream of the region of interest were PCR amplified and fused together by an overlap PCR. The fused fragments were then cloned into the plasmid pBJ114 containing the kanamycin resistance cassette and the *galK* gene for counter selection. Error-free sequenced plasmid was introduced by electroporation into *M. xanthus* cells and integrated by single recombination either at the 5' or 3' end of the target. Colonies were selected on kanamycin and confirmed for plasmid integration at the expected site by colony PCR, performed using a plasmid-specific (M13 reverse primer) and a genome-specific (downstream of the region of interest) oligonucleotide (E primer) (Table 4.8). To select for plasmid excision by homologous recombination, the plasmid integrants were grown in CYE broth overnight and selected by plating cells on CYE plates containing galactose. The resulting kanamycin-sensitive (kan^S) and galactose-resistant (gal^R) colonies were screened by colony PCR to discriminate between wild type versus the desired deletion/point mutation. In order to diagnose point mutants by PCR, two gene-specific oligonucleotides were used where one had the wild type base sequence and the other had the point mutated base at the very 3' end. *M. xanthus* cells can accumulate random

mutations during prolonged manipulation. To ensure that any observed phenotype resulted from the desired deletion/point mutation, at least three independent mutant clones were analyzed.

4.4.4 Isolation of genomic DNA from *M. xanthus*

M. xanthus DZ2 cells were grown in 20 ml of CYE broth at 32°C overnight, harvested by centrifugation at 4600 x g for 10 min at RT (Multifuge 1 S-R) and concentrated to an A_{550} of 7.0 in TE buffer (10 mM Tris, 1 mM EDTA, pH 8.0) in 1.5 ml tube. 5% (w/v) SDS, 100 µg/ml proteinase K and 50 µg/ml DNAse-free RNase A were added to the cell suspension and incubated at 37°C for 1 h. The suspension was then mixed with 0.167 volumes of 5M NaCl and 0.114 volumes of 12.15% (w/v) CTAB/NaCl solution (50 ml water, 5 g CTAB, 2.05 g NaCl) and incubated at 65°C for 10 min. Next, the solution was mixed with 975 µl of a phenol: chloroform: isoamyl mixture (25:24:1). The samples were centrifuged for 2 min (Biofuge) at maximum speed at RT. The top aqueous layer was transferred into a fresh tube and mixed with an equal volume of chloroform: isoamyl mixture (24:1). The mixture was centrifuged at maximum speed at RT for 2 min. After centrifugation, the aqueous layer was again transferred into a fresh tube and 0.6 volumes of isopropanol were added. The solution was mixed by inverting until the thread-like genomic DNA precipitated. The DNA was transferred with a pipette tip into a fresh tube containing 1 ml of 70% (v/v) ethanol and centrifuged (Biofuge) for 5 min at maximum speed at RT. The supernatant was discarded and the DNA was washed again in 1 ml of 70% (v/v) ethanol and centrifuged. After this step, the supernatant was removed, the DNA pellet was dried until the smell of ethanol was gone and later resuspended in 50 µl in daH_2O.

4.4.5 Isolation of plasmid DNA from *E. coli*

E. coli cells containing the desired plasmid were grown as described in section 4.3.2. Plasmid DNA was isolated using the QIAprep Spin Miniprep Kit (Qiagen) as recommended by the supplier.

4.4.6 Amplification of DNA fragments by PCR

The amplification of specific DNA fragments for cloning was performed by polymerase chain reaction (PCR) using the Platinum® *Pfx* DNA-polymerase (Life Technologies). PCRs to confirm plasmid integration or deletion mutants were carried out using *Taq* DNA polymerase (Thermo Scientific).

A standard 25µl PCR reaction mixture contained:
Genomic DNA: 2 µl (100 ng/µl)
Forward primer (50 µM stock): 0.25 µl
Reverse primer (50 µM stock): 0.25 µl
2 x FailSafe™ PCR PreMix BufferJ (Bioline): 12.5 µl
DNA Polymerase: 0.25 µl
daH_2O: add upto 25 µl

A standard PCR program followed:
Initial denaturation: 95°C - 3min
Denaturation: 95°C - 30 sec
Primer Annealing: 62°C - 15sec
Elongation: 68°C - 2 min
Final elongation 68°C - 5 min
Hold: 4°C

The elongation temperature was 68°C for *Pfx* polymerase and 72°C for *Taq* polymerase. The elongation time was usually calculated as 1000 bases/min depending on the length of the product. Routinely, 25-35 cycles of amplification were used for each PCR reaction. The melting temperature of the primers was calculated using the software NetPrimer (http://www.premierbiosoft.com/ netprimer/index.html) and the annealing temperature was calculated by subtracting ~5°C from the melting temperature. PCR products were purified using the QIAquick® PCR Purification Kit (Qiagen) or extracted from agarose gels using the QIAquick® Gel Extraction Kit (Qiagen) according to supplier's instructions.

4.4.7 PCR confirmation of *M. xanthus* integrants in the *attB* site

In order to confirm *M. xanthus* integrants in the *attB* site, an attachment (*att*) site PCR was performed. A crude genomic DNA preparation was made from the transformed *M. xanthus* colonies by scraping off some cells from a CYE plate with a wooden stick into an Eppendorf tube containing 20 µl sterile daH_2O. This tube was boiled at 99°C for 7 min, centrifuged at 13000 rpm for 5 min (Biofuge Pico) and thereafter, placed on ice. The supernatant containing the genomic DNA (gDNA) was used as a template for three PCR reactions.

PCR reactions I-III contained the following ingredients:
2 µl crude gDNA
0.25 µl 50 µM oPH primer A
0.25 µl 50 µM oPH primer B
12.5 µl Buffer J 2X Premix (Bioline)
9.75 µl daH2O

0.25 µl Taq polymerase (Thermo Scientific)

PCR I, PCR II and PCR III used the primer pairs oPH477/oPH480, oPH478/oPH479 and oPH477/oPH478, respectively. The PCR machine was programed as follows:

Initial Denaturation: 95°C- 1 min
Denaturation: 95°C - 15 sec
Annealing: 51°C - 15 sec
Elongation: 72°C - 1 min
Final elongation: 72°C - 5 min
Hold: 4°C
The PCR reaction was cycled 25 times.

An appropriate integration could be determined from the length of the PCR product obtained in the three PCR reactions; PCR I (700-800 bp), PCR II (840 bp) and PCR III (no product). A PCR product of ~495 bp in PCR III, the absence of a product in PCR I and II would be expected in case of a non-altered chromosomal *attB* site, indicating that the plasmid integration did not occur in the genome. For each transformed strain, 3-5 clones which were positive for PCR I, II and showed no product in PCR III were inoculated in liquid CYE to prepare freezer stocks (section 4.3.3).

4.4.8 Restriction digestion, dephosphorylation and ligation of DNA

PCR amplified DNA fragments (~500 ng) or plasmid DNA (~1 µg) were digested using 1 µl FastDigest® restriction endonucleases (Fermentas) in a total volume of 20 µl 1x FastDigest® reaction buffer for 30 min to 2 h at 37°C. For dephosphorylation of a digested plasmid, 1 µl antarctic phosphatase (NEB) was added to the restriction reaction alongwith 3 µl 10x antarctic phosphatase buffer and the final reaction volume was adjusted with daH_2O to be 30 µl. This reaction was further incubated for 20 min at 37°C. Finally, this reaction mixture was purified using the QIAquick® PCR Purification Kit (Qiagen) according to the supplier's instructions. Ligation of DNA fragments was achieved by incubation with 1 µl T_4 DNA ligase (Thermo Scientific) in a total reaction volume of 20 µl of 1x T_4 DNA ligase buffer overnight at 16°C. In general, 3-30 fmol of linerarized plasmid DNA was ligated with 3-4 times more insert DNA. The ligation mixture was inactivated at 65°C for 20 min and 5 µl of the reaction was used for transformation of *E. coli* cells.

4.4.9 Agarose gel electrophoresis

DNA fragments or digested plasmid DNA were size-separated with agarose gel electrophoresis in 0.5x TAE (40 mM Tris, 1 mM EDTA, pH 8.0 with acetic acid) buffer using 1-2% TAE agarose gels. To detect DNA, ethidium bromide was added to the agarose at a concentration of 0.01% (v/v). 6x sample loading buffer (0.2% bromophenol blue and 0.2% xylene cyanol dissolved in 50% glycerol) was mixed with samples to a 1x final concentration. A *BstEII* digested λ phage DNA (Thermo Scientific) was used as a standard for fragment size. The gels were run for ~30 min at 150V. For DNA visualization, the gels were exposed to a 2UV-Transilluminator (UVP-Bio-Doc-IT-System, UVP) at a wavelength of 365 nm and images were recorded using an electronic P93E thermo video printer (Mitsubishi). DNA fragments were gel excised and purified with the QIAquick® Gel Extraction Kit (Qiagen).

4.4.10 Determination of nucleic acid concentration

The concentration and purity of DNA/RNA was determined by NanoDrop ND-1000 spectrophotometer.

4.4.11 Sequencing of DNA

PCR amplified DNA fragments or plasmid DNA was sent for commercial sequencing by MWG Operon (Ebersberg) and the sequencing data was analyzed by VectorNTI™ contig express (Invitrogen).

4.4.12 Preparation and transformation of electro competent *E.coli* cells

To prepare electro competent *E. coli* cells, a 5ml overnight culture was sub-cultured into 1L LB medium and incubated at 37°C. Cells were grown to an optical density of 0.7 A_{550} and harvested by centrifugation at 4600 x g for 20 min at 4°C (Multifuge 1 S-R). To remove media components and salts, the cell pellet was washed four times by subsequent resuspension in 10% (v/v) sterile glycerol solution (1000 ml, 500 ml, 250 ml, 40 ml) followed by centrifugation as described earlier. Finally, the pellet was resuspended in 2 ml ice cold sterile 10% (v/v) glycerol and 50 µl aliquots were stored at -80°C after flash freezing.

For transformation, 5 µl ligation reaction or plasmid (~1 µg) was gently mixed with 50 µl ice-cold electro competent cells and transferred to an ice-cold 0.1 cm electroporation cuvette (BioRad). The cuvette was assembled in the GenePulser (BioRad) and pulsed at 1.25 kV, 25 µF and 200 Ω followed by recovery of cells in 1 ml LB medium at 37°C for 1 h. 100 µl and 900 µl of the cell suspension was plated on LB agar plates containing an appropriate antibiotic for selection and incubated at 37°C overnight.

4.4.13 Preparation and transformation of chemocompetent *E.coli* cells

To prepare chemically competent *E. coli* cells, cells were inoculated into 25 ml LB-broth and incubated at 37°C until the culture reached an optical density of 0.7 A_{550}. The cell culture was centrifuged at 4600 x g, for 10 min at 4°C (Multifuge 1 S-R) and resuspended in 2.5 ml sterile, ice cold TSS (1% tryptone, 0.5% yeast extract, 1% NaCl, 10% PEG (MW 3350), 5% DMSO, and 50 mM $MgCl_2$ or $MgSO_4$, pH 6.5) medium. 100 µl aliquots were flash freezed and stored at -80°C.

For transformation, 5 µl ligation reaction or plasmid (~1 µg) was gently mixed with 100 µl of ice-cold chemo competent cells and incubated on ice for 30 min. The cells were then heat shocked at 37°C for 2 min, immediately recovered in 500 µl LB medium and incubated at 37°C for 1 h. Finally, 100 µl and 900 µl of the cell suspension was plated on LB agar plates containing an appropriate antibiotic for selection and incubated overnight at 37°C.

4.4.14 Preparation and transformation of electrocompetent *M. xanthus* cells

To prepare electro competent *M. xanthus* strains, cells were inoculated in 100 ml CYE in a 250 ml flask, incubated at 32°C and grown to approximately 0.3-0.5 $A_{550.}$ The cell culture was centrifuged at 4620 x g for 10 min at RT (Multifuge 1 S-R). The cell pellet was washed in 25 ml daH_2O and centrifuged again as earlier. The wash step was repeated. The pellet was then resuspended in 1 ml water and centrifuged at 4000 x g for 5 min. Finally, the cells were resuspended in 150 µl daH_2O and aliquoted (50 µl) and stored at -80°C after flash freezing.

For the transformation, 1 µg plasmid DNA or 5 µg genomic DNA was added to 50 µl electro competent *M. xanthus* cells, mixed and transferred to a 0.1 cm electroporation cuvette (BioRad). Electroporation was performed at 0.65 kV, 25 µF and 400 Ω; the cells were recovered in 1 ml of CYE medium and incubated for 5 h at 32°C. 100, 300 and 600 µl of the cell culture was mixed with 3 ml molten CYE top agar (at ~50°C), vortexed briefly and plated on CYE agar plates containing an appropriate antibiotic for selection. The plates were incubated at 32°C for 5 to 7 days till transformed colonies appeared.

4.4.15 RNA isolation, cDNA synthesis and quantitative real time PCR

To isolate the total RNA from *M. xanthus* cells, the hot-phenol method was applied. Cells were grown under vegetative conditions or developed in 16 ml Petri-dish format as described previously. Cells were harvested by centrifugation at 4620 x g for 10 min at 4°C (Multifuge 1 S-R). The cell pellet was resuspended in 1ml of ice-cold solution 1 (0.3 M sucrose; 0.01 M sodium acetate, pH 4.5) and transferred into a 15 ml Falcon tube containing 1ml of solution 2 (2% SDS; 0.01M Na Ac, pH 4.5) at 65°C. The sample was gently mixed by inverting the tubes 5 times. 2 ml of hot (65°C) phenol was added to the sample tube, gently mixed by inversion and the sample tube was incubated at 65°C for 5 min. The sample tube was then chilled using liquid nitrogen, thereby avoiding the sample to freeze and centrifuged at 4620 x g for 5 min at 4°C. The aqueous layer was transferred to a fresh 15 ml tube containing 2 ml of hot phenol and again the sample tube was chilled and centrifuged as described earlier. Next, the aqueous layer was transferred to a tube containing 2 ml of Phenol: chloroform: isoamyl alcohol (25:24:1) mixture, mixed by inversion and centrifuged. The aqueous layer was subsequently transferred to a tube containing 2 ml of chloroform: isoamyl alcohol (24:1) mixture and centrifuged. To precipitate RNA, the aqueous layer (~1 ml) was transferred to a fresh tube containing 100 µl of 3 M sodium acetate (pH 4.5) and 2.5 ml of 96% EtOH and was incubated at -80°C for 30 min or overnight. After this incubation, the sample was centifuged at 4620 x g for 30 min at 4°C and the supernatant was removed carefully. To wash the pelleted RNA, 5 ml of ice-cold 75% EtOH was added to the tube and centrifuged at 4620 x g for 5 min at 4°C. The washing step was repeated. Finally, the supernatant was removed and the pellet was air dried and dissolved in 100 µl of RNase-free water. The concentration and purity of the RNA isolated was measured by NanoDrop. 10 µg of the total extracted RNA was incubated in the presence of 10 µl RNase-free DNase I (EN0521, 1000 U, Thermo Scientific) in a 100 µl 1x reaction buffer solution for 1 h at 37°C. 1 µl of 25 mM EDTA was added and the reaction was incubated 65°C for 10 min to inactivate the enzyme. Finally, the RNA was purified using the precipitation method described above.

For the RNA isolation from the separated cell fractions, a fixed number of *E. coli* cells (counted using a cell chamber) were added directly to the lysis solution 1; proportionate volumes of this mixture were added to the two cell fraction pellets such that the ratio of *E. coli* to *M. xanthus* cells (previously counted with a cell counter) was 1:1000. Subsequently, solution 2 was also added in proportionate volumes as solution 1 and 2 ml of sample from each fraction were finally used to continue with the rest of the procedure from the hot-phenol step.

For the cDNA synthesis, 1 µg of DNA-free RNA was used as a template for reverse transcription using the Superscript III kit (Invitrogen). The recommended protocol was followed. A 13 µl reaction mixture containing RNA (1 µg, <10 µl), random hexamers or specific cDNA synthesis primer (2 µl, 100 ng/µl), DNTPs (1

µl, 10 mM) was prepared in RNase-free water in a thin wall PCR tube which was incubated at 65°C for 5 min and snap cooled on ice. To this reaction, 4 µl of 5x RT-buffer, 1 µl of RNasin (RNase inhibitor), 1 µl of Superscript III RT enzyme and 1 µl of 0.1 M DTT (prepared as a master mix, 7 µl per reaction) was added. This reaction mix was incubated in a PCR machine programmed at 25°C for the first 5 min; at 55°C for the next 50 min and at 70°C for the last 15 min.

The quantitative real time PCR (qRT-PCR) was performed using the SYBR® Green PCR master mix kit (Applied Biosystems). Each reaction containing cDNA (2 µl, diluted 1:20 / 1:100 / 1:1000 etc.), 2X PCR-solution (13 µl), specific qPCR primer-mix (2 µl, 5 µM each primer, always diluted fresh) and water (9 µl) in a total volume of 26 µl was performed in triplicates. Control reactions contained no cDNA (no reverse transcriptase) and H_2O (no template) as negative controls and gDNA as positive control. The real time PCR system was programmed as follows:

Initial denaturation: 95°C – 10 min
Denaturation: 95°C – 10 min
Primer annealing and elongation*: 60°C – 15 sec
Denaturation*: 95°C – 1 min
Recording of dissociation curve: 60°C – 30 sec
95°C – 15 sec
Hold: 4°C
(*=40 cycles)

Data were analyzed by averaging the C_t values for each triplicate sample. For analysis of mRNA levels in the total population, the ΔC_t value for each sample was determined by subtraction of the C_t value for the wild type from the respective sample and the fold difference in mRNA levels was calculated by normalizing to the native 16sRNA levels in each sample. For analysis of mRNA levels in the non-aggregated and aggregated cell populations, the ΔC_t value for the non-aggregated fraction was determined by subtracting the average C_t value for the corresponding aggregated cell fraction. Thus, the fold difference in mRNA levels was expressed as the ratio of NA/A *mrpC* mRNA levels. To control for efficiency of RNA extraction and cDNA generation, the levels of *mrpC* mRNA were normalised to *E.coli* 16S rRNA isolated from *E. coli* cells spiked in proportion to the number of *M. xanthus* cells in each fraction (as described above). Appropriate controls were performed to ensure that the *E. coli* 16S rRNA was not amplified by *M. xanthus* 16S rRNA primers and also that *M. xanthus mrpC* specific primers did not amplify *E. coli* mRNA.

4.5 Biochemical methods

4.5.1 Protein sample preparation & total protein concentration determination

To perform immunoblot analysis, protein samples were prepared in two ways, namely, samples with an equal protein concentration or with an equal cell number.

Protein samples with equal protein concentration

Cells were developed in 16 ml submerged culture format and harvested by centrifugation at 4620 x g for 10 min at 4°C (Multifuge 1 S-R) and directly frozen at -20°C. Cell pellets were resuspended in 200 µl of 100 mM Tris buffer (pH 7.6), diluted with 200 µl 2x clear LSB (without β-mercap and blue dye) and heated at 95°C for 5 min. The protein concentration of each sample was determined using a BCA™ Protein Assay Kit (Thermo Scientific). The samples were further diluted in 2x LSB to 1 µg/µl and briefly boiled at 99°C before loading onto a gel. Additionally, samples from 36 h developmental samples were transferred into 2 ml screw cap tubes filled with 0.5 g 0.1 mm zirconia/silica beads (BioSpec, Bartlesville). Spores were mechanically disintegrated using a FastPrep®24 tissue and cell homogenizer (MP Biomedicals) six times at 6.5 m/s speed for 45 s each. Samples were shortly boiled again before loading on a gel/ determining the protein concentration.

Protein sample as equal cell number

Cells were harvested from 16 ml of submerged culture and separated into the non-aggregated and aggregated cell fraction as described earlier. To determine the cell number, cells in each fraction were resuspended in equivalent volumes of MMC starvation buffer (16 ml) in 50 ml Falcon tubes, parafilm sealed and dispersed using the FastPrep®24 tissue and cell homogenizer (MP Biomedicals) at 5 m/s speed for 45 s at least twice. Cell numbers were counted using a cell counter. The cell pellets from these counted samples were later resuspended as 4.3 x 10^6 cells/µl in hot (80°C) LSB containing 1:20 mammalian protease inhibitor cocktail (Sigma) by flushing the walls of the tube. Samples were boiled at 99°C for 10 min. Also, like earlier, 36 h old samples were bead beated after resuspension to lyse spores and briefly boiled again and centrifuged before loading on a gel.

Determination of total protein concentration

To determine the total protein concentration of samples, the BCA™ Protein Assay Kit (Thermo Scientific) was used according to the instructions of the manufacturer, except that the test sample was in total 50 µl and 950 µl of the developer from the kit was used. To check the concentration of over-expressed proteins, the Bradford assay was used as recommended in the Bio-Rad protein

assay kit (Bio-Rad, Munchen). The absorbance of samples was measured using an Ultrospec 2100 pro spectrophotometer (Amersham).

4.5.2 SDS Polyacrylamide Gel Electrophoresis (SDS-PAGE)

For the analysis of proteins under denaturing conditions, a discontinuous sodium dodecyl sulphate-polyacrylamide gel electrophoresis (SDS-PAGE) was performed. Protein samples were mixed with equal volumes of 2x Laemmli sample buffer (LSB; 0.125 M Tris-HCl pH 6.8, 20% glycerol, 4% SDS, 10% β-mercaptoethanol, 0.02% bromophenol blue) and heated at 99°C for 5 min. PageRuler™ prestained protein ladder plus (Thermo Scientific) was used as a size standard. Electrophoresis was performed using Bio-Rad electrophoresis chambers (Bio-Rad, München) at 150-175 V for ~1.5h in Tris-glycine-SDS running buffer (25 mM Tris; 190 mM Glycine; 0.1% SDS) until the dye front reached the bottom of the gel. Proteins were visualized by soaking the gel in staining solution (70% ethanol, 7% acetic acid, 0.25% Coomassie brilliant blue R250) for 30 min to overnight and then by incubation in the destaining solution (70% ethanol, 7% acetic acid) until the protein bands became clearly visible or alternatively, an immunoblot analysis was performed.

The resolving gel of the SDS-PAG was composed of x% Rotiphorese® NF-acrylamide/bis-solution (29:1), 0.35 mM APS and 0.06% (v/v) N,N,N,N- TEMED in 1x resolving buffer (4x, 1.5 M Tris-HCl pH 8.8, 0.4% SDS). The desired concentration of acrylamide (x) was adjusted depending on the protein size to be analyzed and is mentioned in the relevant sections. The stacking gel was composed of 5% Rotiphorese® NF-acrylamide/bis-solution (29:1), 0.44 mM APS and 0.076% (v/v) TEMED in 1x stacking buffer (4x, 0.5 M Tris-HCl pH 6.8, 0.4% SDS).

4.5.3 Immunoblot analysis

For the immunoblot analysis, the protein samples were prepared as described in section 4.5.1. 20 µg of total protein or 4.6 x 10^7 cells in each fraction were resolved by denaturing SDS-PAGE in 12% polyacrylamide gels. After electrophoresis, the protein in the gels was transferred onto a PVDF membrane in a transfer buffer (25 mM Tris, 192 mM glycine, 10% methanol, 0.1% SDS, pH 8.3) using a wet tank transfer system (Hoeffer). Briefly, in the transfer cassette, the gel containing the proteins was placed over a PVDF membrane (activated in methanol and washed in daH_2O) which was tightly packed between two pieces of thick Whatman® paper and a piece of foam on either sides. The apparatus was connected to the power supply to transfer proteins from the gel to the membrane overnight at 20V at 4°C. After the transfer, the PVDF membrane was

dried, rehydrated briefly in 100% methanol, washed with daH2O and incubated in blocking milk (5% non-fat milk powder, 0.1% tween-20 dissolved in 1x PBS buffer pH 7.4, see below) for 1 h at room temperature or overnight at 4°C. After blocking, the membrane was incubated with milk containing an appropriate dilution of the primary antibody (anti-FibA, 1:5000; anti-mCherry, 1:10,000 and anti-MrpC, 1:1000) for 1 h at room temperature or overnight at 4°C. The membrane was washed three times with blocking milk for 10 min and then incubated with the secondary antibody for 1 h at room temperature. This antibody was an anti-rabbit IgG conjugated to horseradish peroxidase (HRP) (Thermo Scientific) and was used at a dilution of 1: 20,000. Next, the membrane was washed three times with PBS buffer (137 mM NaCl, 10 mM phosphate, 2.7 mM KCl pH 7.4) for 10 min. Signals on the membrane were detected with a chemiluminescence substrate (Thermo Scientific) followed by exposure to an X-ray film (Thermo scientific). The relative intensity of proteins was quantified using the software Image J.

4.5.4 Radiolabeled *in-vitro* phosphorylation assay

To carry out the i*n vitro* phosphorylation of Pkn14 and MrpC, the protocol of Nariya and Inouye was slightly modified and adopted (Nariya and Inouye, 2005). 10 µM of each recombinant protein was incubated in 30 µL of buffer P (50 mM Tris-HCl pH 8.0, 10 mM $MgCl_2$, 2 mM DTT) containing 175 µM ATP with 1.5 µCi of [γ^{32} P]-ATP 222 TBq/mmol; Hartmann Analytic, Braunschweig) for 30 minutes at 30°C. The reaction was quenched with an equal volume of 2x LSB and 20 µl were loaded on a 15% SDS-PAGE to resolve the radiolabeled proteins. The gel was exposed to a Storage Phosphor Screen (GE Healthcare) overnight and analyzed using a Storm^{TM} 800 imaging system (GE Healthcare). Later, the SDS-PAGE gel was stained with Coomassie brilliant blue to detect the total protein.

4.5.5 MrpC turnover assay

For the MrpC turnover experiment in the developmental cell populations, a previously established protein turnover assay was modified and adopted (Schramm, PhD Thesis 2012). Wild type DZ2 cells were developed in 16 ml submerged culture format for 18 h, cells were harvested from three plates and the non-aggregated and aggregated cell fractions separated (as described in section 4.3.5) from each plate were pooled together in one 50 ml Falcon tubes and resuspended in MMC buffer such that in total, the non-aggregated fraction was in 48 ml and the aggregated cell fraction was in 18 ml of buffer. The number of cells in each fraction was counted with the cell counter (Beckman Coulter Inc.) after dispersing the cell fractions twice with the FastPrep®24 cell and tissue homogenizer (MP Biomedicals) at 5m/s for 45s. Each fraction was then

divided into three portions; non-aggregated fraction was divided as 3 x 15 ml while the aggregated fraction was divided as 3 x 5 ml. Each fraction was treated with 34 µg/ml chloramphenicol block *de novo* protein synthesis or ethanol or Sigma Mammalian Protease Inhibitor cocktail (1:20) at 32°C in an orbital shaker. At 0, 20 and 40 min after addition, cells were quickly harvested by centrifuging. 4ml of the non-aggregated cell fraction was harvested at 4600 x g, 4°C for 2 min (Multifuge 1 S-R) and 1 ml of the aggregated cell fraction was harvested at 13000 rpm, 4°C for 2 min (Biofuge fresco) and stored at -20°C for further analysis. Cells of the two fractions were resuspended in hot (70°C) LSB so as to have 4.6 x 10^6 cells/µl in each fraction and heated at 99 °C for 5 min. 20 µl of protein samples were analyzed by MrpC immunoblot as described in section 4.5.3. Band intensities were quantified with the software ImageJ. The MrpC half-life in the two cell fractions was calculated assuming a first order kinetic degradation reaction (Schramm *et al.*, 2012). Each background-subtracted band intensity value was normalized to the intensity at t=0 in the respective sample and the natural log of the resulting values was plotted versus minutes after the chloramphenicol treatment using Microsoft Excel. The slope (k) of the linear fit of the data was used to calculate the MrpC half-life ($t_{1/2}$) using the equation $t_{1/2}$ = ln(2)/-k.

4.5.6 Over-expression and purification of recombinant proteins

The plasmids encoding the recombinant proteins are described in section 4.4.1 and 4.4.2. To induce protein over-expression, the respective plasmids were freshly transformed into BL21/ λDE3 *E.coli* strain. Overnight pre-cultures were prepared in 5 ml LB medium with an appropriate antibiotic.

Pkn14 and Pkn14$_{K48N}$

For the over-expression of Pkn14 and its point mutant Pkn14$_{K48N}$, the plasmids pPH166 and pVG130 were used, respectively. The overnight pre-culture was sub-cultured (1:100) into 250 ml LB broth containing 100 µg/ml ampicillin, grown to an optical density of ~ 0.7 A_{550} at 37°C, and induced with anhydro-tetracycline (0.2µg/ml dissolved in DMF) at 18°C overnight or 37°C for 2-3 hours. The induced culture was harvested in a GS3 rotor at 7000 rpm for 20 min at 4°C. The supernatant was removed and the pellets were frozen at -20°C.

For purification, the induced cell pellet was resuspended in 10 ml of ice cold Buffer W (100 mM Tris pH 8.0, 150 mM NaCl, 1 mM EDTA) and protease inhibitor cocktail (1:100) solution and lysed by three passages through French® Pressure Cell Press at 18,000 psi. The cell lysate was pelleted at 600 x g for 30 min at 4°C (Multifuge 1 S-R). The supernatant fraction containing the soluble protein was purified by affinity chromatography using the Strep-tag II®

purification kit as per manufacturer's instructions (IBA BioTAGnology, Goettingen). Briefly, 2ml 50 % slurry of Strep-Tactin® Sepharose® beads was applied to a disposable chromatography column and allowed to settle for ~15min. The column was drained (bed volume = 1 ml) and equilibrated with 5 ml Buffer W. 1 ml of supernatant fraction containing the recombinant protein (50-100 nmol) was applied to the column and simultaneously, the flow through fraction was collected (~ 1ml). The column was washed with 5 ml Buffer W and 5 wash fractions (1 ml each) were collected. The recombinant protein was eluted with 3 ml of Buffer E (100 mM Tris pH 8.0, 150 mM NaCl, 1 mM EDTA, 2.5 mM desthiobiotin) and 4 elution fractions (1 ml each) were collected. The column was regenerated with 15 ml Buffer R (100 mM Tris pH 8.0, 150 mM NaCl, 1 mM EDTA, 1 mM HABA) and stored at 4°C by overlaying with 2 ml of Buffer R for future use. All the collected fractions were analysed by SDS-PAGE. The elution fraction (E2) containing the purified protein was dialyzed against a buffer containing 100 mM Tris pH 8.0, 150 mM NaCl and 20 % w/v glycerol and stored at -20°C for subsequent use in phosphorylation assays.

MrpC, MrpC2, MrpC$_{T22A}$, MrpC$_{T21-22A}$ and MrpC$_{T21-22A,S23-24A}$

For the over-expression of MrpC, MrpC2, MrpC$_{T22A}$, MrpC$_{T21-22A}$ and MrpC$_{T21-22A,S23-24A,}$ the plasmids pPH158, pPH167, pPH168, pPH169 and pVG131 were used, respectively. The overnight pre-culture was sub-cultured (1:100) into 250 ml LB broth containing 50 µg/ml kanamycin, grown to an optical density of ~0.7 A_{550} at 37°C and induced with 0.5 mM IPTG at 37°C for 3 hours. The induced culture was harvested in a GS3 rotor at 7000 rpm for 20 min at 4°C. The supernatant was removed and the pellets were frozen at -20°C.

For purification, the induced cell pellet was resuspended in 30 ml of ice cold Lysis Buffer A (50 mM HEPES pH 7.4, 500 mM NaCl, 20 mM imidazole) and protease inhibitor cocktail (1:100) solution and lysed by three passages through French® Pressure Cell Press at 18,000 psi. The cell lysate was pelleted at 100000 x g for 30 min at 4°C (T865 rotor). The supernatant fraction containing the soluble protein was purified by nickel affinity chromatography at 4°C (ÄKTApurifier™, GE Healthcare) using a 1 ml His Trap FF1 nickel affinity column (GE Healthcare). The column was washed with 5 column volumes (CV) of 20% ethanol, 5 CV of water and finally, 5 CV of Buffer A. The supernatant was applied to the column at a flow rate of 1 ml/min and the flow through was collected as one fraction. The column was washed with 5 CV of Buffer A and 5 wash fractions were collected (1 ml each). The recombinant protein was eluted with a linear gradient of 20-500 mM imidazole using Buffer B (50 mM HEPES pH 7.4, 500 mM NaCl, 500 mM imidazole) and subsequently, 10 elution fractions were collected (1 ml each). The column was washed with 5 CV of Buffer B, 5 CV of Buffer A, 5 CV of water and finally stored in 5 CV of 20%

ethanol. All the collected fractions were analysed by SDS-PAGE. The elution fraction containing the purified protein was dialyzed against a buffer containing 100 mM Tris pH 8.0, 150 mM NaCl and 20 % w/v glycerol and stored at -20°C for subsequent use in phosphorylation assays.

4.6 Bioinformatic analysis

Orthologs of Mxan_5126 and MrpC were identified within the Myxococcales genomic sequences using a reciprocal BLASTp (Altschul *et al*., 1997) analysis. The protein sequence of either Mxan_5126 or MrpC was used as query in a BLASTp analysis against the publically available protein database from *Myxococcus fulvus* HW-1 (accession no. CP002830), *Myxococcus stipitatus* DSM 14675 (accession no. CP004025.1), *Corallococcus coralloides* DSM2259 (accession no. CP003389), *Stigmatella aurantiaca* DW4/3-1 (accession no. CP002271), *Anaeromyxobacter dehalogenans* 2CP-C (accession no. CP000251.1), *Haliangium ochraceum* SMP-2 (accession no. CP001804.1), *Sorangium cellulosum* So ce 56 (accession no. AM746676). The protein with the highest bitscore was then used as a query in a second Blastp analysis against the protein database from *Myxococcus xanthus* DK1622 (accession no. CP000113). If the highest scoring match in the second Blastp analysis was identical to the protein sequence originally used for the first Blastp analysis, the two proteins were considered orthologs. Additionally, the unpublished genome *M. macrosporus* provided by Stuart Huntley was also analysed using the Artemis Comparison Tool (Wellcome Trust Sanger Institute).

4.7 Plate reader experiments

Strains were induced to develop under submerged conditions in 24-well dishes (as described in section 4.3.4) and harvested in 2-ml screw cap tubes at various time points. The cells were dispersed (without beads) at 5 m/s for 45 sec in a FastPrep® 24 cell and tissue homogenizer (MP Biomedicals) at 4°C. Cells were dispersed once till 24 h and twice at the later time points and 200 µl of the dispersed cell culture was analyzed for the mCherry fluorescence signal intensity at an excitation/emission wavelength of 582/613 nm with the Infinite M200 plate reader (Tecan, Austria) in 24-well glass bottom plates (Greiner Bio-One). Simultaneously, the total number of cells in each strain was counted with a cell counter. The average fluorescence was calculated by normalising to the total number of cells. A wild type strain lacking the fluorescent reporter was used as the background control. All measurements were done from biological triplicate experiments.

4.8 Microscopic methods

For fluorescent microscopic analysis, 10 µl of *M. xanthus* cells were spotted on agar pads made of 1.5% (w/v) agarose in A50 starvation buffer (10 mM MOPS pH 7.2, 1 mM $CaCl_2$, 1 mM $MgCl_2$, 50 mM NaCl), covered with a cover slip and stored in a humidity chamber (for ~5-10 min) to prevent desiccation and at the same time allowing the cells to settle on the agar surface before analysis under the fluorescent microscope. Phase contrast and fluorescent pictures with the Dsred and Gfp channels were taken with 40x magnification with the Zeiss Axio Imager.M1 microscope (Carl Zeiss, Jena). The pictures were taken using the Cascade 1K camera, HXP-120 Light Source for Fluorescence Illumination (Visitron Systems, Puchheim) and analyzed using the software Metamorph® v.7.5 (Molecular Devices).

4.8.1 Single cell fluorescence analysis with the software Metamorph® v.7.5

Pictures (both phase contrast and fluorescent) of single cells taken under the fluorescent microscope were opened in the software Metamorph® v.7.5 (Molecular Devices). On a phase contrast image, a rectangular region (size 64 x 64) was drawn around as well as just adjacent to each single cell so as to measure the fluorescence intensity and the background fluorescence for each single cell, respectively. The regions drawn around various single cells on each image were transferred to the corresponding fluorescent image and the average intensity of all the marked regions was recorded. The background fluorescence was subtracted from the fluorescence signal for every cell analyzed in order to get its absolute fluorescence value without any error due to varying background fluorescence in various areas of the agar pad. In case, the absolute fluorescence intensity measurement had a negative value, it was zeroed. Thus, the single cell intensity measurement of cells ($n \geq 100$) was used to calculate either the population average or to look at the single cell heterogeneity in a population with the aid of box plots.

5. APPENDIX

Table 5.1 Biological replicates of the MrpC turnover assay. Chloramphenicol chase experiments were performed as described in section 2.2.2 (Fig. 2.11). The MrpC band intensities for each time point (0, 20, 40 minutes) normalized to T=0 of the respective sample and fraction (NA, non-aggregated; A, aggregated) are indicated for five biological replicates. Cm, Chloramphenicol; PI, Protease inhibitor; +/-, with/without. Tick mark (✓) means a control/test worked as expected, cross (x) means a control/test did not work as expected and question mark (?) means not defined.

1	NA	0	20	40	Result	A	0	20	40	Result
	Cm- PI-	1.00	1.70	1.78	✓	Cm- PI-	1.00	1.23	1.26	✓
	Cm+ PI-	1.00	0.94	0.79	✓	Cm+ PI-	1.00	0.91	0.51	✓
	Cm- PI+	1.00	2.26	3.69	✓	Cm- PI+	1.00	1.38	1.47	✓
2	**NA**	0	20	40	Result	**A**	0	20	40	Result
	Cm- PI-	1.00	1.63	2.39	✓	Cm- PI-	1.00	1.49	2.67	✓
	Cm+ PI-	1.00	1.41	2.44	x	Cm+ PI-	1.00	0.82	0.66	✓
	Cm- PI+	1.00	1.95	2.27	x	Cm- PI+	1.00	1.53	1.64	x
3	**NA**	0	20	40	Result	**A**	0	20	40	Result
	Cm- PI-	1.00	3.30	4.02	✓	Cm- PI-	1.00	1.22	1.91	✓
	Cm+ PI-	1.00	1.34	1.74	x	Cm+ PI-	1.00	1.10	0.87	x
	Cm- PI+	1.00	2.30	2.62	x	Cm- PI+	1.00	1.36	1.59	x
4	**NA**	0	20	40	Result	**A**	0	20	40	Result
	Cm- PI-	1.00	5.55	11.44	✓	Cm- PI-	1.00	0.85	0.80	x
	Cm+ PI-	1.00	0.79	0.83	✓	Cm+ PI-	1.00	0.78	N.D.	?
	Cm+ PI+	1.00	1.57	1.69	x	Cm+ PI+	1.00	0.39	0.43	x
5	**NA**	0	20	40	Result	**A**	0	20	40	Result
	Cm- PI-	1.00	1.78	2.04	✓	Cm- PI-	1.00	1.83	1.53	✓
	Cm+ PI-	1.00	1.12	1.53	x	Cm+ PI-	1.00	0.91	0.75	✓
	Cm+ PI+	1.00	1.21	1.22	x	Cm+ PI+	1.00	0.74	0.31	x

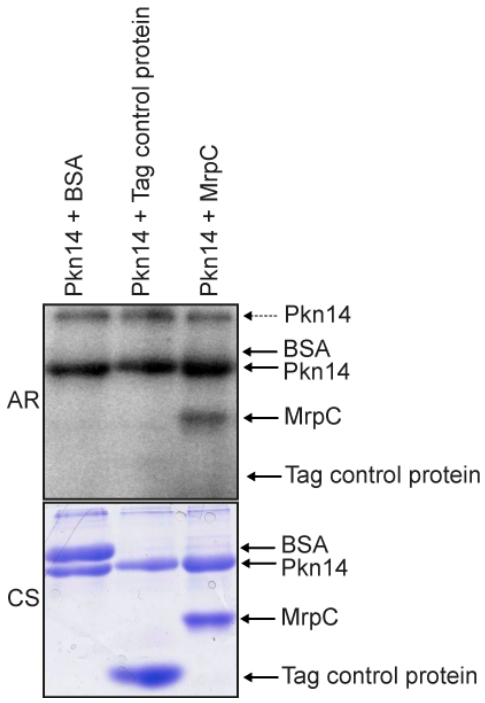

Fig 5.1 Control reactions for the *in vitro* phosphorylation assay of MrpC and MrpC mutants by Pkn14. A. 10 µM of each recombinant protein was incubated in 30 µL of buffer P containing 175 µM ATP with 1.5 µCi of [γ^{32} P]-ATP for 30 minutes at 30ºC, quenched and analyzed on a 15% SDS-PAGE. The radiolabel was detected by exposure to a Storage Phosphor Screen (AR). The dashed arrow represents a phosphorylated Pkn14 oligomer. B. The SDS-PAGE gel in A was subsequently stained with Coomassie brilliant blue to detect the total protein (CS). BSA, bovine serum albumin; tag control protein contains the same tag as on the purified recombinant MrpC proteins used in the assay and lacks any kinase or phosphatase activity.

6. REFERENCES

Altschul SF, Madden TL, Schäffer AA, Zhang J, Zhang Z, Miller W & Lipman DJ (1997). Gapped BLAST and PSI-BLAST: a new generation of protein database search programs. *Nucleic Acids Res* 25: 3389–3402.

Amon A (1998). Controlling cell cycle and cell fate: Common strategies in prokaryotes and eukaryotes. *Proc Natl Acad Sci USA* 95: 85–86.

Balaban NQ, Merrin J, Chait R, Kowalik L & Leibler S (2004). Bacterial persistence as a phenotypic switch. *Science* 305: 1622–1625.

Bignell C & Thomas CM (2001). The bacterial ParA-ParB partitioning proteins. *J Biotech* 91:1–34.

Blackhart BD & Zusman D R (1985). “Frizzy” genes of *Myxococcus xanthus* are involved in control of frequency of reversal of gliding motility. *Proc Natl Acad Sci USA* 82: 8767–8770.

Boynton TO, McMurry JL & Shimkets Lawrence J (2013). Characterization of *Myxococcus xanthus* MazF and implications for a new point of regulation. *Mol Microbiol* 87: 1267–1276.

Boysen A, Ellehauge E, Julien B & Søgaard-Andersen L (2002). The DevT protein stimulates synthesis of FruA, a signal transduction protein required for fruiting body morphogenesis in *Myxococcus xanthus*. *J Bacteriol* 184: 1540–1546.

Brenneis M & Soppa J (2009). Regulation of translation in haloarchaea: 5’- and 3'-UTRs are essential and have to functionally interact *in vivo*. *PloS One* 4: e4484.

Chai Y, Chu F, Kolter R & Losick R (2008). Bistability and biofilm formation in *Bacillus subtilis*. *Mol Microbiol* 67: 254–263.

Chastanet A, Vitkup D, Yuan G-C, Norman TM, Liu JS & Losick RM (2010). Broadly heterogeneous activation of the master regulator for sporulation in *Bacillus subtilis*. *Proc Natl Acad Sci US* 107: 8486–8491.

Cho K & Zusman D R (1999). Sporulation timing in *Myxococcus xanthus* is controlled by the *espAB* locus. *Mol Microbiol* 34: 714–725.

Cozy LM & Kearns DB (2010). Gene position in a long operon governs motility development in *Bacillus subtilis*. *Mol Microbiol* 76: 273–285.

Curtis PD, Taylor RG, Welch RD & Shimkets Lawrence J (2007). Spatial organization of *Myxococcus xanthus* during fruiting body formation. *J Bacteriol* 189: 9126–9130.

Davidson CJ & Surette MG (2008). Individuality in bacteria. *Annu Rev Genet* 42: 253–268.

Ding N, Zheng Y, Wu Q & Mao Xiaohua (2008). The 5′ untranslated region of fruA mRNA is required for translational enhancement of FruA synthesis during *Myxococcus xanthus* development. *Arch Microbiol* 189: 279–288.

Dubnau David & Losick R (2006). Bistability in bacteria. *Mol Microbiol* 61: 564–572.

Dworkin, M. & D. Kaiser, (1993). Myxobacteria II. American Society for Microbiology, Washington, DC.

Ellehauge E, Nørregaard-Madsen M & Søgaard-Andersen L (1998). The FruA signal transduction protein provides a checkpoint for the temporal co-ordination of intercellular signals in *Myxococcus xanthus* development. *Mol Microbiol* 30: 807–817.

Fujita M & Losick R (2005). Evidence that entry into sporulation in *Bacillus subtilis* is governed by a gradual increase in the level and activity of the master regulator Spo0A. *Genes Dev* 19: 2236–2244.

Fujita M & Losick R (2003). The master regulator for entry into sporulation in *Bacillus subtilis* becomes a cell-specific transcription factor after asymmetric division. *Genes Dev* 17: 1166–1174.

García-Moreno D, Polanco MC, Navarro-Avilés G, Murillo FJ, Padmanabhan S & Elías-Arnanz M (2009). A Vitamin B12-Based System for Conditional Expression Reveals *dksA* To Be an Essential Gene in *Myxococcus xanthus*. *J Bacteriol* 191: 3108–3119.

Goldman BS *et al*. (2006). Evolution of sensory complexity recorded in a myxobacterial genome. *Proc Natl Acad Sci USA* 103: 15200–15205.

Gómez-Santos N, Treuner-Lange A, Moraleda-Muñoz A, García-Bravo E, García-Hernández R, Martínez-Cayuela M, Pérez J, Søgaard-Andersen Lotte & Muñoz-Dorado José (2012). Comprehensive set of integrative plasmid vectors for copper-inducible gene expression in *Myxococcus xanthus*. *Appl Environ Microbiol* 78: 2515–2521.

González-Pastor JE (2011). Cannibalism: a social behavior in sporulating *Bacillus subtilis*. *FEMS Microbiol Rev* 35: 415–424.

Gottesman S (2003). Proteolysis in bacterial regulatory circuits. *Annu Rev Cell Dev Biol* 19: 565–587.

Graumann PL (2006). Different genetic programmes within identical bacteria under identical conditions: the phenomenon of bistability greatly modifies our view on bacterial populations. *Mol Microbiol* 61: 560–563.

Gronewold TM & Kaiser D (2001). The *act* operon controls the level and time of C-signal production for *Myxococcus xanthus* development. *Mol Microbiol* 40: 744–756.

Hanlon WA, Inouye M & Inouye S (1997). Pkn9, a Ser/Thr protein kinase involved in the development of *Myxococcus xanthus*. *Mol Microbiol* 23: 459–471.

Harris BZ, Kaiser D & Singer M (1998). The guanosine nucleotide (p)ppGpp initiates development and A-factor production in Myxococcus xanthus . *Genes Dev* 12: 1022–1035.

Hengge R (2009). Proteolysis of sigmaS (RpoS). and the general stress response in Escherichia coli. *Res Microbiol* 160: 667–676.

Higgs PI, Cho Kyungyun, Whitworth DE, Evans LS & Zusman David R (2005). Four unusual two-component signal transduction homologs, RedC to RedF, are necessary for timely development in *Myxococcus xanthus*. *J Bacteriol* 187: 8191–8195.

Higgs PI, Jagadeesan S, Mann P & Zusman David R (2008). EspA, an orphan hybrid histidine protein kinase, regulates the timing of expression of key developmental proteins of *Myxococcus xanthus*. *J Bacteriol* 190: 4416–4426.

Hoiczyk E, Ring MW, McHugh CA, Schwär G, Bode E, Krug D, Altmeyer MO, Lu JZ & Bode HB (2009). Lipid body formation plays a central role in cell fate determination during developmental differentiation of *Myxococcus xanthus*. *Mol Microbiol* 74: 497–517.

Iniesta A A, García-Heras F, Abellón-Ruiz J, Gallego-García A & Elías-Arnanz M (2012). Two systems for conditional gene expression in *Myxococcus xanthus* inducible by isopropyl-β-D-thiogalactopyranoside or vanillate. *J Bacteriol* 194: 5875–5885.

Janssen GR & Dworkin M (1985). Cell-cell interactions in developmental lysis of *Myxococcus xanthus*. *Dev Biol* 112: 194–202.

Jelsbak L & Kaiser Dale (2005). Regulating pilin expression reveals a threshold for S motility in *Myxococcus xanthus*. *J Bacteriol* 187: 2105–2112.

Julien B, Kaiser a D & Garza a (2000). Spatial control of cell differentiation in *Myxococcus xanthus*. *Proc Natl Acad Sci USA* 97: 9098–9103.

Kaberdin VR & Bläsi U (2006). Translation initiation and the fate of bacterial mRNAs. *FEMS Microbiol Rev* 30: 967–979.

Kaiser Dale (2004). Signaling in myxobacteria. *Annu Rev of Microbiol* 58: 75–98.

Kaiser Dale, Robinson M & Kroos L (2010). Myxobacteria, polarity, and multicellular morphogenesis. *Cold Spring Harb Perspect Biol* 2: a000380.

Kaplan HB & Plamann L (1996). A *Myxococcus xanthus* cell density-sensing system required for multicellular development. *FEMS Microbiol Lett* 139: 89–95.

Kearns DB & Losick R (2005). Cell population heterogeneity during growth of *Bacillus subtilis*. *Genes Dev* 19: 3083–3094.

Koch MK, McHugh CA & Hoiczyk E (2011). BacM, an N-terminally processed bactofilin of *Myxococcus xanthus*, is crucial for proper cell shape. *Mol Microbiol* 80: 1031–1051.

Kumar K, Mella-Herrera R a & Golden JW (2010). Cyanobacterial heterocysts. *Cold Spring Harb Perspect Biol* 2: a000315.

Kunst F *et al*. (1997). The complete genome sequence of the gram-positive bacterium *Bacillus subtilis*. *Nature* 390: 249–256.

Kuspa A, Plamann L & Kaiser D (1992). Identification of heat-stable A-factor from *Myxococcus xanthus*. *J Bacteriol* 174: 3319–3326.

Laub MT, Shapiro L & McAdams HH (2007). Systems biology of Caulobacter. *Annu Rev Genet* 41: 429–441.

Laue BE & Gill RE (1995). Using a phase-locked mutant of *Myxococcus xanthus* to study the role of phase variation in development. *J Bacteriol* 177: 4089–4096.

Lee B, Higgs P, Zusman DR & Cho Kyungyun (2005). EspC is involved in controlling the timing of development in *Myxococcus xanthus*. *J Bacteriol* 187: 5029–5031.

Lee B, PhD Thesis (2009). The role of negative regulators in coordination of the *Myxococcus xanthus* developmental program.

Lee B, Holkenbrink C, Treuner-Lange A & Higgs PI (2012). *Myxococcus xanthus* developmental cell fate production: heterogeneous accumulation of developmental regulatory proteins and reexamination of the role of MazF in developmental lysis. *J Bacteriol* 194: 3058–3068.

Lee B, Mann P, Grover V, Treuner-Lange A, Kahnt J & Higgs PI (2011). The *Myxococcus xanthus* spore cuticula protein C is a fragment of FibA, an extracellular metalloprotease produced exclusively in aggregated cells. *PloS One* 6: e28968.

Lee J-S, Son B, Viswanathan P, Luethy PM & Kroos L (2011). Combinatorial regulation of *fmgD* by MrpC2 and FruA during *Myxococcus xanthus* development. *J Bacteriol* 193: 1681–1689.

Leisner M, Stingl K, Frey E & Maier B (2008). Stochastic switching to competence. *Curr Opin Microbiol* 11: 553–559.

Leonardy S, Freymark G, Hebener S, Ellehauge Eva & Søgaard-Andersen Lotte (2007). Coupling of protein localization and cell movements by a dynamically localized response regulator in *Myxococcus xanthus*. *EMBO J* 26: 4433–4444.

Letouvet-Pawlak B, Monnier C, Barray S, Hodgson DA & Guespin-Michel JF (1990). Comparison of beta-galactosidase production by two inducible promoters in *Myxococcus xanthus*. *Res Microbiol* 141: 425–435.

Lewis K (2007). Persister cells, dormancy and infectious disease. *Nat Rev. Microbiol* 5: 48–56.

Li S, Lee BU & Shimkets L J (1992). csgA expression entrains *Myxococcus xanthus* development. *Genes Dev* 6: 401–410.

Licking E, Gorski L & Kaiser D (2000). A common step for changing cell shape in fruiting body and starvation-independent sporulation of *Myxococcus xanthus*. *J Bacteriol* 182: 3553–3558.

Lobedanz S & Søgaard-Andersen Lotte (2003). Identification of the C-signal, a contact-dependent morphogen coordinating multiple developmental responses in *Myxococcus xanthus*. *Genes Dev* 17: 2151–2161.

López D & Kolter R (2010). Extracellular signals that define distinct and coexisting cell fates in *Bacillus subtilis*. *FEMS Microbiol Rev* 34: 134–149.

Lopez D, Vlamakis H & Kolter R (2009). Generation of multiple cell types in *Bacillus subtilis*. *FEMS Microbiol Rev* 33: 152–163.

Maamar H & Dubnau David (2005). Bistability in the *Bacillus subtilis* K-state (competence) system requires a positive feedback loop. *Mol Microbiol* 56: 615–624.

Maamar H, Raj A & Dubnau David (2007). Noise in gene expression determines cell fate in *Bacillus subtilis*. *Science* 317: 526–529.

McBride MJ, Köhler T & Zusman D R (1992). Methylation of FrzCD, a methyl-accepting taxis protein of *Myxococcus xanthus*, is correlated with factors affecting cell behavior. *J Bacteriol* 174: 4246–4257.

McBride MJ & Zusman D R (1993). FrzCD, a methyl-accepting taxis protein from *Myxococcus xanthus*, shows modulated methylation during fruiting body formation. *J Bacteriol* 175: 4936–4940.

Mensch B, Bachelor thesis (2009). Analysis of EspA dependent protein accumulation of MrpC, a developmental regulator in *Myxococcus xanthus*.

Meyer TF, Gibbs CP & Haas R (1990). Variation and control of protein expression in *Neisseria*. *Annu Rev Microbiol* 44: 451–477.

Mittal S & Kroos L (2009a). A combination of unusual transcription factors binds cooperatively to control *Myxococcus xanthus* developmental gene expression. *Proc Natl Acad Sci USA* 106: 1965–1970.

Mittal S & Kroos L (2009b). Combinatorial regulation by a novel arrangement of FruA and MrpC2 transcription factors during *Myxococcus xanthus* development. *J Bacteriol* 191: 2753–2763.

Monier J-M & Lindow SE (2003). Differential survival of solitary and aggregated bacterial cells promotes aggregate formation on leaf surfaces. *Proc Natl Acad Sci USA* 100: 15977–15982.

Müller F-D, Treuner-Lange A, Heider J, Huntley SM & Higgs PI (2010). Global transcriptome analysis of spore formation in *Myxococcus xanthus* reveals a locus necessary for cell differentiation. *BMC Genomics* 11: 264.

Muñoz-Dorado J, Inouye S & Inouye M (1991). A gene encoding a protein serine/threonine kinase is required for normal development of M. xanthus, a gram-negative bacterium. *Cell* 67: 995–1006.

Nariya H & Inouye Masayori (2008). MazF, an mRNA interferase, mediates programmed cell death during multicellular Myxococcus development. *Cell* 132: 55–66.

Nariya H & Inouye Sumiko (2006). A protein Ser/Thr kinase cascade negatively regulates the DNA-binding activity of MrpC, a smaller form of which may be necessary for the *Myxococcus xanthus* development. *Mol Microbiol* 60: 1205–1217.

Nariya H & Inouye Sumiko (2005). Identification of a protein Ser/Thr kinase cascade that regulates essential transcriptional activators in *Myxococcus xanthus* development. *Mol Microbiol* 58: 367–379.

Novick A & Weiner M (1957). Enzyme induction as an all-or-none phenomenon. *Proc Natl Acad Sci USA* 43: 553–566.

O'Connor K A & Zusman D R (1991a). Analysis of *Myxococcus xanthus* cell types by two-dimensional polyacrylamide gel electrophoresis. *J Bacteriol* 173: 3334–3341.

O'Connor K A & Zusman D R (1991b). Behavior of peripheral rods and their role in the life cycle of *Myxococcus xanthus*. *J Bacteriol* 173: 3342–3355.

O'Connor K A & Zusman D R (1991c). Development in *Myxococcus xanthus* involves differentiation into two cell types, peripheral rods and spores. *J Bacteriol* 173: 3318–3333.

O'Connor K a & Zusman D R (1988). Reexamination of the role of autolysis in the development of *Myxococcus xanthus*. *J Bacteriol* 170: 4103–4112.

Odorico JS, Kaufman DS and Thomson JA (2001). Multilineage Differentiation from Human Embryonic Stem Cell Lines. Stem cells 19: 193–204.

Ogawa M, Fujitani S, Mao X, Inouye S & Komano T (1996). FruA, a putative transcription factor essential for the development of *Myxococcus xanthus*. *Mol Microbiol* 22: 757–767.

Osterås M & Jenal U (2000) Regulatory circuits in Caulobacter. *Curr Opin Microbiol* 3: 171–176.

Owen P, Meehan M, De Loughry-Doherty H & Henderson I (1996). Phase-variable outer membrane proteins in *Escherichia coli*. *FEMS immunology and medical microbiology* 16: 63–76.

Pessi G, Blumer C & Haas D (2001). mRNA stabilizing or *lacZ* fusions report gene expression , don't they? *Microbiol* 147: 1993–1995.

Rasmussen AA & Søgaard-Andersen Lotte (2003). TodK, a putative histidine protein kinase, regulates timing of fruiting body morphogenesis in *Myxococcus xanthus*. *J Bacteriol* 185: 5452–5464.

Reichenbach H (1993). Biology of the Myxobacteria: Ecology and Taxonomy. In: Myxobacteria II. Dworkin M & Kaiser AD (eds). Washington, DC: American Society for Microbilology, pp. 13-62.

Reichenbach H (1999). The ecology of the myxobacteria. *Environ Microbiol* 1: 15–21.

Robert L, Paul G, Chen Y, Taddei F, Baigl D & Lindner AB (2010). Pre-dispositions and epigenetic inheritance in the *Escherichia coli* lactose operon bistable switch. *Mol Sys Biol* 6: 357.

Rosenberg E, Keller KH & Dworkin M (1977). Cell density-dependent growth of *Myxococcus xanthus* on casein. *J Bacteriol* 129: 770–777.

Schramm A, PhD thesis (2012). Characterization of the Esp signalosome: Two hybrid histidine kinases utilize a novel signaling mechanism to regulate developmental progression in *Myxococcus xanthus*.

Schramm A, Lee B & Higgs PI (2012). Intra- and Interprotein Phosphorylation between Two-hybrid Histidine Kinases Controls *Myxococcus xanthus* Developmental Progression. *J Biol Chem* 287: 25060–25072.

Shi W, Ngok FK & Zusman D R (1996). Cell density regulates cellular reversal frequency in *Myxococcus xanthus*. *Proc Natl Acad Sci USA* 93: 4142–4146.

Shimkets L J (1990). Social and developmental biology of the myxobacteria. *Microbiol Rev* 54: 473–501.

Singer M & Kaiser D (1995). Ectopic production of guanosine penta- and tetraphosphate can initiate early developmental gene expression in *Myxococcus xanthus*. *Genes Dev* 9: 1633–1644.

Smits WK, Kuipers OP & Veening J-W (2006). Phenotypic variation in bacteria: the role of feedback regulation. *Nat Rev Microbiol* 4: 259–271.

Søgaard-Andersen L & Kaiser D (1996). C factor, a cell-surface-associated intercellular signaling protein, stimulates the cytoplasmic Frz signal transduction system in *Myxococcus xanthus*. *Proc Natl Acad Sci USA* 93: 2675–2679.

Søgaard-Andersen L, Slack FJ, Kimsey H & Kaiser D (1996). Intercellular C-signaling in *Myxococcus xanthus* involves a branched signal transduction pathway. *Genes Dev* 10: 740–754.

Son B, Liu Y & Kroos L (2011). Combinatorial regulation by MrpC2 and FruA involves three sites in the fmgE promoter region during *Myxococcus xanthus* development. *J Bacteriol* 193: 2756–2766.

Stein E a, Cho Kyungyun, Higgs PI & Zusman David R (2006). Two Ser/Thr protein kinases essential for efficient aggregation and spore morphogenesis in *Myxococcus xanthus*. *Mol Microbiol* 60: 1414–1431.

Stibitz S, Aaronson W, Monack D & Falkow S (1989). Phase variation in *Bordetella pertussis* by frameshift mutation in a gene for a novel two-component system. *Nature* 338: 266–269.

Sun H & Shi Wenyuan (2001a). Genetic studies of *mrp*, a locus essential for cellular aggregation and sporulation of *Myxococcus xanthus*. *J Bacteriol* 183: 4786–4795.

Sun H & Shi Wenyuan (2001b). Analyses of *mrp* genes during *Myxococcus xanthus* development. *J Bacteriol* 183: 6733–6739.

Turgay K, Hahn J, Burghoorn J & Dubnau D (1998). Competence in *Bacillus subtilis* is controlled by regulated proteolysis of a transcription factor. *EMBO J* 17: 6730–6738.

Tyagi S (2010). *E. coli*, what a noisy bug. *Science* 329: 518–519.

Tzeng L, Ellis T & Singer Mitchell (2006). DNA replication during aggregation phase is essential for *Myxococcus xanthus* development. *J Bacteriol* 188: 2774–2779.

Tzeng L & Singer Mitchell (2005). DNA replication during sporulation in *Myxococcus xanthus* fruiting bodies. *Proc Natl Acad Sci USA* 102: 14428–14433.

Ubersax JA & Ferrell JE (2007). Mechanisms of specificity in protein phosphorylation. *Nat Rev Mol Cell Biol* 8: 530–541.

Ueki T, Inouye S & Inouye M (1996). Positive-negative KG cassettes for construction of multi-gene deletions using a single drug marker. *Gene* 183: 153–157.

Ueki Toshiyuki & Inouye Sumiko (2003). Identification of an activator protein required for the induction of *fruA*, a gene essential for fruiting body development in *Myxococcus xanthus*. *Proc Natl Acad Sci USA* 100: 8782–8787.

Veening J, Hamoen LW & Kuipers OP (2005). Phosphatases modulate the bistable sporulation gene expression pattern in *Bacillus subtilis*. 56: 1481–1494.

Veening J-W, Smits WK & Kuipers OP (2008). Bistability, epigenetics, and bet-hedging in bacteria. *Annu Review Microbiol* 62: 193–210.

Viswanathan P, Murphy K, Julien Bryan, Garza AG & Kroos L (2007). Regulation of *dev*, an operon that includes genes essential for *Myxococcus xanthus* development and CRISPR-associated genes and repeats. *J Bacteriol* 189: 3738–3750.

Vlamakis H, Aguilar C, Losick R & Kolter R (2008). Control of cell fate by the formation of an architecturally complex bacterial community. *Genes Dev* 22: 945–953.

Wall D, Kolenbrander PE & Kaiser D (1999). The *Myxococcus xanthus pilQ* (*sglA*) gene encodes a secretin homolog required for type IV pilus biogenesis, social motility, and development. *J Bacteriol* 181: 24–33.

Waters LS & Storz G (2009). Regulatory RNAs in bacteria. *Cell* 136: 615–628.

Willett JW & Kirby JR (2012). Genetic and biochemical dissection of a HisKA domain identifies residues required exclusively for kinase and phosphatase activities. *PLoS Genetics* 8: e1003084.

Wireman JW & Dworkin M (1977). Developmentally induced autolysis during fruiting body formation by *Myxococcus xanthus*. *J Bacteriol* 129: 798–802.

Wu SS & Kaiser D (1996). Markerless deletions of *pil* genes in *Myxococcus xanthus* generated by counterselection with the *Bacillus subtilis sacB* gene. *J Bacteriol* 178: 5817–5821.

Wu SS & Kaiser D (1997). Regulation of expression of the *pilA* gene in *Myxococcus xanthus*. *J Bacteriol* 179: 7748–7758.

Xie C, Zhang H, Shimkets Lawrence J & Igoshin OA (2011). Statistical image analysis reveals features affecting fates of *Myxococcus xanthus* developmental aggregates. *Proc Natl Acad Sci USA* 108: 5915–5920.

Yewdell JW, Lacsina JR, Rechsteiner MC & Nicchitta C V (2011). Out with the old, in with the new? Comparing methods for measuring protein degradation. *Cell Biol Intl* 35: 457–462.

Zhang D, Iyer LM & Aravind L (2011). A novel immunity system for bacterial nucleic acid degrading toxins and its recruitment in various eukaryotic and DNA viral systems. *Nucleic Acids Res* 39: 4532–4552.

Zusman D & Rosenberg E (1970). DNA cycle of *Myxococcus xanthus*. *J Mol Biol* 49: 609–619.

CURRICULUM VITAE

This page contains personal data; hence it is not a part of the electronic version of the thesis.

Diese Seite enthält persönliche Daten. Sie ist deshalb nicht Bestandteil der Online-Veröffentlichung.

ACKNOWLEDGEMENTS

This page contains personal data; hence it is not a part of the electronic version of the thesis.

Diese Seite enthält persönliche Daten. Sie ist deshalb nicht Bestandteil der Online-Veröffentlichung.